UNIVERSITY *of the*
WESTERN CAPE

INVESTIGATING SUBSURFACE HETEROGENEITIES AND ITS IMPACT ON THE VARIATION IN INTERVAL VELOCITIES: IMPLICATIONS TO VELOCITY MODELLING IN THE BREDASDORP BASIN

A mini thesis in Petroleum Geoscience

*By **MUAZZAM ALI HASHIM***

Submitted in partial fulfilment of the requirements for the degree of Magister Scientiae (MSc) in the Faculty of Science, Earth Science Department, University of the Western Cape, South Africa.

Supervisor: Dr. M. Opuwari

ABSTRACT

Velocity modelling forms an integral part of the seismic interpretation process initially completed in two-way time. In order for a representative depth conversion, it is obligatory to construct a velocity model that serves the bridge between velocity and respective two-way time. This study deals with the investigation of subsurface heterogeneities and its impact on the variation of velocities. Interpretation of time domain reflection data results in one or more seismic horizons, however these horizons should represent the variation in subsurface geology as a result of acoustically different layers displaying varying reflection amplitudes.

The purpose of this study was fulfilled by examining the variation of these velocities in relation to the geology and its significance towards building a velocity model. It is evident that complexities, such as an existing heterogeneous subsurface is present in the study area. Using velocities only considered at formation well tops, as a result, does not completely honour the variation in these velocities. The velocity profile as calculated from the sonic log was characterized into zones representing unique velocity trends. The analyses to understand the impact of subsurface heterogeneities on the velocities was completed by the application of seismic facies analysis which entailed the study of the seismic reflector patterns and amplitudes; a study of the lithologies present and the generation of mineral plots using available wireline logs, all of which in close relation to the variation in velocities.

The characterized zones, as a result have shown that shaly sediments are typically associated with higher velocities (~2800 – 4600m/s) compared to sandstones of lower densities. Mineral plots however, have also indicated that where quartz minerals were present (specifically zone L), sandstones as a result have shown higher velocities (~4800m/s) as compared to the shales (~3600m/s). These higher velocities are also associated with more organised seismic reflectors with brighter amplitudes and strong contrasts in acoustic impedance as shown by the seismic. Uniform velocities were observed in zones such as zone Ia, typically associated with a low acoustic impedance contrast and minimal variation in its lithological make-up.

The integrated investigation of subsurface heterogeneities has shown that velocities vary to a substantial degree as a result of existing subsurface heterogeneities. The variation of these velocities are hence significant enough that it should be considered when constructing a velocity model which aims to respect the geology of the study area. The result of understanding the relation between the geology and resultant velocities may prove to advance the results of the velocity model in a manner that it is more complete and representative of the subsurface.

KEYWORDS

Heterogeneity

Velocity modelling

Interval velocities

Seismic Facies

Lithologies

Mineral composition

Subsurface

Two-way time

Time-depth relation

Acoustic impedance

DECLARATION

I declare that the thesis entitled: **Investigating subsurface heterogeneities and its impact on the variation in interval velocities: Implications to velocity modelling in the Bredasdorp Basin** is my own work, that it has not been submitted before for any degree or examination in any other University, and that all the sources I have used or quoted have been indicated and acknowledged by means of complete references.

Muazzam Ali Hashim **November 2015**

Signed:.....

DEDICATION

This project is dedicated to

The

ALMIGHTY ALLAH, the most Beneficent, the most Merciful

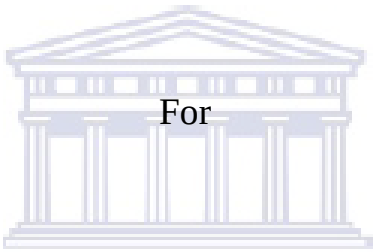

For

All things are possible through the Almighty's grace.

ACKNOWLEDGEMENT

I wish to thank the Almighty for guiding and blessing me with the ability to pursue this project. All praise, glory and honour is due to Allah. It is through His mercy and blessings that has made it possible for me to accomplish the undertaking of this research.

An immense gratitude is due to my supervisor, Dr. M. Opuwari for his support and guidance throughout this research project and Jody Frewin for her generous assistance. I wish to thank Mr. Nehemiah Dominick and Mr. Chris McClean for their comprehensive advice and guidance through the trials that was encountered throughout this research project.

I am deeply grateful to my parents Mr. and Mrs. Hashim for their utmost care and support throughout this journey, and for granting me the opportunity to develop myself academically. A special acknowledgement goes to my dearest friend, Ms. Nabeelah Kader for her continuous support, advice and motivation which inspired me to remain steadfast. To my brother and sister, Shuaib and Hafeezah for their continuous encouragement and confidence in me.

Gratitude is given to the Petroleum Agency of South Africa and PetroSA for the provision of data required to undertake this endeavour. To my fellow postgraduate colleagues and lecturers of the Earth Science Department at the University of the Western Cape for all the advice and support.

CONTENTS

LIST OF FIGURES

LIST OF TABLES

CHAPTER 1 – Synopsis of Research

1.1 Introduction

Subsurface heterogeneities are conclusively existent in any given area of study. The term subsurface heterogeneity is used to describe geological complexities, which may include assemblages of depositional facies, sub-facies or changes in the lithological make-up of the subsurface. These heterogeneities serve as key indicators for important geological boundaries or markers in history that may be of significance to the oil and gas industry. The understanding of the variation in geology with the incorporation of seismic studies may unlock periods of key interest, of which may also improve on methods previously used in exploring for oil and gas.

While interpretation of seismic data is completed in two-way time, the end result is represented in its depth position in space. The method for this conversion is known as Velocity modelling, whereby seismic and well data are jointly interpreted for the purpose of locating significant intervals of interest.

This study focusses on capturing the heterogeneity of the subsurface by means of investigating the constraints that impact this variation. The study will also focus on how these changes in geology can be incorporated into the Velocity model for the purpose of constructing a model which not only respects a continuous velocity profile but at the same time, the heterogeneity of the subsurface.

The responses of the velocities that are determined from seismic and well data are solely the result of complexities or changes within the geology of the subsurface. Hence, these changes may represent areas of value to the study that may have been ignored when only considering specific intervals. Studying the velocity profile, it is evident that significant intervals represented by substantial variations in velocities are present.

The construction of a velocity model using data at only specified intervals may result in averaging out significant variations in interval velocities, which may have been indicative of changes in subsurface geology. Appreciation to the aspect of geological heterogeneity may as a result be excluded.

With the understanding of subsurface heterogeneities and their respective response to the velocities, this study addresses the possibility of using such information to construct a velocity model that respects the geology of the subsurface by means of incorporating significant

changes in velocities. The completion of such a study may serve to improve the proficiency of a previous model as a result of conjointly necessitating subsurface geology and velocities in a mutual study.

The velocity profile for this study was determined using the sonic log. Using this profile, the identified velocity intervals signified by their distinct variation were used to characterize zones of geological importance. The velocity model V=V0+Kz (Slotnick, 1936 cited in Ugbor and Alaminiokuma, 2010), was used in order to incorporate these lithological boundaries/zones, characterized by a variation in velocity at its top and a constant linear gradient. Further analyses on these respective zones were completed in order to understand the differences in geology from those above and below them. This was completed in order to understand how velocities vary on a smaller scale and the imperativeness of these changes as a result of existing heterogeneities.

1.2 Location of Study Area

The Bredasdorp basin being the location of the study area is situated off the southern coast of South Africa where analysis was completed using well and 3D seismic data from a field within this basin.

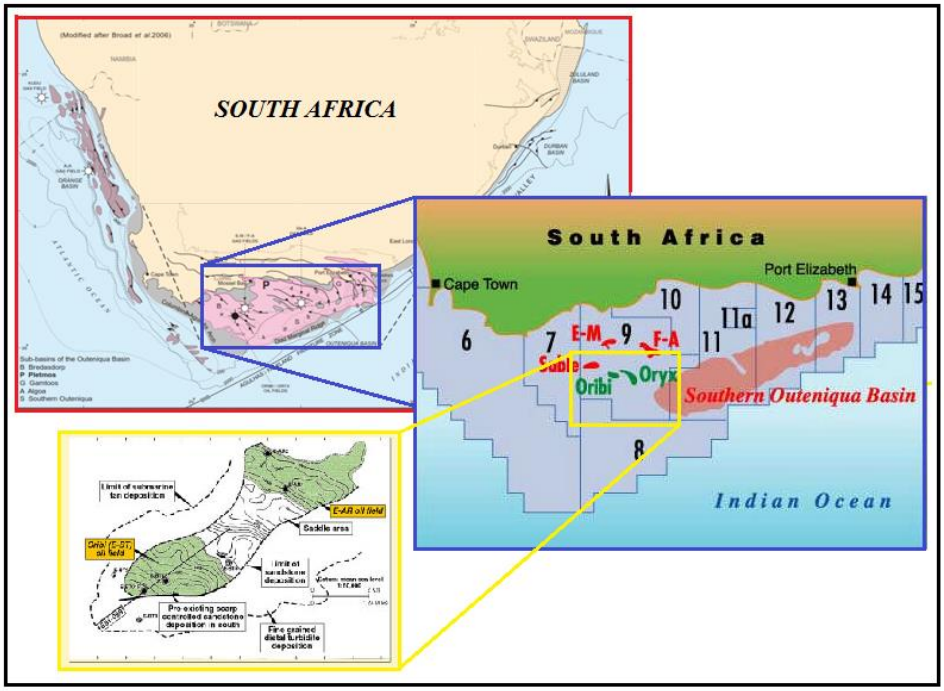

Figure 1: Location Map of the Bredasdorp Basin and study area (Adapted from Envoi, 2014; Roux, 1997).

The Bredasdorp basin, located off the southern South African coast rests beneath the Indian ocean and covers total area of 18 000km². The basin structure is bounded by two arches, namely: the Agulhas Arch and the Infanta Arch with its strata sequenced with Upper Jurassic, Lower Cretaceous & Cretaceous and Cenozoic sediments (Brown et al., 1995, Turner et al., 2000).

1.3 Previous work completed on the Basin

The Petroleum Agency SA being the licensing regulator for the South African region for the oil and gas E & P has been overseeing many projects undertaken off the coast of southern Africa. Extensive exploration for more than 30 years have shown that the southern coast of South Africa is host to numerous small oil and gas fields as compared to the onshore region with no proven hydrocarbon reserves to date as yet. Extensive drilling done by the former SOEKOR (Presently PetroSA) since 1965 had resulted in these numerous petroleum plays.

PetroSA has brought further discoveries of oil and gas deposits in the Bredasdorp Basin within Block 9 and 11A. Oil discoveries in particular are the Oribi and Oryx fields of Block 9 within the respective basin.

The field of interest for this study was discovered in 1988 as part of many fields within the Bredasdorp Basin. The first well drilled started production at a rate of 6000 barrels of oil per day. The second well was drilled in 1990 intersected a massive deep marine channel sandstone that was also found to be oil-bearing.

1.4 Problem Statement

Velocity modelling forms part of an integral process in the seismic interpretation phase, whereby it is of great significance in depth converting the final product. All initial interpretations are captured in two-way time. The velocity model serves to convert initial two way time interpretations to its correct position in depth. Interpretation of time domain seismic reflection data results in one or more seismic horizons. However, do these horizons account for the variation in the subsurface geology? Each horizon should mark, in the time domain, a surface separating significant changes in the geology to account for its heterogeneity of the complete study area. If acoustically different layers can be associated with well -defined

lithostratigraphic layers or key changes in the geology, then it is possible to construct a depth representation of the complete subsurface that incorporates significant variations in subsurface geology.

If the geology of the subsurface is known to be uniform, averaging velocities to represent their uniformity may be accepted. However, it is evident that subsurface complexities, such as existing subsurface heterogeneities are well known in any given area of study. Using limited intervals such as those taken from formation well tops, velocities in between these intervals which may have been of significance to the variations in the geology, as a result are entirely averaged and excluded. The heterogeneity of the subsurface is what governs the responses to velocities and therefore should be considered. Hence, this study focusses on capturing the heterogeneity of the subsurface by studying the velocity profile from well data, as well as the geology of the subsurface using well and seismic data. These heterogeneities will be of key focus to the study and its significance in incorporating such information into a velocity model in order to construct a model that is representative of interval velocities characteristic of key geological variations.

1.5 Aims and Objectives

The study aims at addressing velocity modelling keeping into consideration a geological perspective. The focal point of this study is based upon investigating existing subsurface heterogeneities of the given study area and its impact on the variation of interval velocities. The results of this investigation will focus on the importance of incorporating these subsurface heterogeneities into the velocity model. This is completed in order for the construction of a velocity model that is representative of the geology.

The specific objectives are the following:

- Examine the velocity profile to identify zones (divided by substantial changes in interval velocities) of which may well be representative of key variations in the geology.
- Construct a velocity model incorporating an increased number of interval velocities representative of the variations in geology.
- Investigate the heterogeneity of these zones.
- Identify seismic facies that are unique to these zones.
- Investigate the variations in lithologies that impact the variation in velocities.

- Generate mineral plots to understand the behaviour of similar lithologies with varying resultant velocities.

1.6 Hypothesis

In the case of existing subsurface heterogeneities, the result of the velocity response is based upon variation in the geology such as zones representing distinctive seismic facies, the lithological make-up of the subsurface or even the mineral make-up of similar lithologies. These changes in subsurface geology have significant influences on the variance in velocities, such that it should be considered when constructing a velocity model.

1.7 Summary of Methodology

Quality control of the well and seismic data was completed before commencement of the research. A synthetic seismogram was generated upon completion of a well to seismic tie. This was accomplished using velocity data calculated from the sonic log. The synthetic seismogram was completed in order to increase the control on the accuracy of interpretations that was completed in two-way time. This is done to correlate well data with seismic data.

Extraction of the sonic log from the desired well has been completed which was used to calculate the velocity profile representative of the entire well. These velocities were plotted against depth in order to visualize the behaviour of the velocities with respect to depth. Zones or boundaries characterized at the top by substantial variation in velocities are selected from this profile. The relationship between two-way and depth was established using data acquired from the velocity computation data. This was completed in order to determine a two-way time point at any selected depth position, as represented on the velocity vs. depth plot.

The velocity model was then constructed using the selected intervals. These intervals are representative of zones characterized by unique geologic properties.

An investigation on the heterogeneity of these zones were accomplished to understand how significant these variations impact the resultant velocities. Analysis completed included, a study to analyse seismic facies, varying lithologies between the selected zones as well as the mineralogy of these lithologies which impact the variation in velocities.

CHAPTER 2 – Literature Review

2.1 Geological Framework

2.1.1 Regional Setting – Development of the Outeniqua Basin

Several Mesozoic basins occur in South Africa and reside at the southernmost tip of the African plate on the south eastern margin of southern Africa (Malan, 1993). The break-up of Gondwana played a significant role in the development of the basins found off-shore the coast of southern Africa with rifting being the fundamental driving mechanism for their formation. Gondwana, the southern portion of the once integrated Pangaea, stores most of its complete records in the rocks lying below sea level on the continental shelf off southern Africa (McCarthy and Rubidge, 2005). Prior to the Break-up of Gondwana, southern Africa resided between the southern tip of South America, the Falkland Plateau and Antarctica. The break-up of Gondwana, initiated by opening of the Indian Ocean along the east African coast, was due to the eruption of basalts and rhyolites of the Lebombo region. The separation of Gondwana resulted in two individual landmasses, namely: West Gondwana and East Gondwana. West Gondwana comprised of South America and Africa while East Gondwana consisted of Madagascar, India, Antarctica and Australia. The split of Gondwana up till present still remains uncertain but various proposals have been put forward, one of which explains the rise of a mantle plume beneath Gondwana, with its centre situated in Mozambique (McCarthy and Rubidge, 2005).

This mantle plume known as the Karoo plume (Thomson, 1999) started developing ~180 million years (Ma), with extension taking place along the Mozambique-Zimbabwe border which resided along the Lebombo range and Limpopo Valley. As a result of the extensional phase, major fractures formed in the crust which caused East Gondwana to slide southward relative to West Gondwana, which in turn opened rifts which are today known as the Mozambique Channel. This created a seaway between the two landmasses (East and West Gondwana) and an initial formation of an oceanic crust between them (McCarthy and Rubidge, 2005).

60Ma later, succeeding the extension, South America began to detach from Africa, which in its course opened rifts along the southern African west coast. As a result of the rifting,

detachment of a large continental slab from the African continent, off the Southern Cape coast transpired, which today is known as the Falkland Plateau. This continental slab moved in a direction westward as South America separated from southern Africa and in the process created fractures in the oceanic crust. The fracture along where the Falkland Plateau detached is known as the Agulhas Falkland Fracture Zone (AFFZ) (McCarthy and Rubidge, 2005).

As a result of the Falkland Plateau drifting westwards, it stretched and tore the continental margin of Southern Africa resulting in the creation of several depressions, presently known as the Southern Cape region and the Agulhas Bank. These depressions paved the way for the sedimentation and accumulation of organic matter currently of significant interest to the Petroleum exploration industry (McCarthy and Rubidge, 2005).

30Ma later subsequent, the Falkland Plateau cleared the coast of the Southern Cape and in turn gave way for the creation of new oceanic crust. The Agulhas Plateau remains as the only portion left behind by the Falkland Plateau. Sedimentation took place during the break-up of Gondwana during which the interior of southern Africa was uplifted and experienced erosion. Sediment deposition mainly took place in the emerging Indian and Atlantic Oceans with eventual sediment deposition to all offshore areas off the coast of southern Africa. This resulted in extensive offshore sediment accumulations, which directly impacted the formation of the oil and gas reservoirs off the southern coast of southern Africa (McCarthy and Rubidge, 2005).

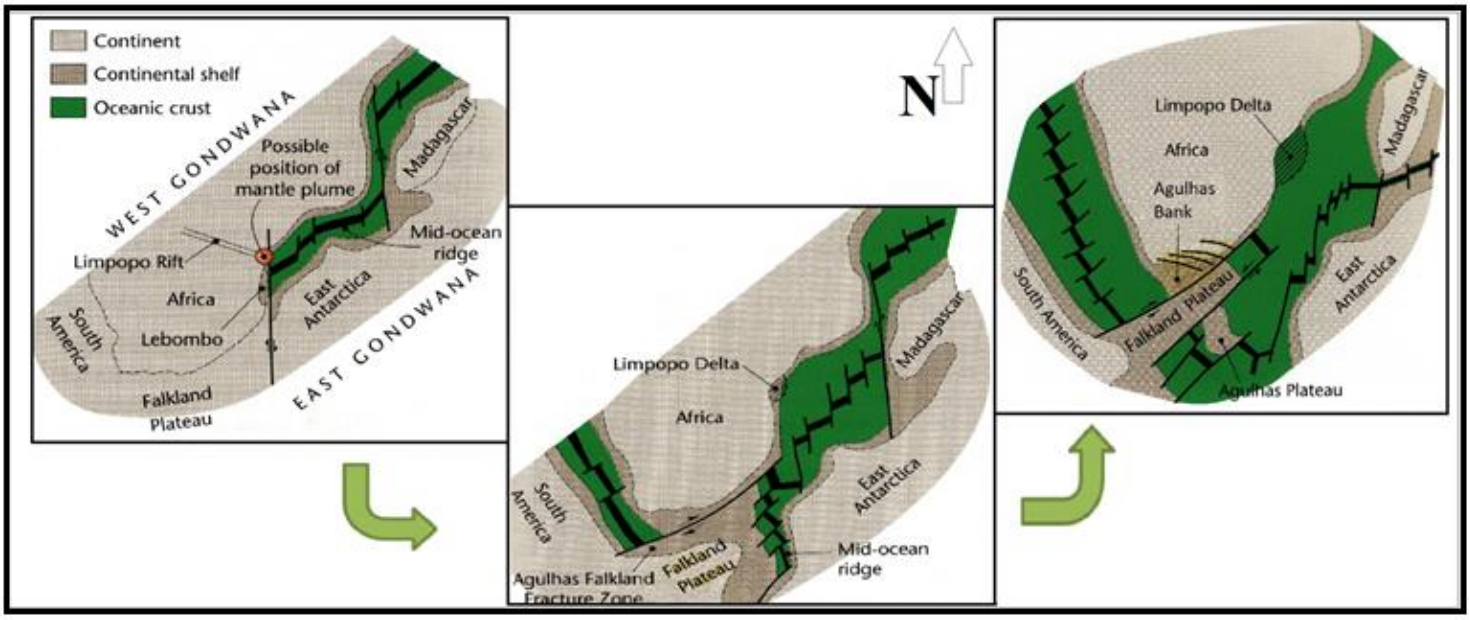

Figure 2: The process of rifting responsible for the formation of the basins (McCarthy & Rubidge, 2005).

The west coast offshore region comprises 45% of the total area for the entire basinal region off the coast of Southern Africa which spans roughly 191 600 km² and is characterised by a broad passive margin. This region is known as the Orange Basin. The eastern offshore region is characterised by limited sediment deposition and contributes a total of 25% of the complete basinal area offshore the southern African coast spanning roughly 107 000 km². This area is characterized by a narrow passive margin (Petroleum Agency SA, 2004/5). The eastern offshore region hosts the Outeniqua Basin which is subdivided into four sub-basins namely: The Bredasdorp, Pletmos, Gamtoos and Algoa Basins.

The Outeniqua Basin can be described to have had a history of strike-slip movement which initiated from the break-up of Gondwana. Each sub-basin within the Outeniqua basin is characterised by half-graben structures which formed as a result of the rifting and is notably overlain by thick sediments that accumulated during the drifting stage. The drifting stage manifested the cycles of sedimentation and accumulation as the basins formed. These four sub-basins of the Outeniqua basin extend outward furthest into the Southern Outeniqua Basinal area (Petroleum Agency SA, 2004/5).

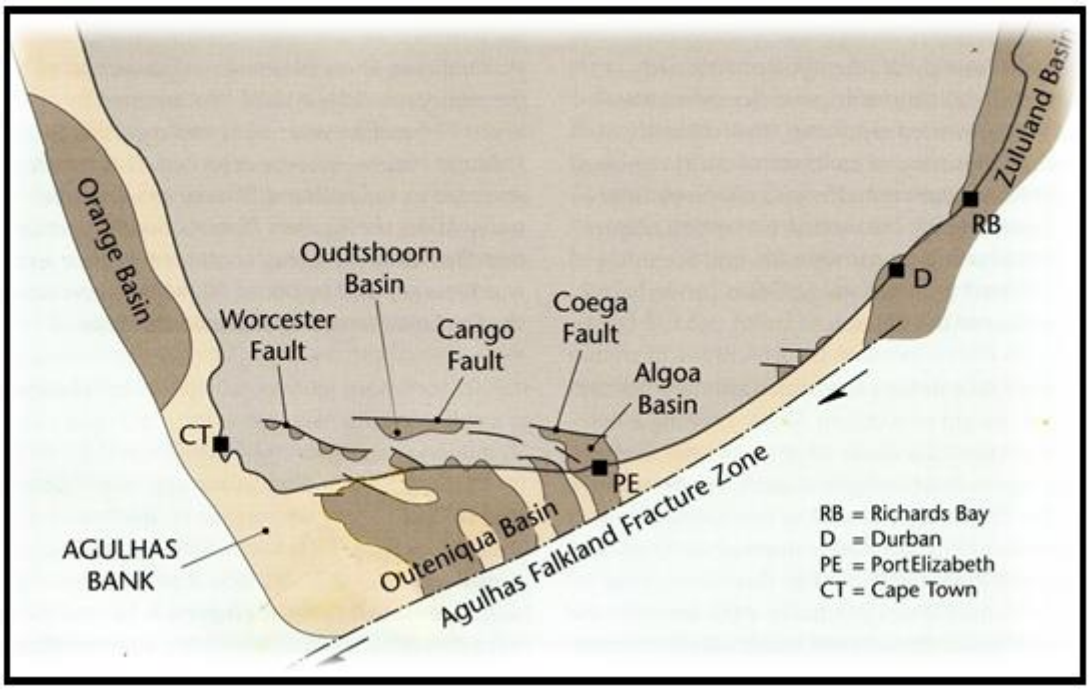

Figure 3: The westerly movement of the Falkland Plateau initiated the development of fractures along the southern Cape coast. As a result, the crust on the southern side dropped downwards, forming depressions, in which sediment was deposited (McCarthy & Rubidge, 2005).

2.1.2 Local Setting – Development of the Bredasdorp Basin

The structure of the Bredasdorp Basin is bounded by two arches, namely: the Agulhas Arch and the Infanta Arch with its strata sequenced with Upper Jurassic, Lower Cretaceous & Cretaceous and Cenozoic sediments (Brown et al., 1995, Turner et al., 2000). The Bredasdorp Basin is representative of a well-developed systems tracts with type 1 erosional unconformities.

The faulting affecting the Bredasdorp Basin during the synrift phase trended in a northwest to south-easterly direction between the Agulhas Arch and the Infanta Arch which resulted in graben and half-graben structures (Brown et al., 1995, McMillan et al., 1997). Throughout the rifting phase of the Bredasdorp Basin, sedimentation to the basin was obtained from the provenance of the Cape Supergroup rocks comprised of orthoquartzites and slates, and sandstones from the Karoo Supergroup located in the north and northeast (McMillan et al., 1997). Upliftment of the Agulhas and Infanta Arches as well as the horst blocks activated the 1At1 unconformity which ended the active rift sedimentation (Brown et al., 1995, McMillan et al., 1997).

Thermal subsidence gave rise to the 1At1 to 13At1 sequences which in turn reactivated the normal faulting. The reactivated faulting induced the deposition of post-rift and on-lap sequences which mostly affected the Bredasdorp Basin. The turbidity currents were the dominant driving force responsible for the sediment flow into the basin for the sequences 5At1 to 13At1. Erosion occurring at 126 to 117Ma incised submarine valleys and canyons into the pre-1At1 units.

The second super-cycle of the post-rift occurred between 117 and 112Ma (Brown et al., 1995). The Early Aptian to mid-Albian (112 to 103Ma) following the second super-cycle, encompassed a drop in sea-level which caused the erosion of sediment from high-stand shelf sandstones. These sandstones were carried by turbidity currents into the centre of the Bredasdorp Basin forming stacked & amalgamated channels and lobes. The channels dominated the western to south western area, whereas the lobes were affinitive in the eastern parts of the basin (Turner et al., 2000).

Glauconitic clays, biogenic clays and minor sands of the high-stand shelf deposits were deposited, starting in the Tertiary up till present day where these sediments were sourced from the erosion of the Agulhas Arch flanks by the process of uplift of the Late Cretaceous deposits

(McMillan et al., 1997). The uplift and biogenic clay deposition affecting the southern parts of the Bredasdorp basin terminated during the early Miocene which were then overlain by unconformities of the Holocene and late Pleistocene (McMillan et al., 1997).

Basin floor fans within the Bredasdorp Basin do not confide to the general radial geometry. Differences contributing to the shape of the basin floor fan are attributed to its relatively confined basin shape being predominantly elongated. The basin maintained a northwest – southwest elongation that is inherent from the syn-rift sub-basins and was open to relatively free marine circulation to the southeast of the Southern Outeniqua Basin. Hence, sedimentation was sourced down the axis from the northwest. The origin of these sandstones consisting of Table Mountain quartzites and Cape granites were derived from the mainland and the Agulhas Arch (Grobbler, 2005).

Presently the Bredasdorp Basin devises a thermal gradient of 35 to 49°C/km (Davies, 1997) characterized by a temperately high heat flow. The thermal gradient underwent a reduction during the late Cretaceous as a result of a reduction in heat flow and subsidence after the rifting. Temperatures within the basin increased until ~80ma at a rate of >3°C/ma. This was followed by a decrease in sedimentation rates which resulted in a reduction in the temperature increase rate during the early Tertiary. The temperature rate decreased from 3°C/ma to a low of <0.3°C/ma. These temperature rates increased again during the Miocene to Pliocene (Davies, 1997). Inconstant heat flow rates during the formation of the Bredasdorp Basin resulted in a strange thermal past within the basins burial history.

The Bredasdorp Basin evolved from fan deltas and river dominated to wave dominated deltas and also associated coastal systems. Slope and basin systems evolved from fine-grained density and suspension deposits to leveed slope and basin floor turbidite fans, this has also been related to the fine-grained turbidite systems. The changes is due to the response to second order tectonic episodes which resulted in the variation in sediment supply rates and subsidence or accommodation rates and increasing open ocean processes. Four relative isolated fault bounded subbasins composing the Bredasdorp Basin during supercycle 1-5 (126-117.5 Ma) were supplied with sediments by high gradient fluvial systems. River dominated deltaic systems progrades southward across the northern margin of the central subbasin. During the second postrift supercycle 6-12 (117.5-112 Ma) well developed river dominated deltaic coastal systems prograded into the expanded basin. This deposition followed major uplift and erosion

of second order erosion of the second order unconformity. Fluvial sediments were introduced to lowstand shorelines through small canyons and eroded into the shelf edge. The Upper Barremian 9A LST (Low-stand systems tract) basin floors comprises of several individual submarine fans. The lowstand prograding wedges does not appear at all of the mouths of all of the entrances of the river systems. It only occurs where the sediment supply rates exceeded accommodation rates for the sediments (Petroleum Agency SA, 2004/5).

In the Bredasdorp Basin it has been established that a total of 24 seismically resolvable postrift Cretaceous unconformities and associated depositional sequences between the drift onset second order unconformity and third order unconformity which is situated at 126Ma and 79Ma. All of the sequences are estimated to be of type 1, of which six of the unconformities exhibit intense tectonically enhanced erosion, also coinciding with the second-order and third-order surfaces. There is a total of 20 third order sequences composing of five second–order supersequences within the Bredasdorp Basin. Most of the sequences is poorly developed fourth order sequences (Mitchum and Van Wagoner, 1988 cited in Schalkwyk, 2005).

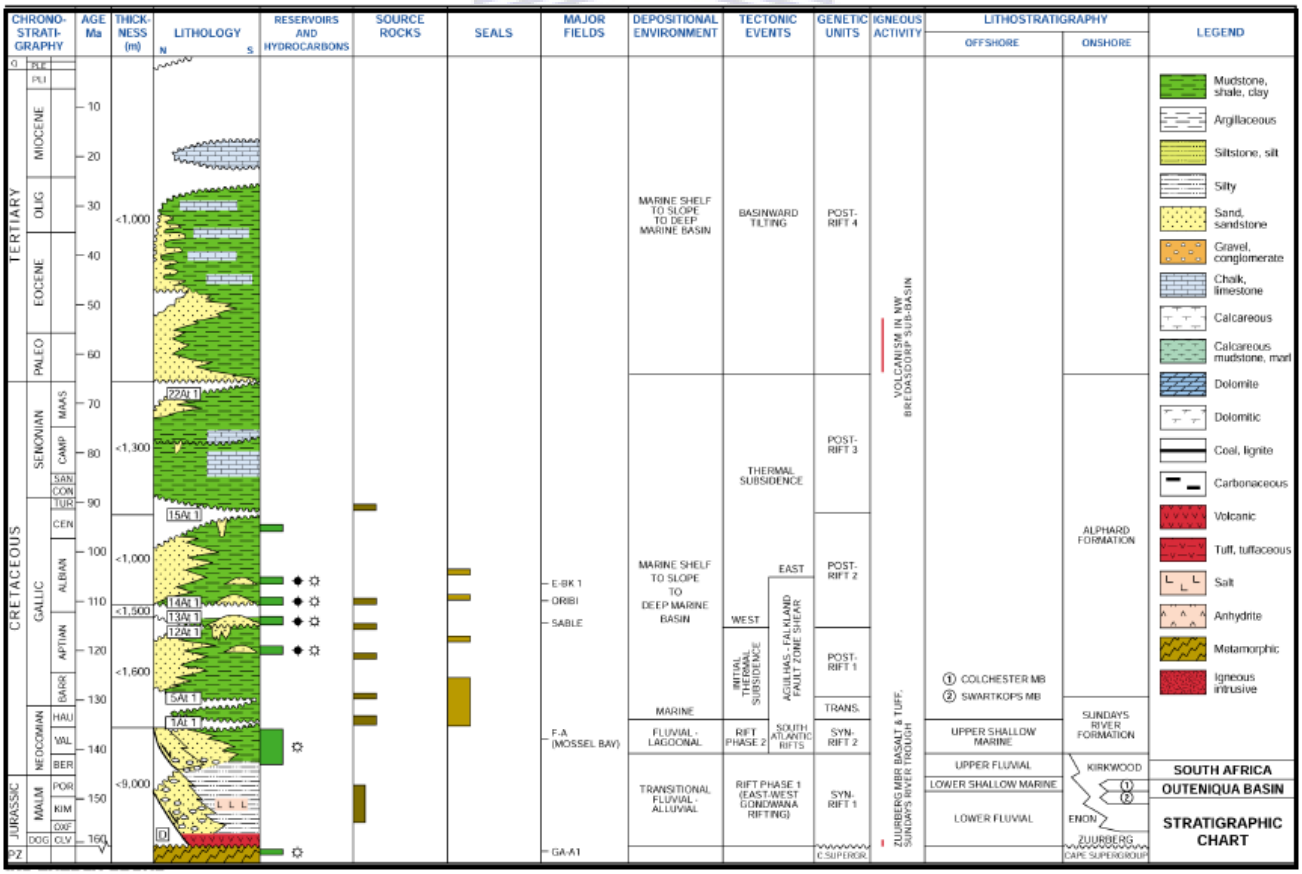

Figure 4: Stratigraphy of the Bredasdorp Basin (IHS Energy, 2010)

2.1.3 Field Setting

Geological models for the field of study show that the overall setting is that of a deep marine fan complex with sand prone channels confined to an erosional valley in the centre of a predominantly mud-rich system (Feddersen and Malan, 2001).

Internally, within the field of study, hydraulic communication is assisted by partial erosion into preceding flow units allowing for amalgamated sand-on-sand contacts (Feddersen and Malan, 2001).

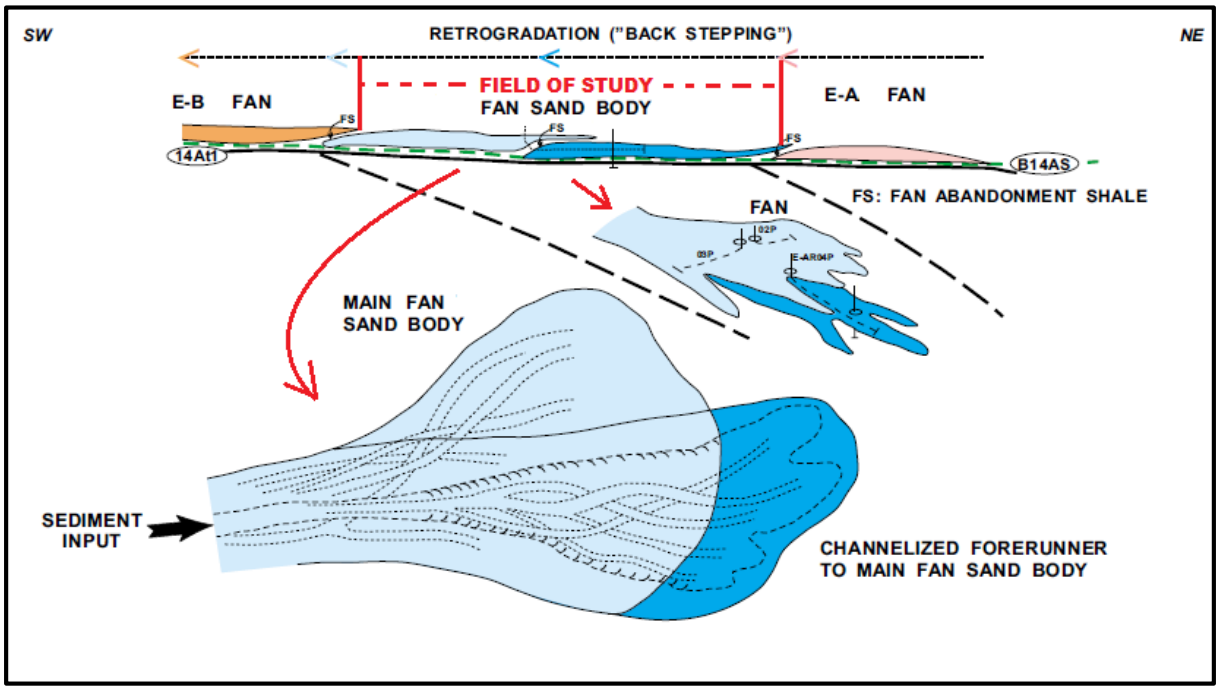

Figure 5: Depositional model for the field of study (Modified from Malan, 2001).

2.2 Velocity Modelling

Velocity modelling is an essential part of seismic processing and interpretation. While all early seismic processing are proceeded in time (two-way time), the velocity model serves as a method to domain convert these interpretations completed in time to their closest approximation to depth. Most of the time, sonic logs are used to help build this depth model, since it is a measure of time over depth (μs/ft) (Sheriff, 1995 cited in Silva, 2008).

A seismic velocity model is necessary to map depth and thickness of subsurface layers that are interpreted in time from seismic reflections. Depth conversion is a method of removing the structural ambiguity inherent in time and verify structure, hence providing a model conforming to the depth domain (Pandey et al., 2013).

Most existing models assume that lithology is sharply discontinuous, discrete, and that velocity is laterally or vertically constant within a particular medium, all of which can be proven otherwise. The application of a velocity model that is able to incorporate variations in the lithologies as well as respect a change in velocity by a particular gradient can be accomplished. An instantaneous linear velocity model is defined by two analytic parameters: 1) top-interface velocity, (V0) and 2) a velocity gradient or compaction factor, *k*. (Ugbor and Alaminiokuma, 2010). By incorporating these factors, it is possible to construct a velocity model that respects the geology.

In areas where there are dramatic variations in velocity, such as thick carbonate or evaporate units alternating with thick elastic units (as those found in the southern North Sea basin), complex structures, tectonic inversions or lateral lithology change, the layer cake model which treats each lithologic unit separately and defines each unit by a different mathematical function may be appropriate for depth conversion. But in areas of uniform lithology which have not undergone tectonic inversion or severe structural deformation, depth conversion can often be performed according to some effective mathematical functions (Instantaneous velocity functions) that respect the geology of the area under consideration (Ugbor and Alaminiokuma, 2010).

Slotnick (1936) and Faust (1951 and1953), as cited in Ugbor and Alaminiokuma describe different types of applicable velocity models. Slotnick describes the linear instantaneous velocity model as V (z) = V0+Kz, where V (z), K and Z represents the top interface instantaneous velocity, constant vertical gradient and z, the lithostratigraphic depth,

respectively. Another method by Slotnick is the exponential method that is described by V (z) + V_a exp ($K_a z/V_a$), where V (z), K_a, and z is representative of the top-interface instantaneous velocity, the gradient at the top interface and the lithostratigraphic depth. Faust (1961 and 1953) describes a method of velocity gradient decrease with depth. This model is shown by [V (z) = $V_a A^k \sqrt{z}, n \approx 6$] or [V (z) $V_a * \sqrt[k]{1 + nk_a z/V_a}$] where n is the root index.

Contrasts in acoustic impedances are achieved at the interfaces of lithostratigraphic layers of varying density and velocity. If these acoustically varying impedances reflect layers with well-defined lithostratigraphic properties, then a velocity model can be constructed that incorporates these changes. For most lithostratigraphic layers, a convenient velocity model represented by the algebraic expression, for this type is the: V=V0+K*Z (Dalfsen et al., 2006).

The end result of any earth model, where a velocity model has been applied, is the representation of the earth model in its depth domain. As previously stated, structural ambiguity inherent of time and the verification of structure can also be achieved after application of a velocity model (Pandey et al., 2013).

2.3 Seismic Interpretation

The objective of seismic data interpretation is to extract all available subsurface information from processed seismic data. This type of extraction includes structure, stratigraphy, subsurface rock properties, velocity, stress and in some cases reservoir fluid changes in time and space. Analysis that is usually involved in seismic interpretation includes components starting from well-log correlation, synthetic seismogram generation, well-to-seismic tie analysis, time-to-depth conversion, fault interpretation, seismic horizon interpretation and mapping (Onajite, 2014).

Seismic analysis begins with the essential seismic data. A seismic section is a display of the seismic data along a line, such as a 2D seismic profile or many profiles extracted from a volume of 3D seismic data. A time section is seismic data that is recorded in two-way travelled time, whereas a depth section can be described as being a section of seismic that has been converted from time to depth (Onajite, 2014)

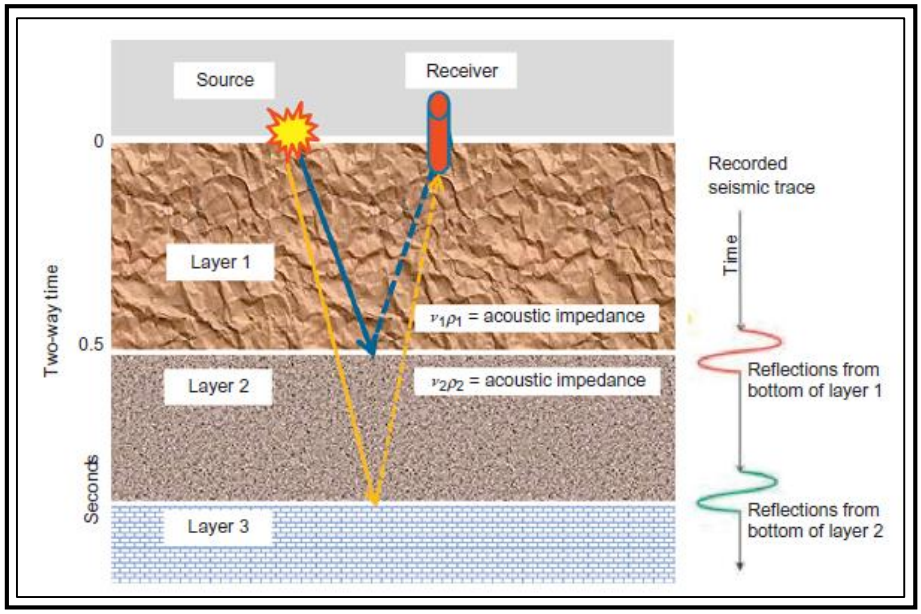

Figure 6: Illustration of a seismic reflection method (Adapted from Onajite, 2014 in Seismic Data Analysis).

A seismic trace can be described as seismic data that has been recorded at the surface due to the responses of subsurface layers to the seismic source. A wiggle trace is a representation of the seismic trace as shown by peaks and troughs associated with acoustic softness and hardness in the earth (Onajite, 2014).

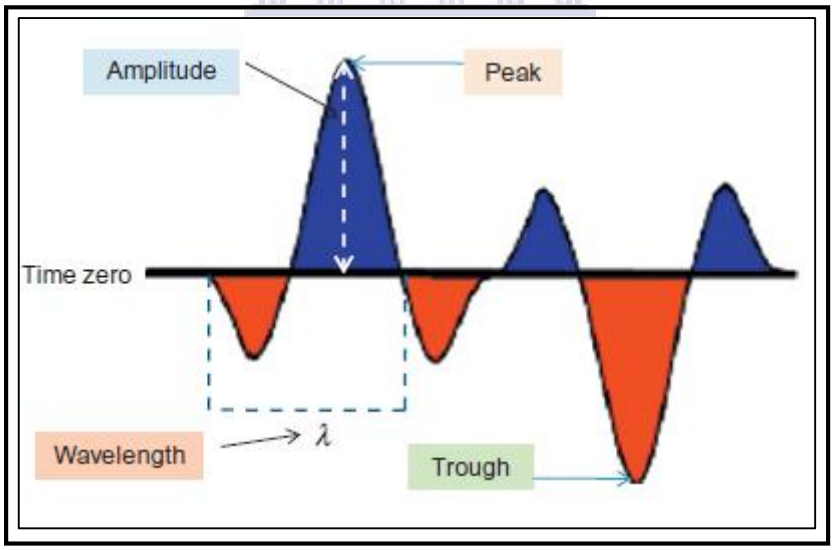

Figure 7: Illustration of a seismic wiggle trace (Adapted from Onajite, 2014 in Seismic Data Analysis).

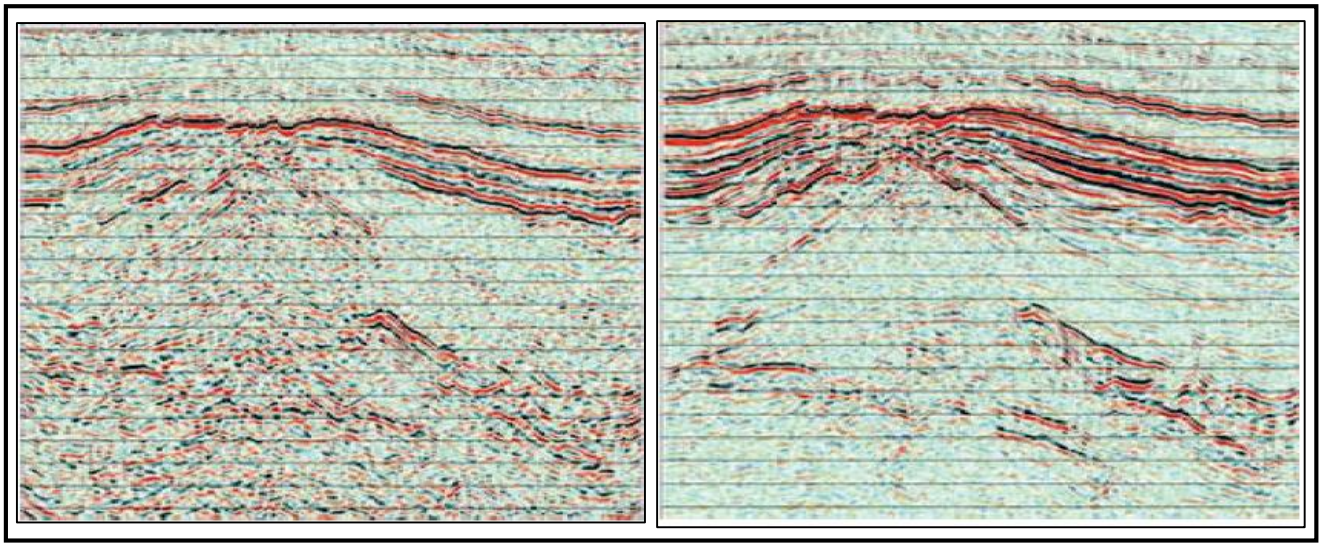

Figure 8: Time (Left) and Depth (Right) seismic sections (Adapted from Onajite, 2014 in Seismic Data Analysis).

Two-Way Time can be defined as the time required for a seismic wave to vertically travel from the source to the reflector within the subsurface and its travel time back to the receiver at the surface. This measurement of time is recorded in milliseconds (Onajite, 2014).

Acoustic impedance can be described as the product of velocity and density, whereby its contrast is controlled by changes in these variables by the next hard or soft lithostratigraphic layer. A seismic reflection is the result of this acoustic impedance between rock layers. The seismic amplitude is determined by the strength of the reflection as a measure of the maximum displacement from the time zero of the seismic trace (Onajite, 2014).

A synthetic seismogram as described by Onajite (2014) is generated using sonic and density logs where it is used to compare the original seismic data collected near the well location. This is completed to improve the accuracy of the interpretations completed in two-way time.

Onajite (2014) describes that the understanding of velocities are significant in seismic interpretation. Average seismic velocities are defined as twice the depth of the seismic wave from the source to receiver divided by the two-way travel time. It is given by the expression:

$$V_a = \frac{2Z_1}{T_1}$$

Seismic interval velocities is described as the thickness of a stratigraphic layer divided by the time it takes to travel from the top of the layer to its base: $Vi = \frac{2\Delta z}{2\Delta t} = \frac{2\Delta z}{\Delta T}$

Fault picking on the seismic sections are completed to delineate the geological structural trend in the study area. This is carried out bearing in mind the nature of the geology of the target study area. Seismic horizon mapping aims to map laterally consistent geologic structures, stratigraphy and reservoir architectures. These horizons represent significant intervals such as geologic sequences or reflections created during seismic processing (Onajite, 2014).

Posamentier and Kolla (2003) describe the use of 3D seismic analysis in deep basin-floor settings offshore Nigeria, Indonesia and the Gulf of Mexico to identify five depositional elements, namely: 1) turbidity-flow leveed channels, 2) channel-overbank sediment waves and levees, 3) distributary- channel complexes, 4) crevasse-splay complexes and 5) debris-flow channels, lobes and sheets. Each depositional element representative of unique morphologies and seismic expressions.

2.4 Seismic Facies

Seismic facies can be described as packages of reflectors with a set of characteristics differing from adjacent units. Seismic facies analysis takes the interpretation process one step beyond seismic sequence analysis by examining within sequences smaller reflection units that may be the seismic response to lithofacies (Lin, 2006).

Lin (2006) describes five reflection patterns that can be identified when undertaking seismic facies analysis. These are namely; Parallel/Subparallel; Divergent; Prograding; Chaotic and Reflection free patterns.

Parallel and Subparallel reflectors generated by strata are representative of uniform depositional rates on a uniformly subsiding shelf or stable basin setting. Divergent configurations are characterized by wedge-shaped units in which lateral thickening of the entire unit is the result of thickening of individual reflection sub-units. These configurations are representative lateral variations in depositional rates or the result of progressive tilting of sedimentary surfaces during deposition (Lin, 2006).

Prograding reflector patterns are generated as a result of deposition by laterally outbuilding or progradation forming gently sloping depositional surfaces (Clinoforms). These prograding reflection configurations include patterns of sigmoid and oblique, complex-sigmoid oblique, shingled and hummocky configured patterns. Chaotic patterns are interpreted to represent a disordered arrangement of reflection surfaces that exhibit little to no continuity. These

configurations are attributed to soft sediment deformation, or deformation of strata in a high-energy environment. Reflection free patterns represent homogenous, non-stratified units such as igneous masses or thick salt deposits, or highly contorted or very steeply dipping strata (Lin, 2006).

The objective of seismic facies analysis is to be able to correlate reflection attributes to the stratigraphic characteristics of identified sequences as well as provide a correlation between seismic and well data. These reflection characteristics are known to correspond to unique geological and depositional history of the sequence (Mitchum et al., 1977 cited in Futalan et al., 2012). Numerous previous studies have shown a direct correlation between seismic facies type and lithology. However, this type of study still remains unique to the basin of interest, hence an independent analysis must be carried out in every basin of interest (Lin, 2006).

Anomneze et al (2015) used this approach in the eastern Niger Delta Basin, Nigeria. Their study incorporated the use of reflection geometries and amplitudes as seen on vertical transects to define seismic facies that are linked to specific stratigraphic bodies. Anomneze et al (2015) also used this approach to make qualitative lithology predictions away from existing well control. It is hence noted that calibration of seismic facies with well control enhances the confidence in the interpretation as a result of unique seismic facies. Also, it is significant to mention that the continuity and configuration of seismic reflectors varies in a predictable manner from one seismic facies to another (Anomneze, 2015).

2.5 M-Lith and N-Lith Plots

The M-Lith and N-Lith plots (M-N plots) is a method used to for the purpose of lithology and mineral identification. In its simplicity, it utilizes three well-known porosity logs, namely: the density, neutron and sonic logs. With the use of these three logs, the cross-plot of the lithology M and N can be used to identify binary and ternary mixtures of minerals (Yin and Wo, 2010).

The terms M and N are defined as follows:

$$M = \frac{\Delta t_{\mathrm{fl}} - \Delta t_{\log}}{\rho_{\mathrm{b}} - \rho_{\mathrm{fl}}} \times 0.01 \qquad N = \frac{\phi_{N\mathrm{fl}} - \phi_{N\log}}{\rho_{\mathrm{b}} - \rho_{\mathrm{fl}}}$$

These plots are used to facilitate the interpretation of lithologies. M and N are simply the slopes of the individual lithology lines on the sonic-density and density-neutron cross-plots charts, respectively.

The advantage of this plot is that, it depends on three porosity logs (ρb, DT, and ΦN) (Burke et al., 1969 cited in Tarek and Ramadan, 2011). Tarek and Ramadan (2011) used this type of analysis to understand the behaviour of lithologies within the Sherouk field, Egypt. From these plots, it could be understood that the mineralogy of the rock units under study were composed of varying volumes of clay minerals which in turn resulted in reduction of effective porosity as well as hydrocarbon saturation within the rock units.

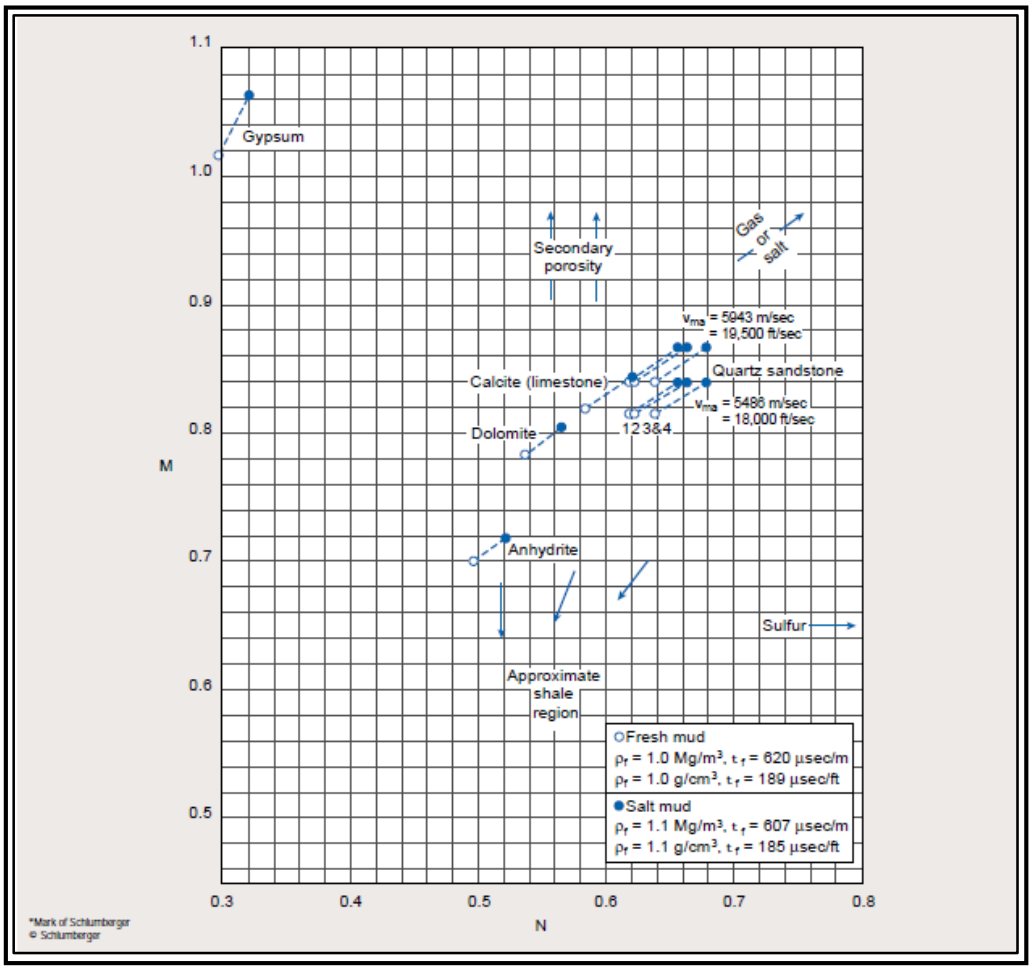

Figure 9: M-N plot for Mineral Identification (Schlumberger, 1997). Arrows indicates the effects of gas, salt, sulphur, secondary porosity and shaliness.

Kadi et al (2015) describes using the mono-porosity cross-plots to determine the water and hydrocarbon saturations, formation water resistivity and sonic, neutron and density derived porosities. Dia- porosity cross-plots were used to determine the shale volume and effective porosity.

CHAPTER 3 – Methodology

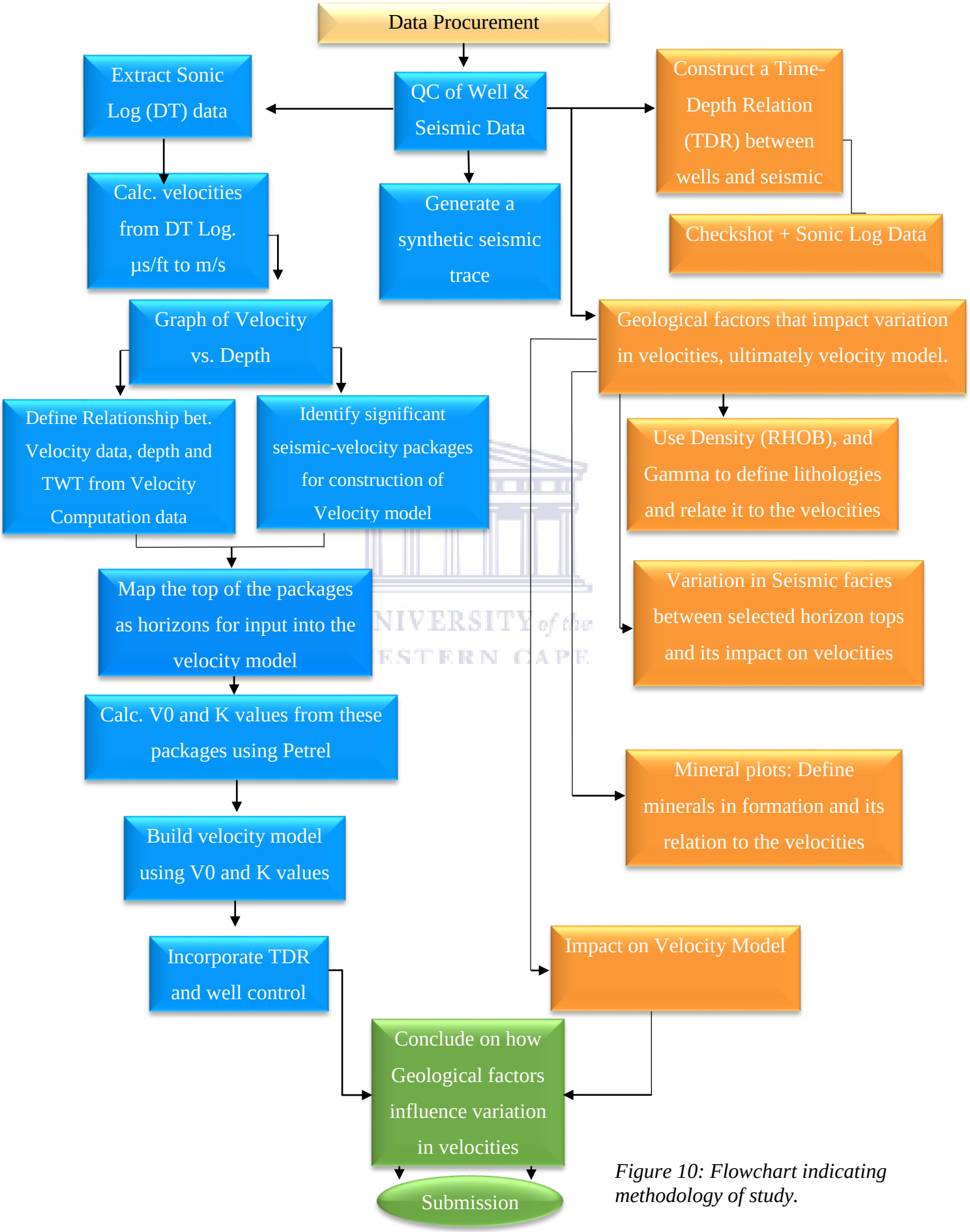

Figure 10: Flowchart indicating methodology of study.

The data set utilized for this study comprises of a 96 Mega 3D seismic data cube. This dataset is a merge of 1989 150m spaced 2D lines reprocessed into a pseudo 3D and 1995 EG 3D seismic + 1992 ECE 3D seismic together with E2000 3D seismic data. Wireline log data were acquired from well E-AX within the study area. Wireline logs used for this study include the Gamma Ray (GR), Sonic (DT), Density (RHOB), Neutron (NPHI), and Resistivity logs.

Seismic interpretation such as horizon and velocity modelling were completed using a software developed by Schlumberger: Petrel 2014. Analysis of wireline logs and the generation of mineral plots were completed using Interactive Petrophysics and Techlog, respectively.

The study is focused on investigating the heterogeneity of the subsurface and the impact of these geological properties on the variation of velocities. The main objective is to study these variations in velocities as a result of the geology and construct a velocity model which incorporates the heterogeneity of subsurface/geology represented by significant variations in the recorded velocities.

3.1 Seismic Data Analysis

This part of the research was carried out first in order to study the seismic data as a whole for the study area. The study of the velocity profile from calculation of the sonic log is completed in this section. This is completed to verify seismic reflector amplitudes with the corresponding velocities.

The velocity profile was calculated from the sonic log, using the formula$(\frac{1}{DT} \times 10^6) \times 0.3048$. This equation converted sonic log data (µs/ft) to m/s. Upon generation of the velocity profile, a representation of the entire well was made possible by means of plotting velocity against depth.

Since seismic data is typically displayed in two-way time (TWT), it is important, for this study, to establish a relationship between TWT and depth. This is done in order to extract significant positions in TWT from the graph of velocity vs. depth. This relationship was determined by means of utilizing the velocity computation data, which included recorded TWT, depth and velocity data taken at multiple intervals in the study area. A linear relationship between TWT and depth was established by means of plotting the TWT points against their respective depth positions. The resultant graph was represented by a linear expression and a correlation

coefficient of 0.9967. This expression was used to calculate TWT as a close approximation to the respective depth position within the well.

Using the graph of velocity vs. depth, key intervals which exhibited strong variations in the velocities were selected. These selected intervals were characterized into zones representing the variation in velocity at the top and a unique constant vertical gradient. Using the Interactive Petrophysics software, zone tops were created and converted to LAS format using the Zone Tops feature.

Sonic calibration was carried out to establish a link between well and seismic data. This is completed prior to the seismic interpretation in Petrel. The sonic calibration was completed by means of utilizing the sonic and checkshot data. This step was followed by the generation of a synthetic seismogram using the sonic and density logs. Calculations for the synthetic is completed in Petrel, whereby the acoustic impedance log is computed. This acoustic impedance was used to compute reflection coefficients at each interface between contrasting velocities. The selected analytical Ricker wavelet was convolved with the reflection series for the entire well survey in order to generate a synthetic seismic trace (Schlumberger, 2014). The synthetic trace was compared to a seismic trace in order to best correlate the well to seismic data, prior to interpretation.

Selected zone tops were imported into Petrel, after which their respective horizons were interpreted. These horizons were mapped as a representation of the lithostratigraphic layers associated with the variation in velocities. The mapped horizons and established well time-depth relation (TDR) were used as inputs for the velocity model.

The velocity model which incorporates the V0, K and Z values was used in this study. This model is represented by $V = V0 + K*Z$ (Slotnick, 1936). The model was built using Petrel 2014. V0 and K values were calculated using the software by means of plotting the velocity profile against depth, where each selected zone was treated independently.

The model V=V0+K*Z explains that at each point in an interval, the velocity at that point is V0+K*Z (Schlumberger, 2014).

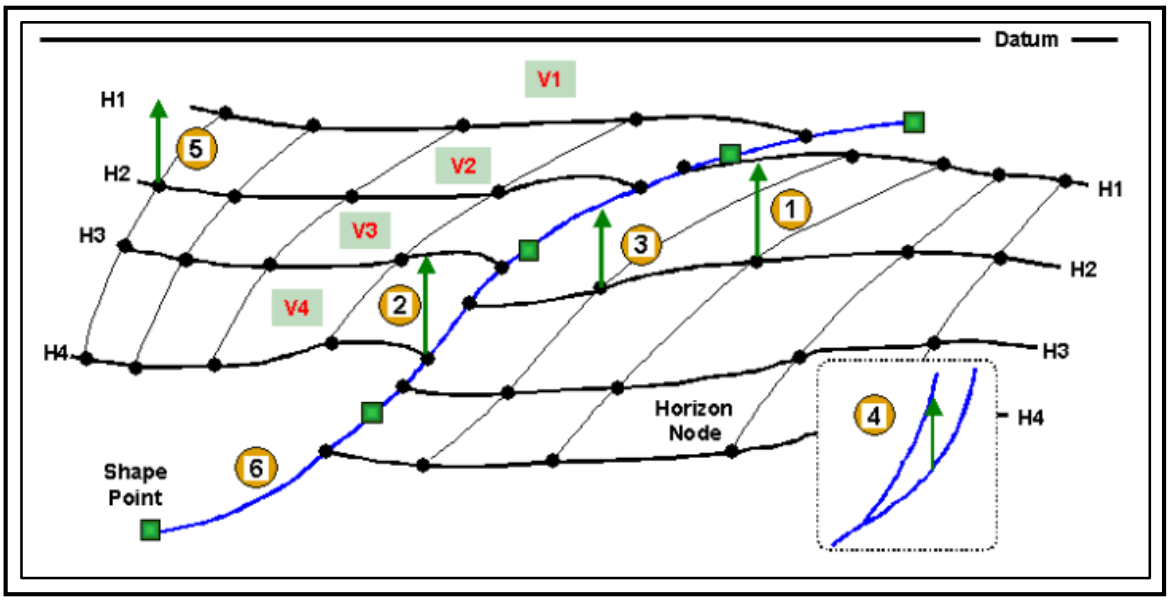

Figure 11: The figure above displays the depth conversion of different nodes of the horizons using the linear velocity algorithm (Schlumberger, 2014).

The incorporation of these zones and respective V0 and K values were used in the model in order to construct such a model that is representative of the subsurface geology.

3.2 Seismic Facies Analysis

The primary objective for carrying out the seismic facies analysis was to bring about an understanding between the relationship of the seismic reflector patterns within the selected zones of interest, the geology and the variation in velocities.

The significant variation in velocities marked at the top of each zone followed by a constant vertical gradient for each zone should be linked to a certain type of deposition, rate of deposition or the variation in inter-depositional systems, related to distinct seismic reflector patterns and reflector amplitudes within each zone.

These seismic facies were characterized based on the reflector amplitudes and patterns so as to understand the response of these facies to the variation in velocities.

3.3 Log and Lithology Analysis

The principal objective for this analysis was to describe the configuration of the lithologies within each zone and its relation to the variation in velocities. This analysis is also carried out to understand how significant the responses of velocities are to the change in certain lithologies, either in terms of their lithological or mineralogical make up.

The analysis was carried out using a suite of logs from the well data. These logs include: the gamma ray, density, neutron, sonic, velocity and resistivity logs.

Rider (2002) describes a geophysical well log as the production of a continuous recording of a geophysical parameter along a borehole. This value is usually plotted against depth. These measurements may be spontaneous, such as natural radioactivity (gamma ray log) or induced, such as the formation velocity log (sonic log). Geophysical well logging is essential such that it accounts for the loss of precision when undertaking geological sampling during drilling (Rider, 2002).

The following are descriptions of well logs used in this study as described by Rider (2002).

Gamma ray log: Records the formations radioactivity which emanates from naturally-occurring uranium, thorium and potassium. The simple gamma ray log gives a measurement of the combinations of all three elements while the spectral gamma shows the amount per element. The gamma ray log is used for the identification of lithologies as a result of unique radioactive compositions.

Density log: A continuous record of a formations bulk density. This bulk density is the overall density of a rock including solid matrix and the fluid enclosed in the pores.

Neutron log: A continuous record of a formations reaction to fast bombardment of neutrons. It is a measure of the concentration of hydrogen in the formation and can be used as a measure of the hydrogen richness as well as an indication for the formations porosity.

Sonic log: This log provides a measure of the formations interval transit time, (designated $\Delta t - the\ reciprocal\ of\ the\ velocity$). It is a measure of the formations capacity to transmit sound.

Resistivity log: Simply, the measurement of the formations resistivity, derived from its resistance to the passage of an electric current. This measurement is used to infer the type of fluids present in the formation, since certain formations conduct or resist the flow of current.

3.4 M-Lith and N-Lith Plots

The primary objective for generating the M-N plots was to understand the impact of various mineralogical compositions within the analysed lithologies in order to determine whether the influence on the variation on velocities can be traced to this scale of analysis.

Mineral plots were generated using the three primary porosity logs and were completed based on the created zones from the seismic data. The generation of these plots were completed using software developed by Schlumberger: Techlog. The method in the software computes lithology indicators from the three logs, namely: density, sonic and neutron porosity curves. From these inputs, the software generates the following lithology indicators:

Lithology P $$P = \frac{1 - NPHI}{\Delta t_f - \Delta t}$$

Lithology M $$M = \frac{\Delta t_f - \Delta t}{\rho_b - \rho_f} * 0.01$$

Lithology N $$N = \frac{1 - NPHI}{\rho_b - \rho_f}$$

Lithology A $$A = \frac{\rho_b - \rho_f}{1 - NPHI}$$

Lithology K $$K = \frac{\Delta t_f - \Delta t}{1 - NPHI}$$

The lithology indicators, M and N are extracted from the software in order to generate the mineral plots. The M-N plots are generated by cross-plotting lithology M (y-axis) against lithology N (x-axis) and interpreted using the M-N Schlumberger overlay (Schlumberger, 2014).

CHAPTER 4 – Results

The study undertaken was completed to understand the heterogeneity of the subsurface and to validate it significance in velocity modelling. This subdivision of the chapter presents how the velocity model was built using the desired interval velocities representative of the responses to the geology. This is followed by the investigation of the subsurface heterogeneities and its impact on the velocities.

4.1 Velocity Model

To acquire the velocity profile for well E-AX, sonic data was extracted from the well and was used to calculate the velocities. Using the sonic log data, the formula $(\frac{1}{DT} \times 10^6) \times 0.3048$ was used to convert µs/ft to m/s.

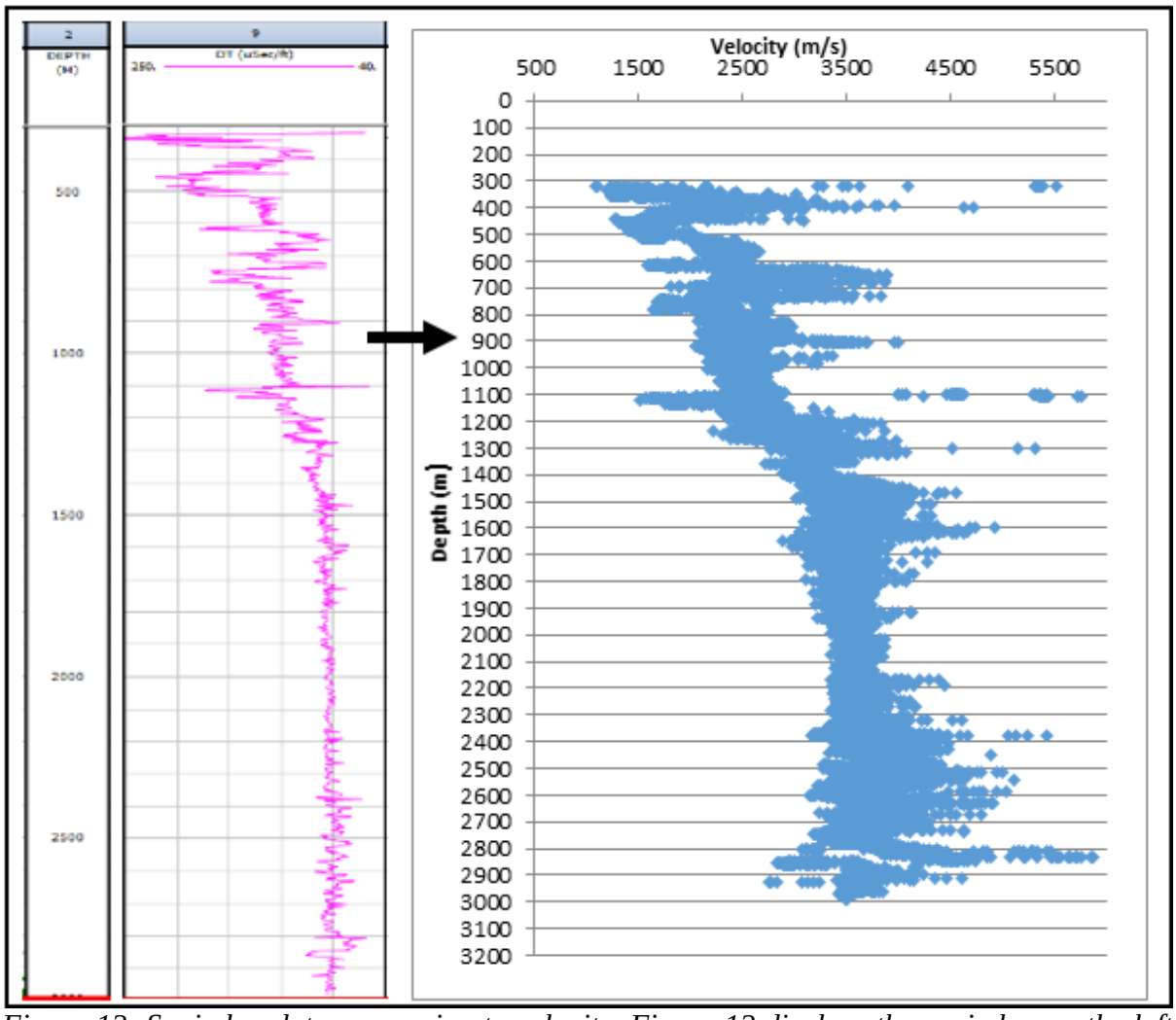

Figure 12: Sonic log data conversion to velocity. Figure 12 displays the sonic log on the left and the velocity profile on the right.

Multiple intervals exhibited by significant variation in velocities (interval velocities) were selected from the velocity profile and were used to build the velocity model. In the general case, a velocity model is built only using targeted intervals such as formation well tops for the sole purpose of depth conversion. In this study, the significant variations in velocities will be used as boundaries (characterized into zones) for the model which ideally respects the possibility of an existing heterogeneous subsurface.

Using the velocity computation file acquired from the well data, a linear relationship between TWT (2TC- Two way vertical time) and depth was established by means of cross plotting these two data sets. This was completed in order to determine respective TWT positions of the selected interval velocities, as determined from the velocity vs. depth graph.

Table 1: Table of measured depth and correlating two-way time from the graph of two-way time vs. depth.

E-AX	
MD	TWT
300	313
400	399
500	502
600	592
700	672
800	762
900	846
1000	930
1100	1012
1220	1105
1325	1175
1425	1238
1525	1298
1625	1356
1725	1418
1825	1476
1925	1533
2025	1591
2125	1645
2225	1705
2325	1763
2425	1813
2525	1872
2650	1940
2700	1966
2780	2013
2900	2076
2975	2120

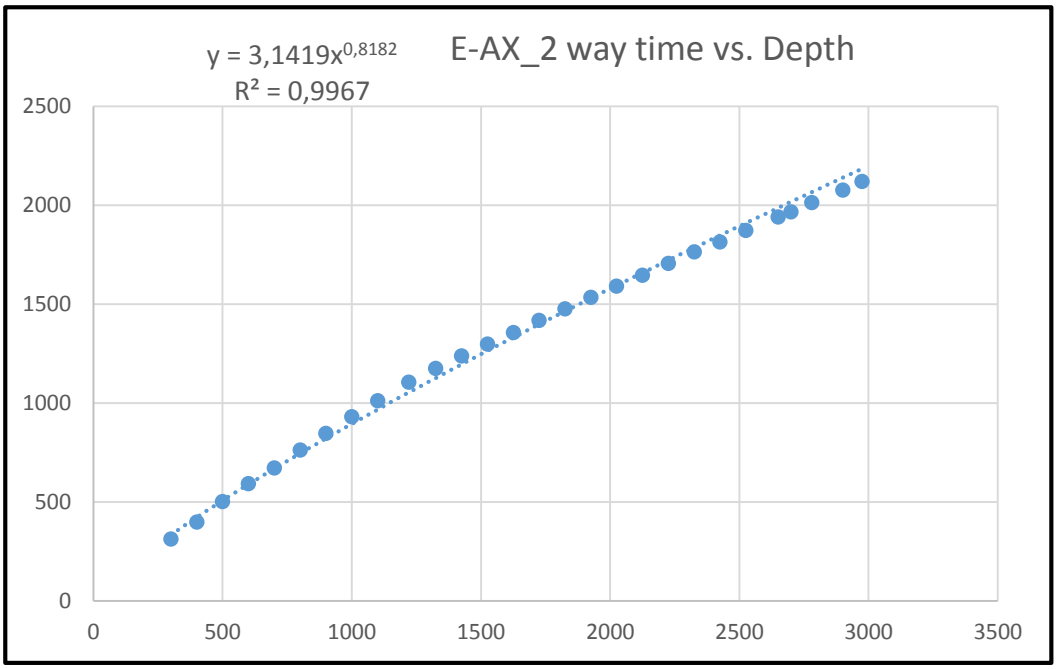

Figure 13: Graph displaying relationship between two-way time and depth as collected from the velocity computation data.

Upon establishing the relationship between the depth and TWT, using the expression $y = 3.1419x^{0.8182}$ it is possible to determine from this relationship a TWT point at any depth position within the well. This is done in order to extract key velocity changes from the velocity profile and calculate its TWT point from a depth at which the specific velocity measurement was selected. The result of this relationship is represented by a correlation coefficient of 0.9967.

The substantial variation in velocities from the velocity profile were characterized into zones. These zones were characterised by a significant variation in velocity at the top following a unique gradient, K.

Figure 14: Velocity profile subdivided into zones representing distinct trends. Zones are headed in accordance of velocity responses with depth.

Surfaces/horizons were constructed using the tops of each zone characterized from the velocity profile and were utilized as inputs for the velocity model.

Figure 14 displays the entire velocity profile from which the selected velocity zones were identified. It can be expected that these zones, exhibited by distinct patterns in velocity are a response to various lithological boundaries, seismic facies, or the mineral composition of the lithologies present.

Table 2: Two-way time extraction from depth using the expression: (y=3.1419x^0.8182).

Zone	Depth (m)	TWT (s)
A	335.64	365
B	433.14	450
C	515.56	520
D	627.45	610
E	751.02	707
F	859.76	790
Fa	949.39	857
G	1076.35	950
H	1289.66	1102
I	1430.71	1200
Ia	1681.29	1370
J	2400.23	1835
K	2560.51	1935
L	2763.41	2060

Upon the selection of zones A to L, the individual top depth values were computed into the expression representing the relationship between the two-way time and depth: ($y = 3.1419x^{0.8182}$). The two-way time position could be calculated as a close estimate to the selected depth point. The confirmation of the calculated two-way time position can be appreciated on the seismic where these zone tops position themselves on reflectors that indicate high acoustic impedances or a significant reflection strength represented by the wiggle trace.

These new zone tops are used to construct the surfaces in Petrel for later inputs in the velocity model.

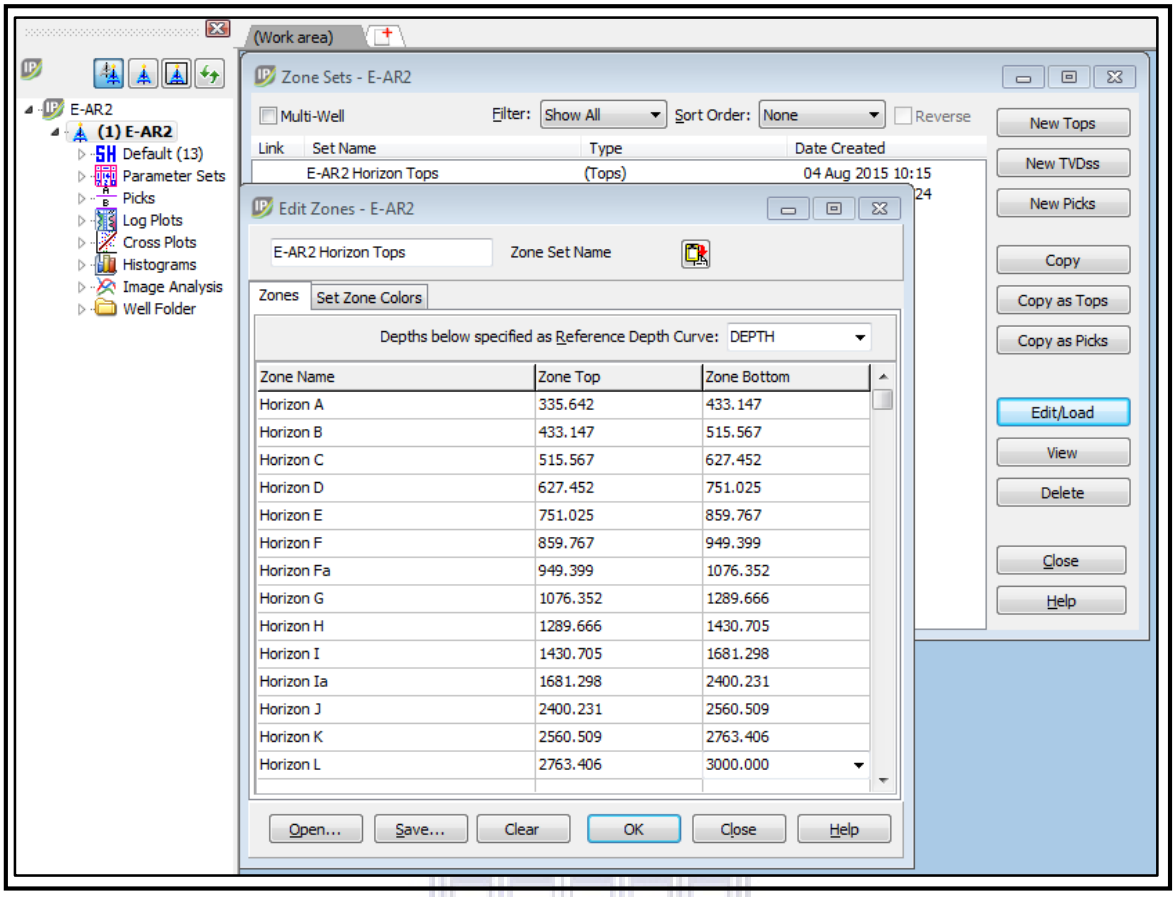

Figure 15: Displays the process of creating the zone tops for input into the modelling software.

These zone tops (figure 15) are converted to LAS format before importing them into Petrel. The creation of these zone tops were completed using the Interactive Petrophysics® software (IP). Once created, the newly created zone tops were saved in LAS format. Data imported into Petrel included the well; seismic; checkshot data and the created zone tops file.

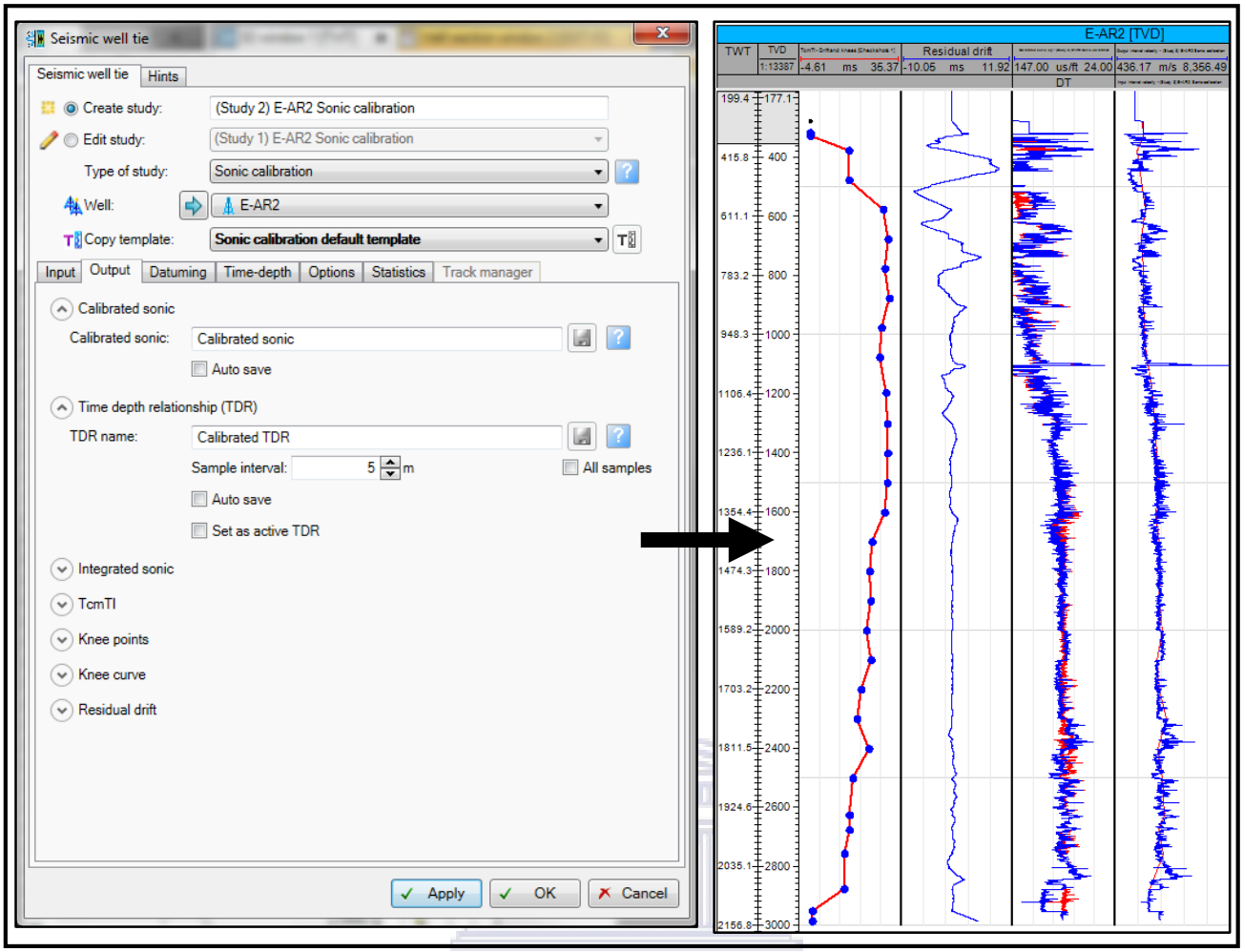

Figure 16: Sonic calibration between the well and seismic data. The left figure represents the window in Petrel used to carry out the time-depth relation (TDR) and the right figure is indicative of the TDR results.

The results display knee points, representative of the checkshot data, calibrated with the continuous sonic log.

In order to establish a representative link between time and depth (TDR), the sonic log was calibrated with the checkshot data (figure 16). Since the checkshot data is acquired at the same time as the seismic data and the sonic data which is collected during logging, it is vital to establish a good relationship between the two. The velocity model in this study will be constructed using the existing time to depth relation (TDR) as established from the sonic and checkshot calibration. This is done to ensure that the zone top correction fits the velocity model after being tied between the well and the seismic.

A synthetic seismogram was generated in order to verify the accuracy of the seismic mapping related to both seismic and well data. The control on the accuracy is achieved by correlating the seismic to the well data. Velocity data as calculated from the sonic log, as well as the density log were used to generate the synthetic seismic trace. This trace closely approximates a trace from a seismic line within the data set that passes through well E-AX where the sonic log was acquired.

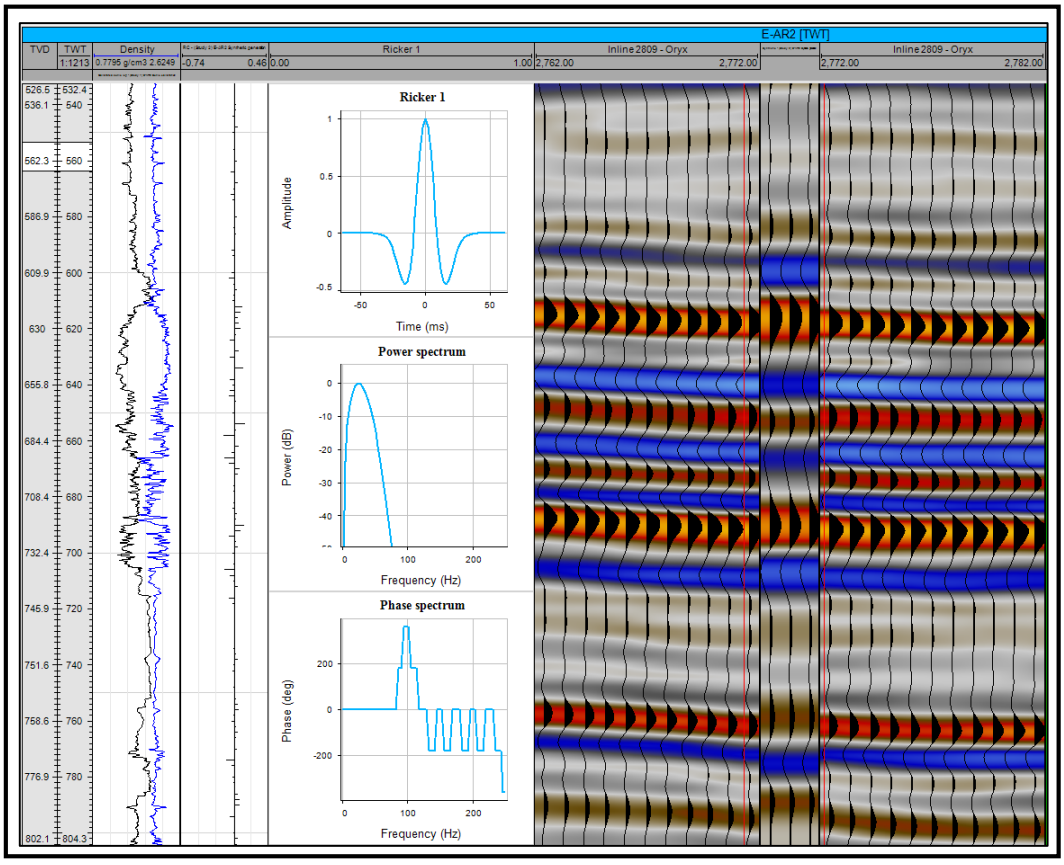

Figure 17: Generation of a synthetic seismic trace, using the analytical Ricker wavelet.

A synthetic seismic trace was generated (figure 17) using the analytical Ricker wavelet. The next figure shows the seismic data at zero-phase wavelet.

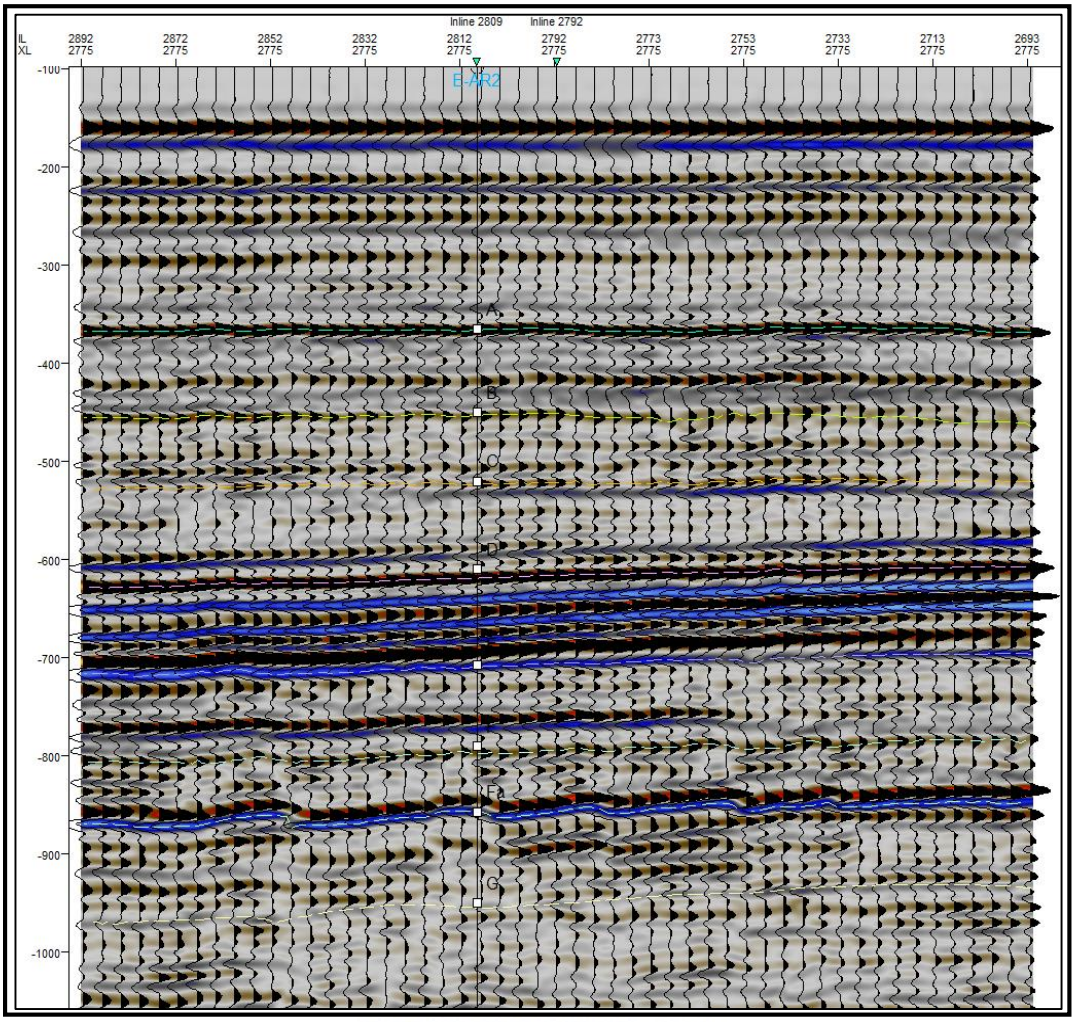

Figure 18: Wiggle traces overlaying a seismic section from the data set.

Zero-phase wavelets are present which show changes in amplitude signatures at the interface of two seismic reflectors (as shown in figure18). Zone tops position where amplitudes vary significantly as shown by the wiggle trace and the brightness in amplitude at each specific zone top. These amplitude reflections could either represent changes in lithology, the mineral composition of these lithologies or the extent of a change in depositional environment that could be derived from a change in seismic facies represented by the seismic data.

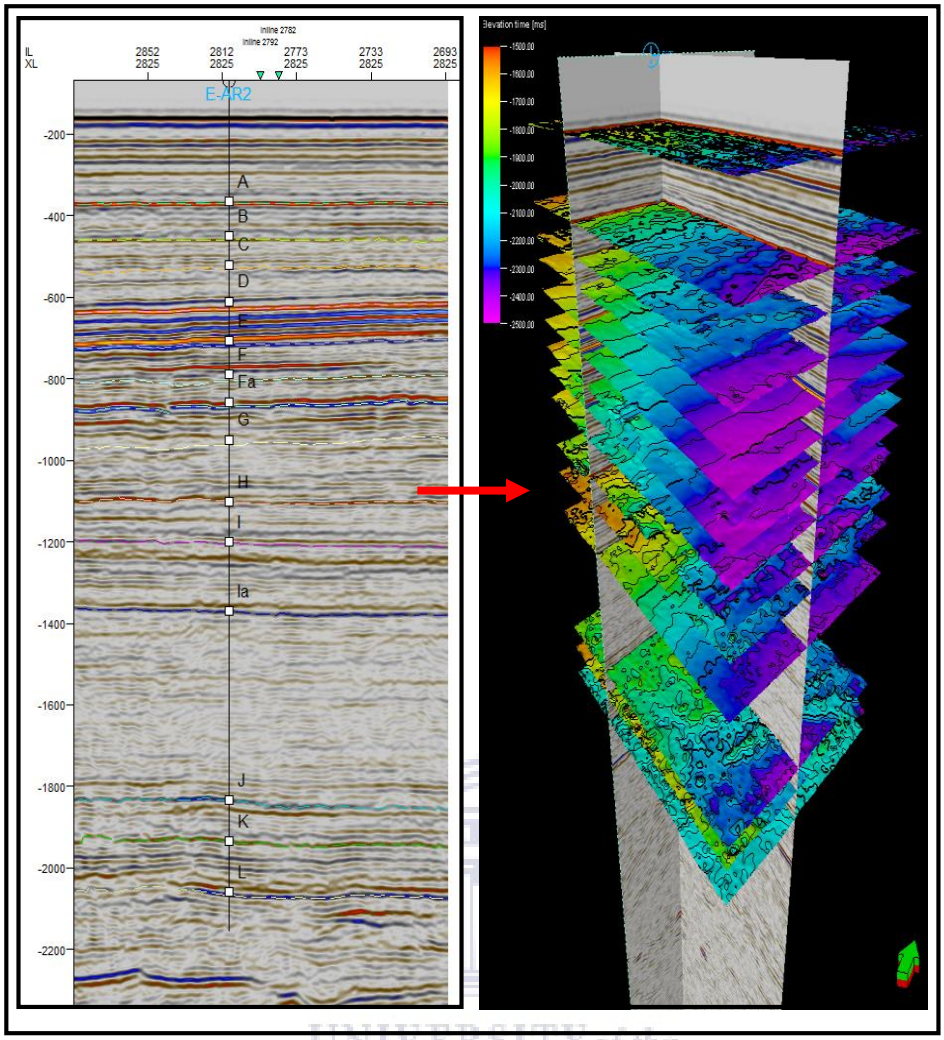

Figure 19: The above figure displays the zone tops tied to the seismic (Figure on the left) and the resultant interpretation of the zone tops as surfaces (Figure on the right).

The zone tops were imported into Petrel as shown above and are seen (figure 19) to correlate with significant amplitudes on the seismic profile. These high amplitudes are representative of the significant variations in velocities that were initially identified using the velocity data plotted against depth. This seismic section together with the heterogeneous distribution in velocities strongly suggests that using velocities taken at formation tops for any depth conversion exercise will not completely respect the heterogeneous nature/behaviour of the subsurface. These significant changes in velocities are mainly due to the heterogeneous nature of the subsurface. The factors responsible for the heterogeneity of the subsurface will be further investigated in this study and its impact on the variation in velocities, ultimately the velocity model.

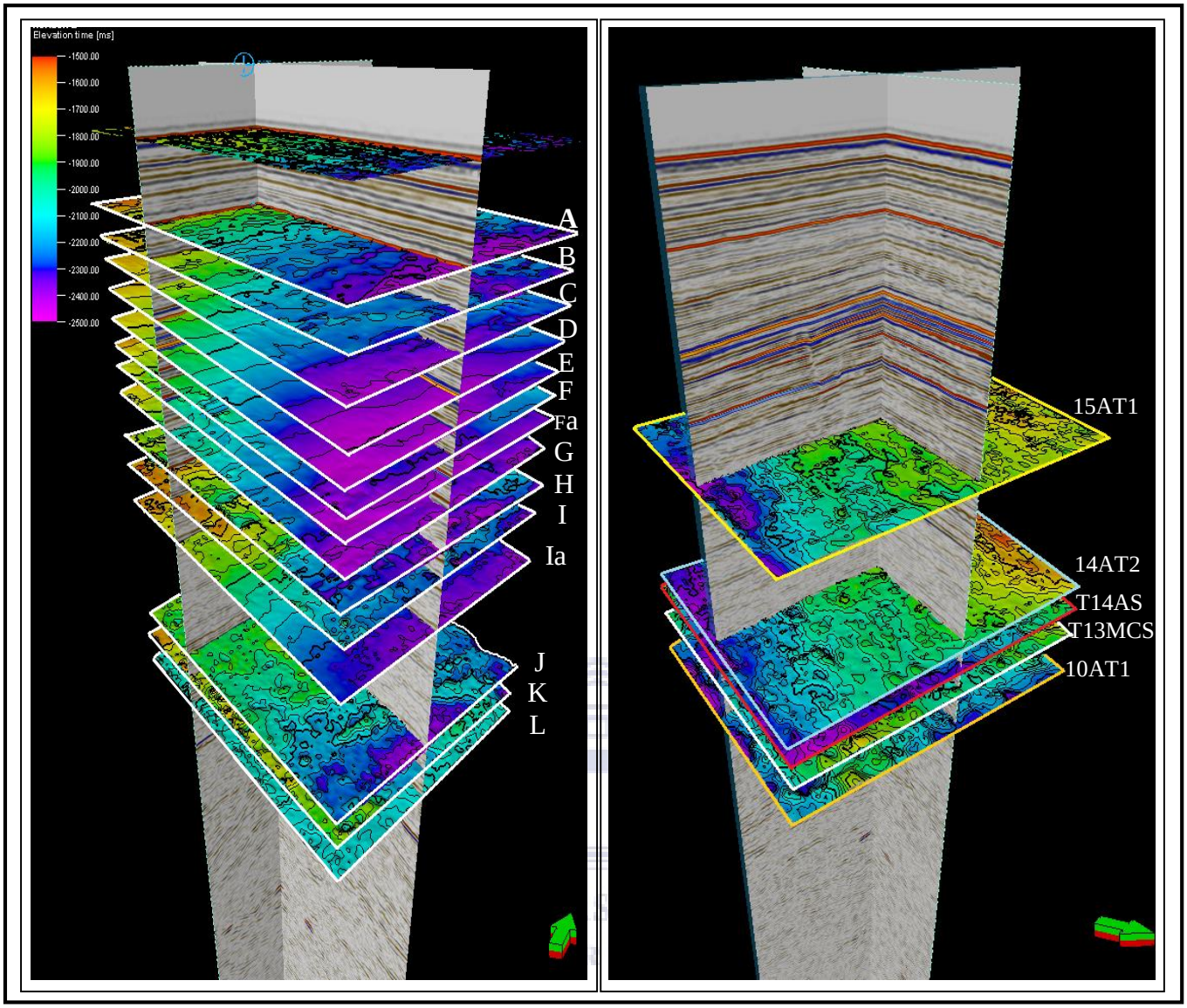

Figure 20: The above figure displays on the left, the surfaces built from the selection of significant velocities representing the zones of interest and the figure on the right is an indication of significant formation well tops recorded within well E-AX.

The figure above (figure 20) is a depiction of the mapped surfaces, so as to bring across an idea of the heterogeneity of the subsurface in terms of velocities (Figure on the left) as compared to the mapped formation well tops as shown by the figure on the right. Formation well tops start from 15At1 (Surface marked by a yellow border) which is the first recorded formation top for well E-AX. The remaining formation well top surfaces are those recorded below 15At1.

Figure 20 also indicates that the velocity model built in this study comprises of velocities that would not be considered when building a velocity model which only takes into account those velocities at the formation well tops.

The velocity model was built using the algebraic expression ($V = V0 + K * Z$), where V0 represents the initial velocity, K represents the constant vertical gradient and Z represents the z-value in depth. Petrel requires the initial velocity V0 and vertical gradient K in order calculate the depth position from these inputs. The V0 and K values were determined by plotting velocity vs. depth in petrel. A 1D (one-dimensional) filter was assigned to this plot to isolate each zone from the plot as a whole. Using the linear function in Petrel, the V0 and K values were determined after filtering each zone individually.

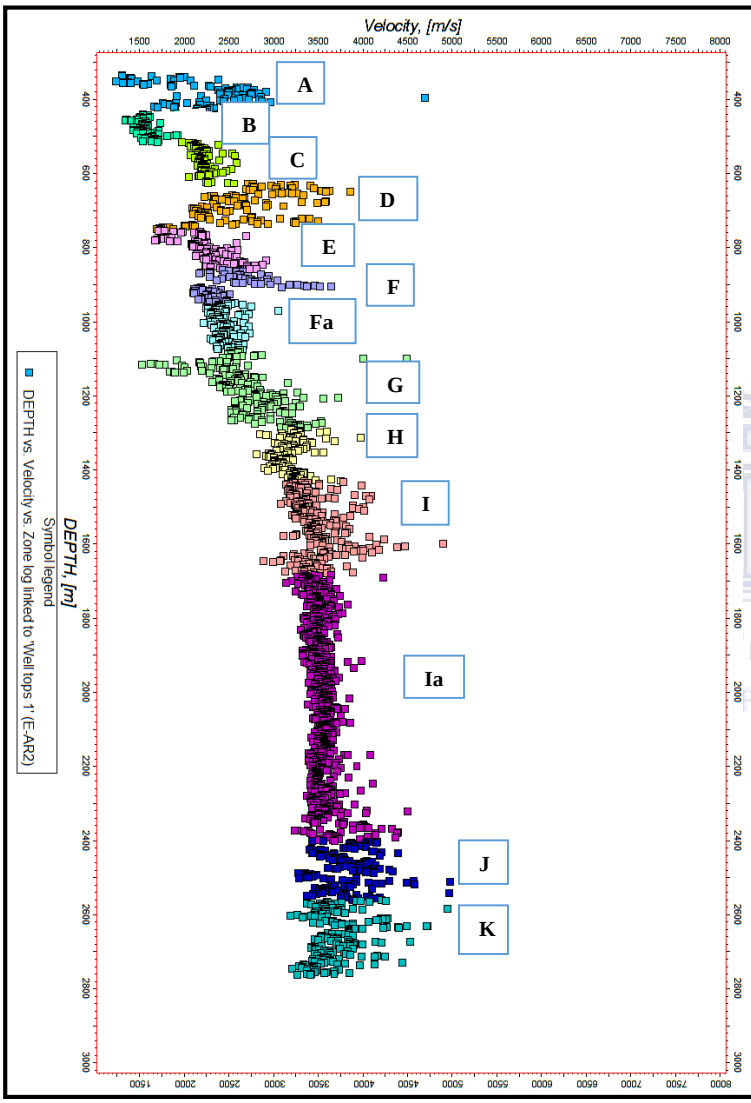

Table 3: V0 and K values extracted from Petrel using a linear function.

Zone	V0 (m/s)	K
A	Vi: 1303.12	/
B	1090.71	1.13581
C	1752.83	1.15560
D	3890.01	-0.74907
E	Vi: 1880.32	/
F	6309.07	-4.17815
Fa	2314.87	0.14668
G	35.6396	2.31052
H	4495.39	-0.94592
I	2404.27	0.69955
Ia	3043.15	0.25211
J	4333.28	-2.07338
K	6792.34	-1.1543

The above table shows the results for the V0 and K values as extracted from each velocity zone from the figure on the left using the linear function in Petrel.

Figure 21: The above figure represents the velocity profile indicating the zones as plotted in Petrel as well as the table on the right displaying the V0 and K values used to build the velocity model.

The velocity model was constructed by means of incorporating the interpreted surfaces representative of the significant interval velocities. The construction of the model included the established TDR, using the zone tops as a measure of correction.

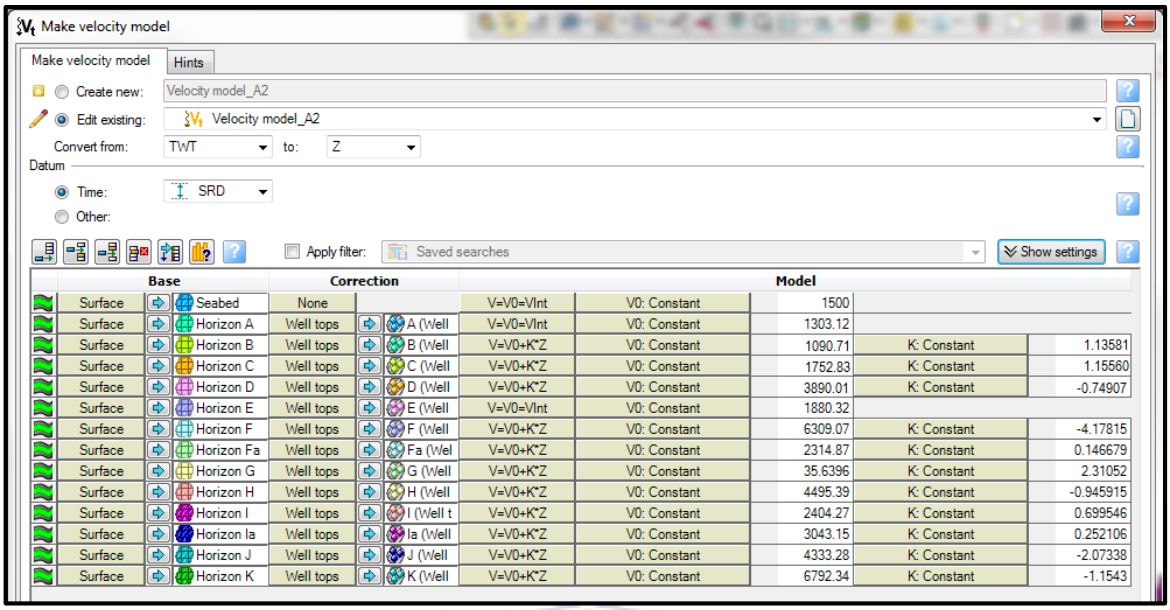

Base			Correction				Model		
Surface	Seabed	None		V=V0=Vint	V0: Constant	1500		
Surface	Horizon A	Well tops	A (Well	V=V0=Vint	V0: Constant	1303.12		
Surface	Horizon B	Well tops	B (Well	V=V0+K*Z	V0: Constant	1090.71	K: Constant	1.13581
Surface	Horizon C	Well tops	C (Well	V=V0+K*Z	V0: Constant	1752.83	K: Constant	1.15560
Surface	Horizon D	Well tops	D (Well	V=V0+K*Z	V0: Constant	3890.01	K: Constant	-0.74907
Surface	Horizon E	Well tops	E (Well	V=V0=Vint	V0: Constant	1880.32		
Surface	Horizon F	Well tops	F (Well	V=V0+K*Z	V0: Constant	6309.07	K: Constant	-4.17815
Surface	Horizon Fa	Well tops	Fa (Wel	V=V0+K*Z	V0: Constant	2314.87	K: Constant	0.146679
Surface	Horizon G	Well tops	G (Well	V=V0+K*Z	V0: Constant	35.6396	K: Constant	2.31052
Surface	Horizon H	Well tops	H (Well	V=V0+K*Z	V0: Constant	4495.39	K: Constant	-0.945915
Surface	Horizon I	Well tops	I (Well t	V=V0+K*Z	V0: Constant	2404.27	K: Constant	0.699546
Surface	Horizon Ia	Well tops	Ia (Well	V=V0+K*Z	V0: Constant	3043.15	K: Constant	0.252106
Surface	Horizon J	Well tops	J (Well	V=V0+K*Z	V0: Constant	4333.28	K: Constant	-2.07338
Surface	Horizon K	Well tops	K (Well	V=V0+K*Z	V0: Constant	6792.34	K: Constant	-1.1543

Figure 22: The figure above shows the process of constructing the velocity model using the V0 and K values as required by the modelling software.

Table 4: Results from the velocity model. Results of the model display the assignment of surfaces to the closest approximation of the z-value as determined from the initial plot of velocity vs. depth.

Velocity model	Velocity model_A2						
User name	user						
Project	Oryx_with logs1.pet						
Date	Thursday, July 09 2015 14:19:31						
From:	TWT [ms]						
To:	Z [m]						
XY:	[m]						
Seabed	**Well**	**X-value**	**Y-value**	**Z-value**	**Horizon after**	**Diff after**	**Corrected?**	**Information**
Horizon A	**Well**	**X-value**	**Y-value**	**Z-value**	**Horizon after**	**Diff after**	**Corrected?**	**Information**
	E-AR2	548992.0	6105754.0	-335.64	-335.64	-0.00	Yes	
Horizon B	**Well**	**X-value**	**Y-value**	**Z-value**	**Horizon after**	**Diff after**	**Corrected?**	**Information**
	E-AR2	548992.0	6105754.0	-433.15	-433.15	-0.00	Yes	
Horizon C	**Well**	**X-value**	**Y-value**	**Z-value**	**Horizon after**	**Diff after**	**Corrected?**	**Information**
	E-AR2	548992.0	6105754.0	-515.54	-515.54	0.00	Yes	
Horizon D	**Well**	**X-value**	**Y-value**	**Z-value**	**Horizon after**	**Diff after**	**Corrected?**	**Information**
	E-AR2	548992.0	6105754.0	-627.45	-627.45	-0.00	Yes	
Horizon E	**Well**	**X-value**	**Y-value**	**Z-value**	**Horizon after**	**Diff after**	**Corrected?**	**Information**
	E-AR2	548992.0	6105754.0	-751.03	-751.03	0.01	Yes	
Horizon F	**Well**	**X-value**	**Y-value**	**Z-value**	**Horizon after**	**Diff after**	**Corrected?**	**Information**
	E-AR2	548992.0	6105754.0	-859.77	-859.77	0.00	Yes	
Horizon Fa	**Well**	**X-value**	**Y-value**	**Z-value**	**Horizon after**	**Diff after**	**Corrected?**	**Information**
	E-AR2	548992.0	6105754.0	-949.40	-949.40	-0.00	Yes	
Horizon G	**Well**	**X-value**	**Y-value**	**Z-value**	**Horizon after**	**Diff after**	**Corrected?**	**Information**
	E-AR2	548992.0	6105754.0	-1076.35	-1076.35	0.00	Yes	
Horizon H	**Well**	**X-value**	**Y-value**	**Z-value**	**Horizon after**	**Diff after**	**Corrected?**	**Information**
	E-AR2	548992.0	6105754.0	-1289.67	-1289.67	-0.00	Yes	
Horizon I	**Well**	**X-value**	**Y-value**	**Z-value**	**Horizon after**	**Diff after**	**Corrected?**	**Information**
	E-AR2	548992.0	6105754.0	-1430.70	-1430.71	0.01	Yes	
Horizon Ia	**Well**	**X-value**	**Y-value**	**Z-value**	**Horizon after**	**Diff after**	**Corrected?**	**Information**
	E-AR2	548992.0	6105754.0	-1681.30	-1681.30	-0.00	Yes	
Horizon J	**Well**	**X-value**	**Y-value**	**Z-value**	**Horizon after**	**Diff after**	**Corrected?**	**Information**
	E-AR2	548992.0	6105754.0	-2400.23	-2400.23	0.00	Yes	
Horizon K	**Well**	**X-value**	**Y-value**	**Z-value**	**Horizon after**	**Diff after**	**Corrected?**	**Information**
	E-AR2	548992.0	6105754.0	-2560.51	-2560.51	0.00	Yes	

The study will now explore the existing heterogeneities within the subsurface which influence the variation in velocities as well as why these heterogeneities should be considered when building the velocity model. The variation in velocities, as analysed by the velocity profile, are the response to these subsurface heterogeneities.

4.2 Seismic Facies Analysis

Lin (2006) describes seismic facies as those packages of reflectors with a set of features differing from adjacent units. The analysis involves examining smaller reflector units that may be the response to lithofacies.

The seismic facies were interpreted according to the zones characterized by the velocity profile. Seismic facies were analysed to compare how variable the selected zones were to each other by means of studying their variation in velocities in relation to the reflector amplitude and patterns.

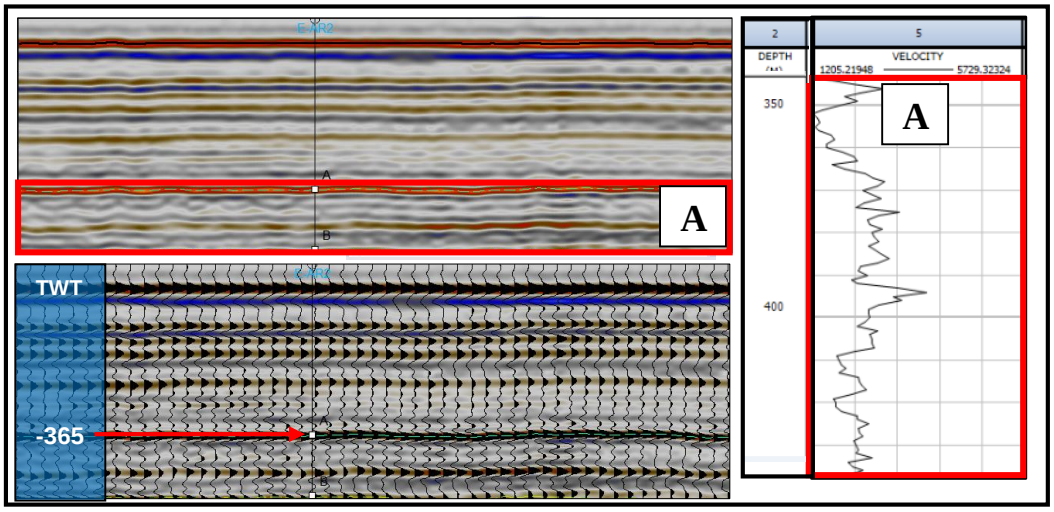

Figure 23: Seismic section displaying zone (A) encircled in red. Velocity profile for zone (A) to the right as well as an overlay of the wiggle traces on the same seismic section.

Zones A to H are located above the first recorded formation top for well E-AX (15AT1). Above zone A, seismic reflector patterns display a dimmed parallel pattern which is suggestive of a uniform depositional rate on a uniformly subsiding surface. The velocities above zone A depict a relatively positive gradient, however do not increase constantly. This is shown on the seismic section by the variation in amplitudes recorded within this zone.

Between zone A and B, the seismic reflectors transition to a sub-parallel pattern, with positive amplitudes dimming below and above the mid-point of this zone. A stronger negative amplitude is found at the mid-point of this zone signifying high acoustic impedance contrasts as a result of a change in velocity and density. The variation in amplitudes can be linked to an increase in velocity and density. This indicates a change in the depositional rate or lithology.

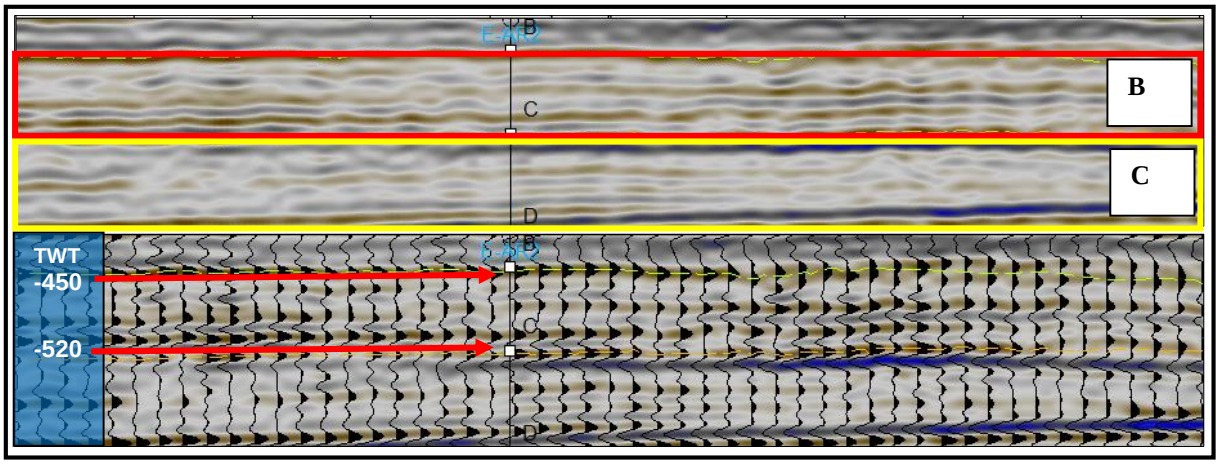

Figure 24: Seismic section displaying zone B and C respectively.

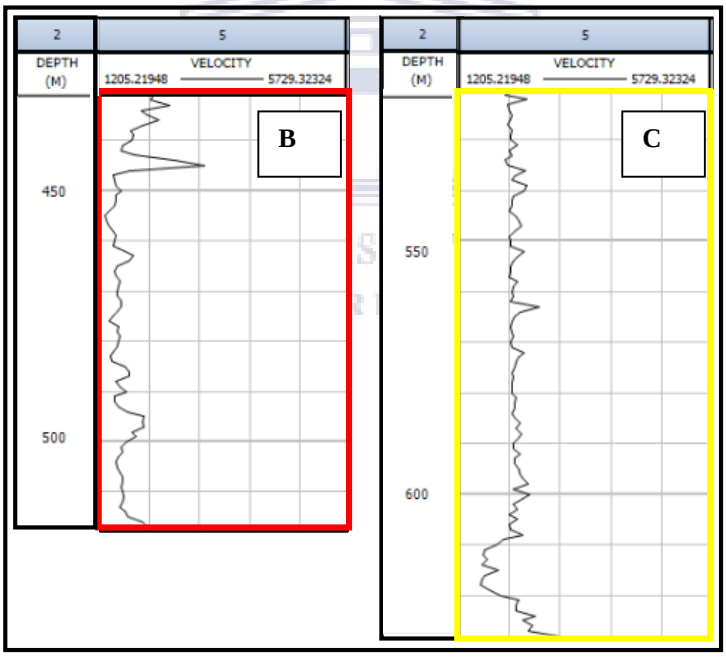

Figure 25: Velocity profiles for zone B and C respectively.

Seismic facies from zone B to the base of zone C exhibits a similar reflection pattern, however amplitude reflections dim with depth. A uniform trend in velocity is represented within this zone, specifically in zone C. Areas of contortion are prominent in zone C. The uniformity of the velocity profile together with the seismic facies suggests a uniform depositional rate. Zone B and C are seen to be quite similar however are different in terms of amplitude reflectivity as well as micro structures such as the contorted seismic reflectors.

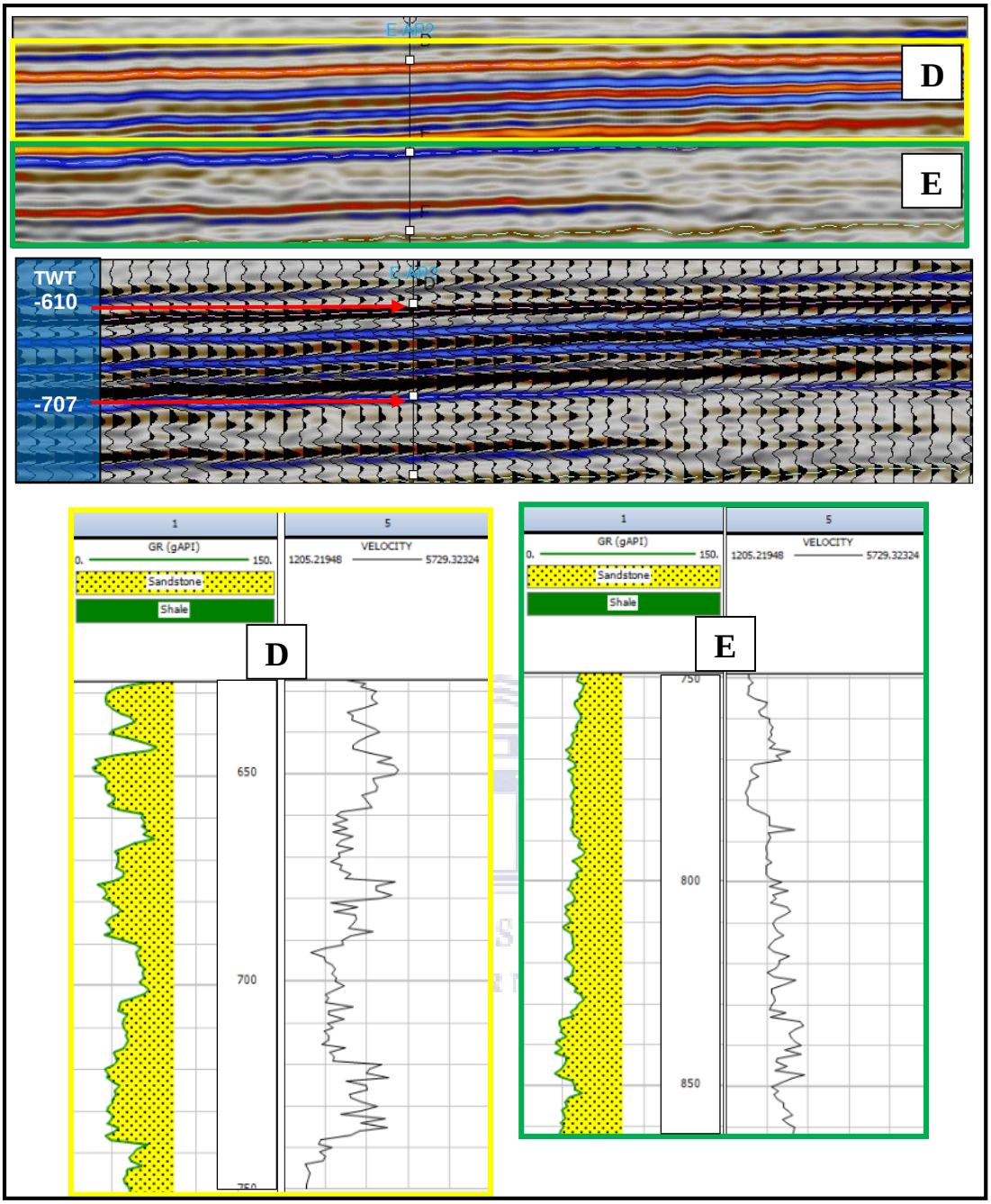

Figure 26: Seismic sections for zone D and E with accompanying gamma and velocity profiles encircled in yellow and green respectively.

Zone D exhibits an entirely different seismic facies in terms of amplitudes and reflection patterns. Amplitude reflections are noticeably brighter with strong parallel reflectors that are highly continuous. Pulses of higher velocities are also noticeable within this zone. The gamma ray log records intervals of thicker coarse sand packages divided by finer sand intervals. Sharp variations in velocities can be attributed to the higher amplitude reflections that is linked to the changes in the composition of lithology present. This type of variation indicates a possible change in the inter-depositional system and may suggest a possible feeder channel on a lobe of

the fan set. The seismic facies represented by zone D is generally interpreted as a marine deposit with the higher amplitude reflections indicative of an increase in depositional rates.

High contrasts in acoustic impedance are characteristic at the top of zone E represented by subparallel seismic reflector patterns. Contorted reflectors are present within zone E as well. Zone E is noticeably less wavy as compared to zone B. The gamma ray log indicates a relatively fining upward sand package. A brighter sub-parallel reflector reveals a strong acoustic impedance contrast within the sand interval, indicative of a change in composition of the sand package. The velocity profile does not vary greatly where there is no significant change in the reflector patterns.

It can be understood thus far that varying rates of deposition are evident and these intervals are represented by significant variations in velocity.

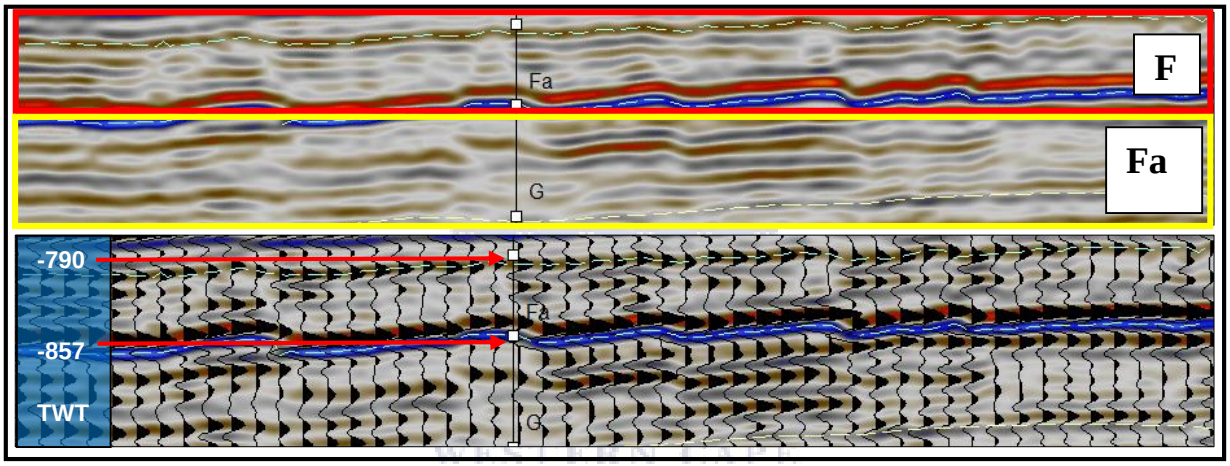

Figure 27: Seismic section and wiggle traces for zone (F) and (Fa)

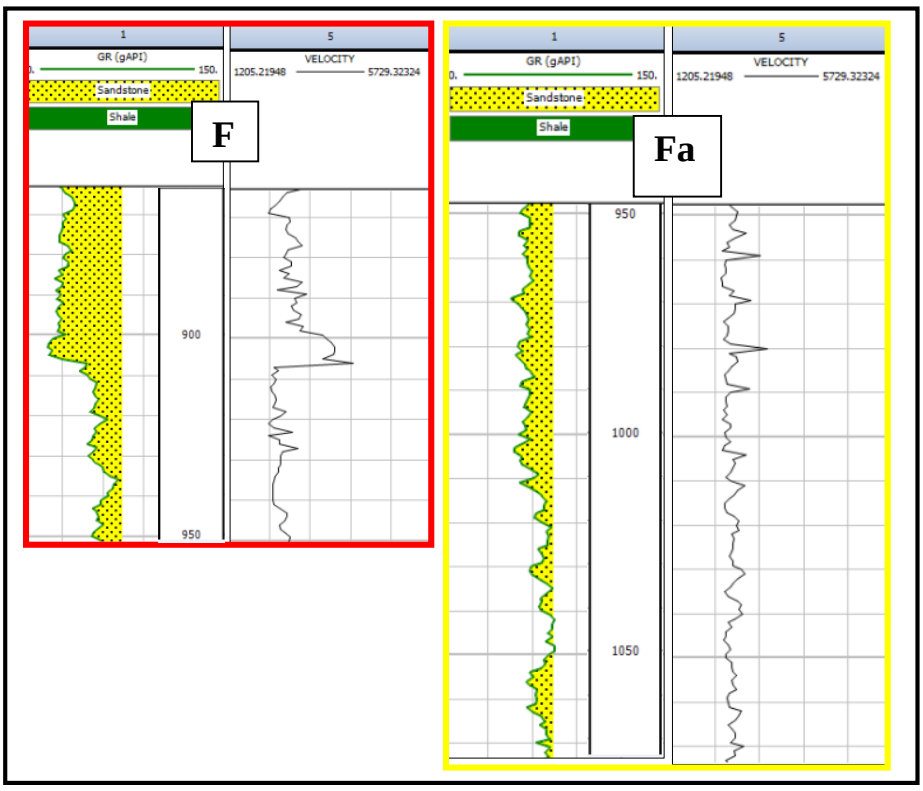

Figure 28: Gamma ray and velocity profiles for zones (F) and (Fa) respectively.

Zone F is characteristic of disrupted sub-parallel seismic reflector patterns that is marked at the top by a brighter amplitude reflection forming the base of zone E. These disruptions may be indicative of a change in lithology or composition. The gamma ray confirms a change in composition, either by grain size or mineral make-up at 935 m. The top of this sand package is marked by a base of channel as shown by the gamma ray at 906 m which is followed by a relatively aggrading sand interval. Lower amplitude reflections within this zone are characteristic of lower depositional rates.

Zone Fa is mapped at a strong change in acoustic impedance and is characteristic of relatively continuous sub-parallel reflectors that are variable in amplitude. The sandstone package as seen from the gamma ray log displays a finer sand package as compared to zone F, which thins out towards the base of zone Fa. Moderate amplitudes in this zone with areas displaying discontinuous seismic reflectors may be structurally related. The variable continuity and moderate amplitude reflections within this zone are indicative of a low deposition rate, however the top is marked by a brighter amplitude in the presence of coarser sand. This is suggestive of a variation in depositional rates.

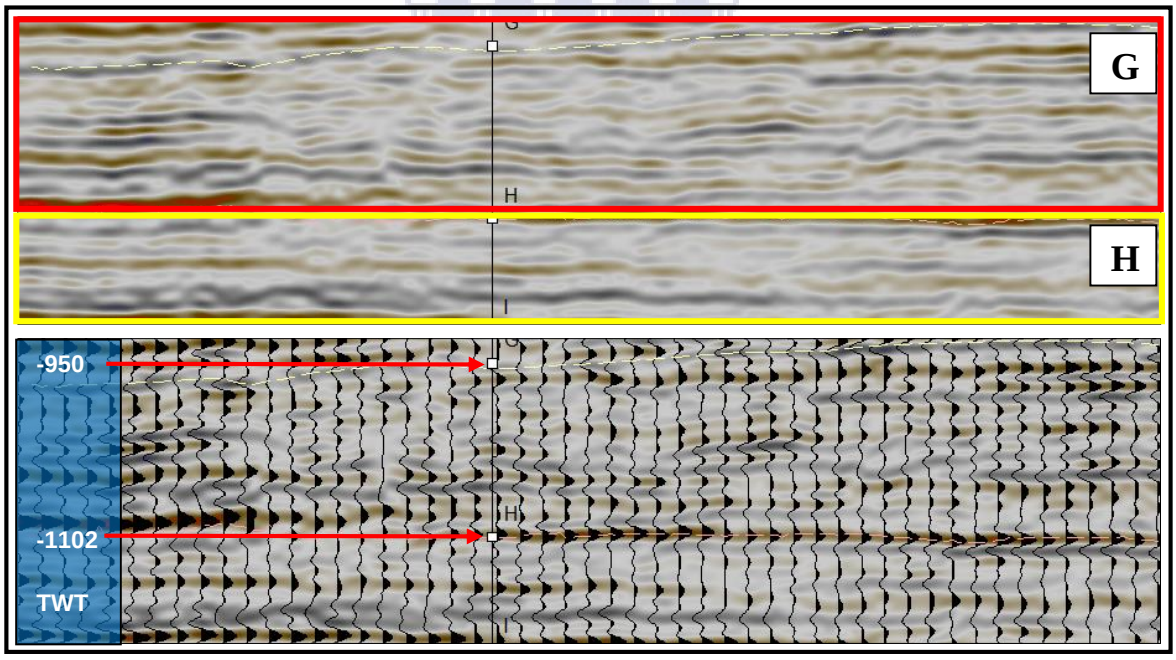

Figure 29: Seismic sections and wiggle traces for zones (G) and (H) respectively.

Zone G is marked by a change in seismic reflector patterns. This zone is characteristic of more hummocky-type features which may be indicative of a possible crevasse splay that diverged from a feeder channel on the fan system. The seismic facies for this zone is represented by a chaotic structure that displays disorganised, discontinuous low amplitude reflections.

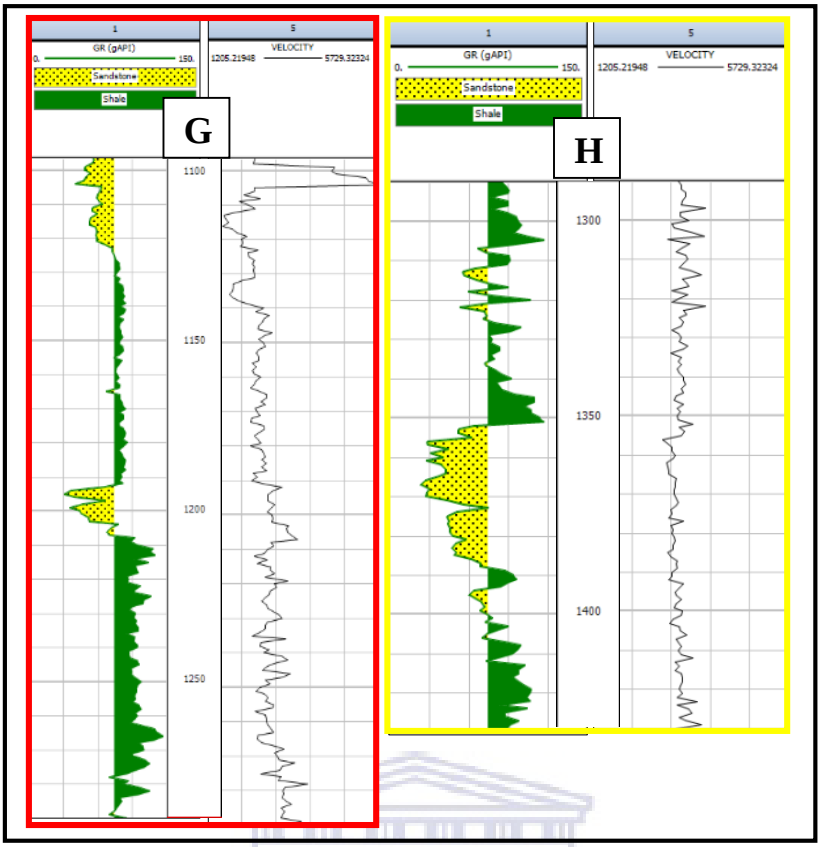

Figure 30: Gamma ray and velocity profiles for zones (G) and (H)

This can be interpreted as debris flow or slump deposition which mainly occurs along the flanks of submarine fans in deeper parts of the basin. The gamma ray log shows an increased concentration of shale sediments. Sharp increases in velocities can be found at the top of zone G, represented by a possible base of channel that is preceded by two shale intervals of varying composition. The velocity profile exhibits a response to this type of deposition.

Zone H is represented by a repetitive seismic facies that can be found in zone E. Low amplitude reflections with sub-parallel reflection features are characteristic of this zone. Amplitudes vary from low to moderate and are thus indicative of a slow depositional rate on a relatively uniform surface. At 1352 m, a change in lithology is observed (Shale to Sand – possible low energy conditions). This is noticeably present on the seismic by an increase in amplitude within zone H. A sudden increase in gamma ray at the top of the sand package indicates the change in deposition and energy in the system. Chaotic features are present to the east of zone H, which may be indicative of a turbidite channel fill. This is supported by the thickness of the sand interval that indicates a possible channel fill overlain by shaly deposits. Velocities are fairly

constant in the sand package, however varies greater in the shale interval as well as at the interface between the shale and sand sediments.

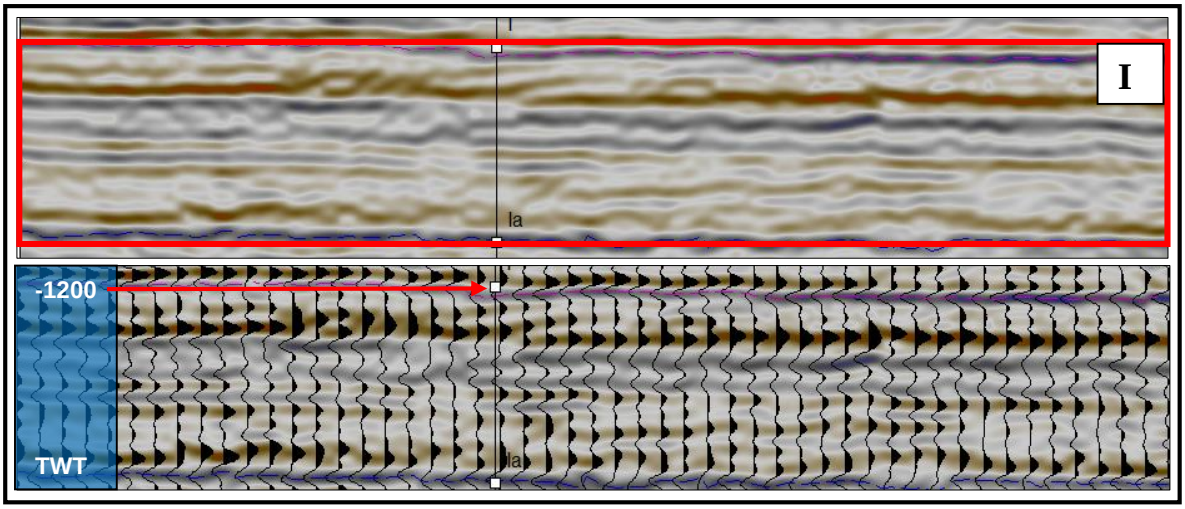

Figure 31: Seismic section and wiggle trace for zone (I)

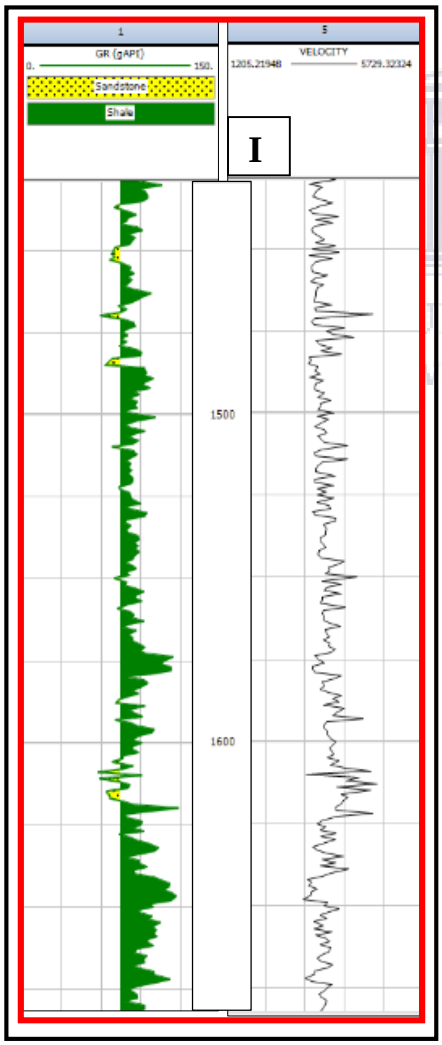

Zone I is representative of seismic facies which vary slightly from that observed within zone H. Seismic facies found within zone I display sub-parallel reflector patterns, however with the presence of prominent wavy reflectors. Amplitudes reflections are fairly low in zone I, except where changes between shale and silty sand sediments are present. These facies represent slow depositional rates on a uniformly subsiding surface, again however, a different trend in velocities are evident in the shale sediments as compared to the sand packages. The variable amplitude strength characteristic of this zone is a measure of varying depositional rates as well as lithological changes. This variation is evident by examining the gamma and velocity profile for zone I.

Figure 32: Gamma ray and velocity profile for zone (I)

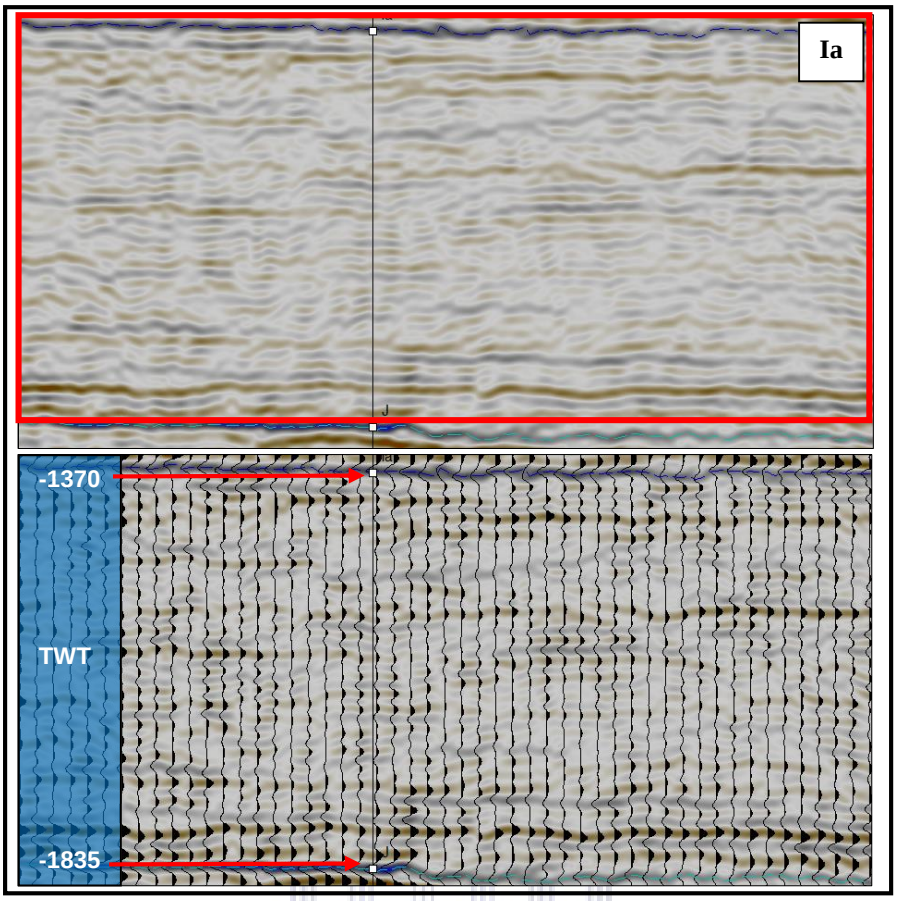

Figure 33: Seismic section and wiggle trace representative of zone (Ia).

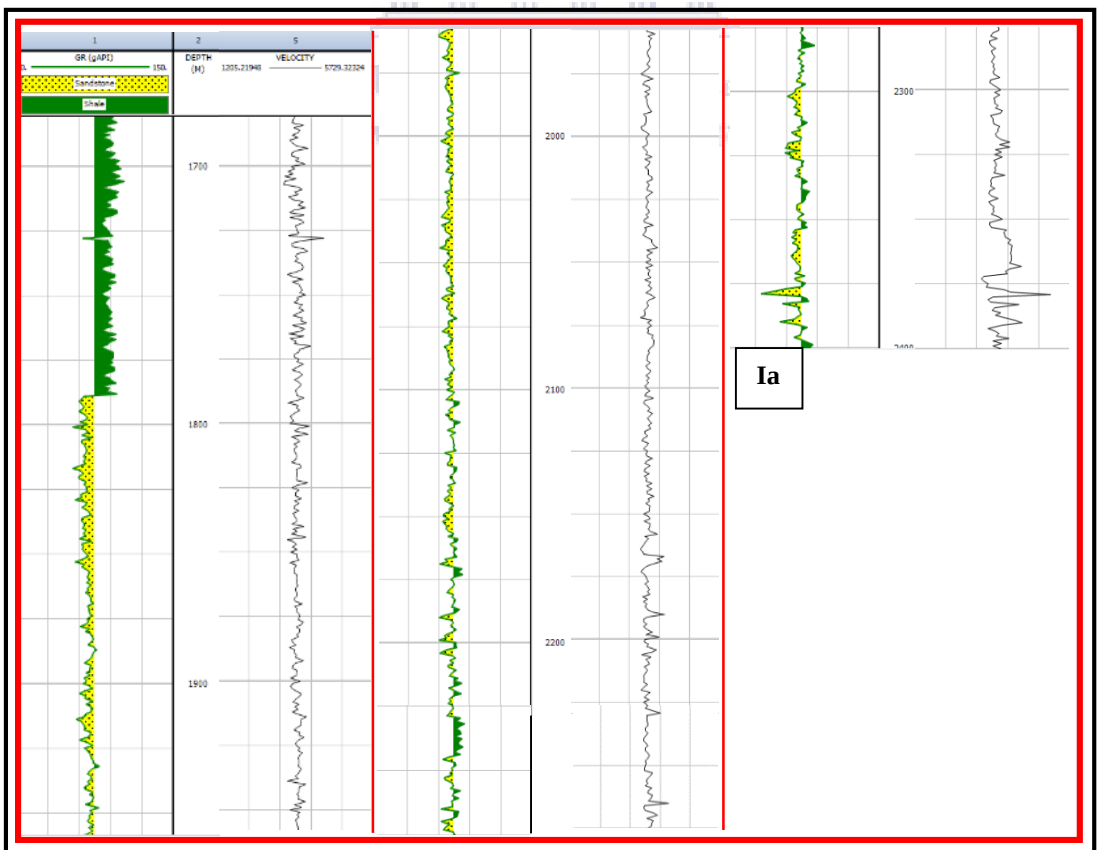

Figure 34: Continuous gamma ray and velocity profile for zone Ia.

Zone Ia displays an entirely different seismic facies that is predominantly chaotic. The reflectors are less continuous and the entire zone is characteristic of very low amplitude reflections. The seismic reflectors exhibit contortion as well. Contorted features indicate shale prone debris flows, which are evident between 1675 to 1780 m on the gamma ray within this zone. The contorted seismic features are evident above the top half of zone Ia. The lower half of zone Ia is characteristic of more chaotic features which may indicate coarser sediments or a turbidite channel fill deposit. The gamma ray reveals that the upper section of zone Ia is predominantly shale sediments that is preceded by a lower gamma ray interval indicating a sediment type that is coarser than the shales above it. The silty-sand package is very continuous and deposited at a slow depositional rate, as presented by the low amplitude reflections on the seismic section. Velocities are fairly constant throughout the silty-sand interval however sharply increase at the base of zone Ia.

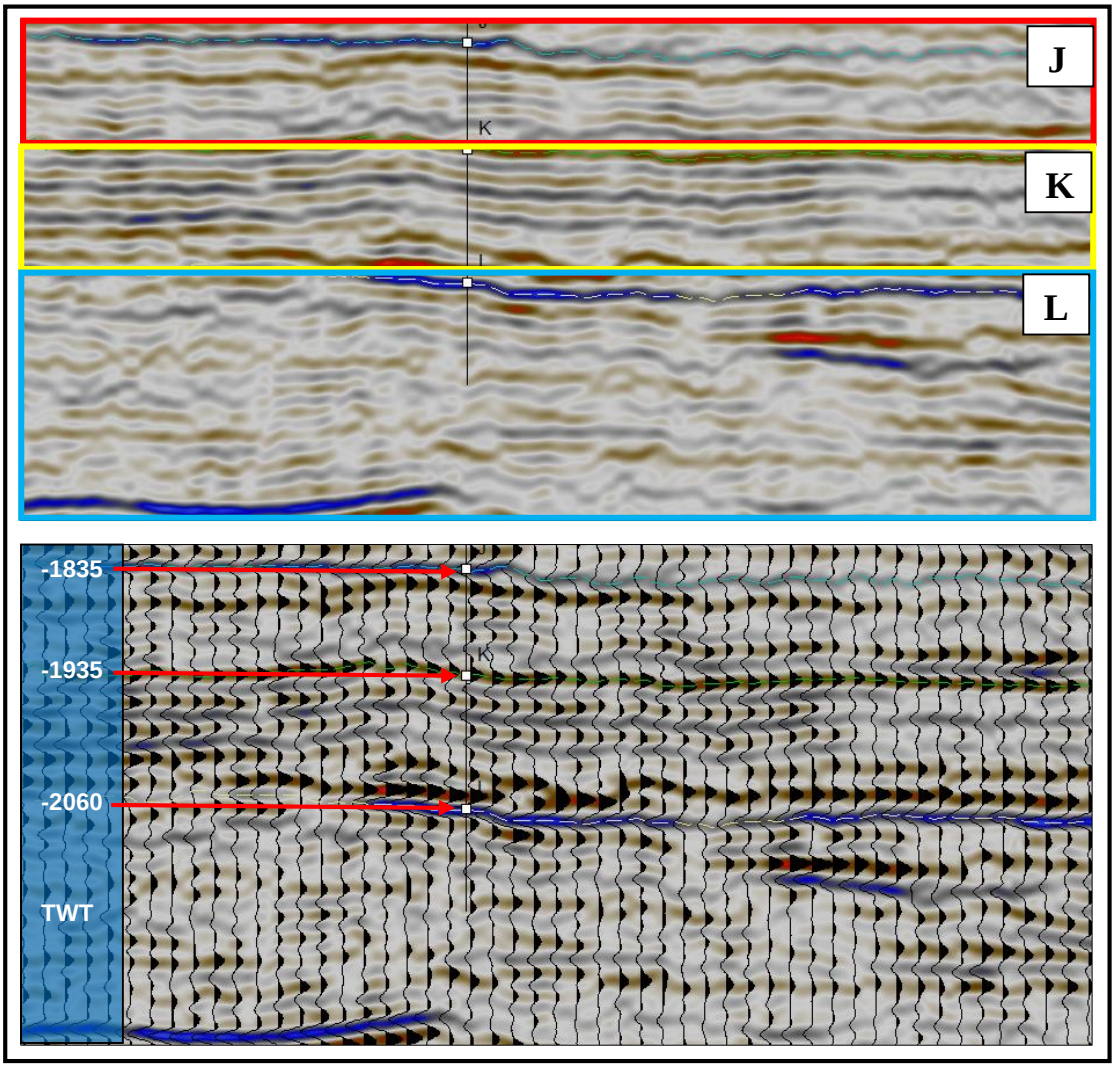

Figure 35: Seismic sections of zones (J), (K) and (L) with their accompanying wiggle traces below.

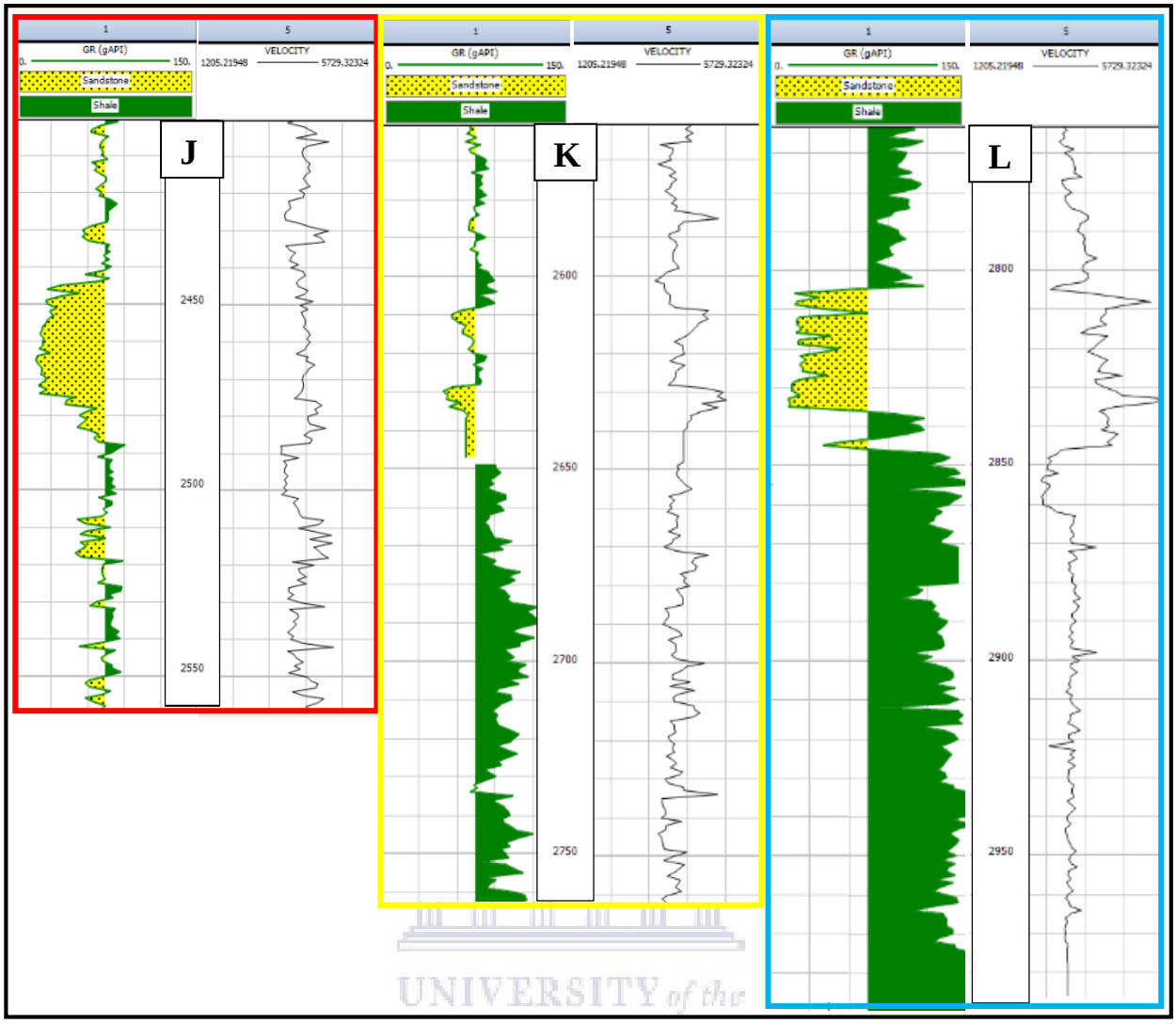

Figure 36: Gamma ray and velocity profiles for zones (J), (K) and (L).

Brighter amplitudes are represented at the top of zone J. This amplitude change is related to a significant change in velocity. Slow depositional rates are indicative of this zone and are suggestive of a debris flow followed by low energy deposition. Sub-parallel facies with chaotic features are also present in this zone. Zone J is characteristic of a thick sand package that can be seen from the brighter amplitude reflection on the seismic as well as on the gamma ray log. This may indicate a higher deposition rate by a possible coarser sediment channel fill deposit. Velocity trends are noticeably different within these packages.

Zone K is representative of brighter amplitude reflections that show more well-defined sub-parallel seismic reflector patterns near the top and chaotic features at the base of zone K. Velocities vary continuously within this zone due to the top of zone K being intercalated with sand and shale intervals. The upper section of zone K is indicative of higher energy level depositional rates that is preceded by turbiditic deposits. The gamma ray provides supporting

evidence to the type of deposition within zone K. This type of deposition can be found along flanks of submarine fans. This zone is also characteristic of discontinuous reflectors which may be indicative of a possible crevasse splay.

Zone L is representative of highly discontinuous seismic reflectors with predominant chaotic features. A sharp change in velocity can be found at the top of zone L that represents a possible change in inter-depositional systems. Zone L is characteristic of a ~40 m thick sand package that represents a distinct trend in velocity as compared to the sediments above and below it. These shale deposits explain the chaotic features found within this zone and may be related to slump or debris flow along flanks of the fan system, mainly made up of finer deposits. The chaotic features of zone L are very similar in structure to that of zone Ia, however differences in the amplitude reflections are due to varying depositional rates and lithologies. The trend in velocity is very similar in both zone Ia and L represented by low amplitude reflections.

The overall depositional environment for this study is a submarine fan set, however it is evident by studying the heterogeneity of the seismic, that multiple inter-depositional systems are present. These variations in seismic facies are the result of many inter-depositional systems which ultimately impact on the significant variations in velocities as shown by the velocity profile.

4.3 Log and Lithology Analysis

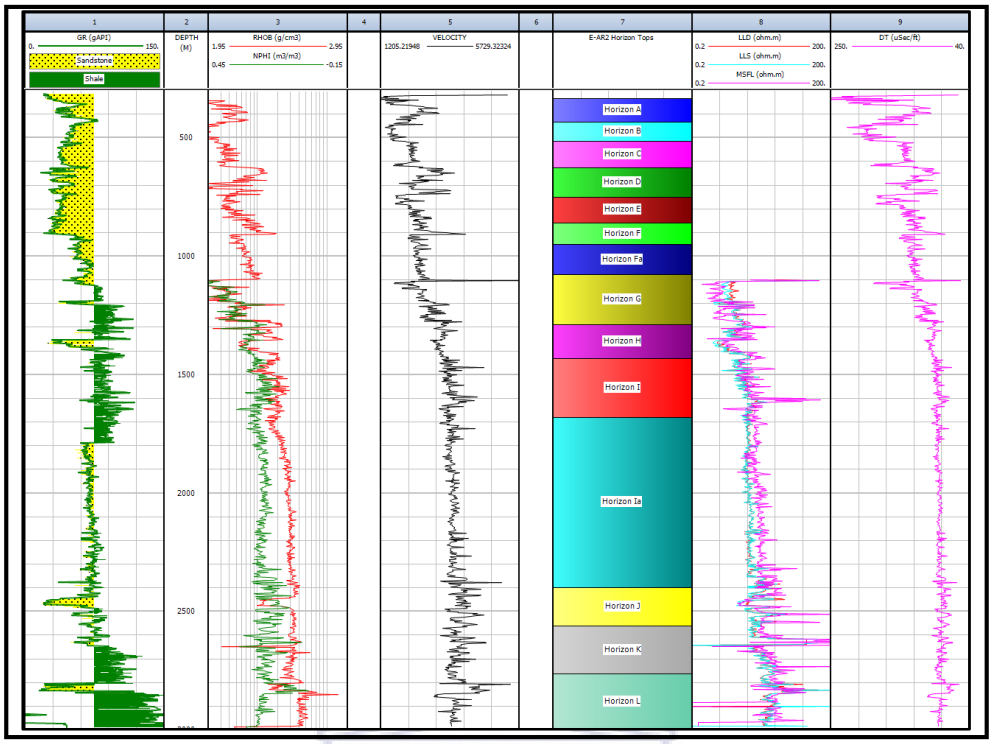

Figure 37: Complete well view displaying wireline logs used, as well as zones (A) to (L).

Lithology and log descriptions are studied per zone for this section of the chapter.

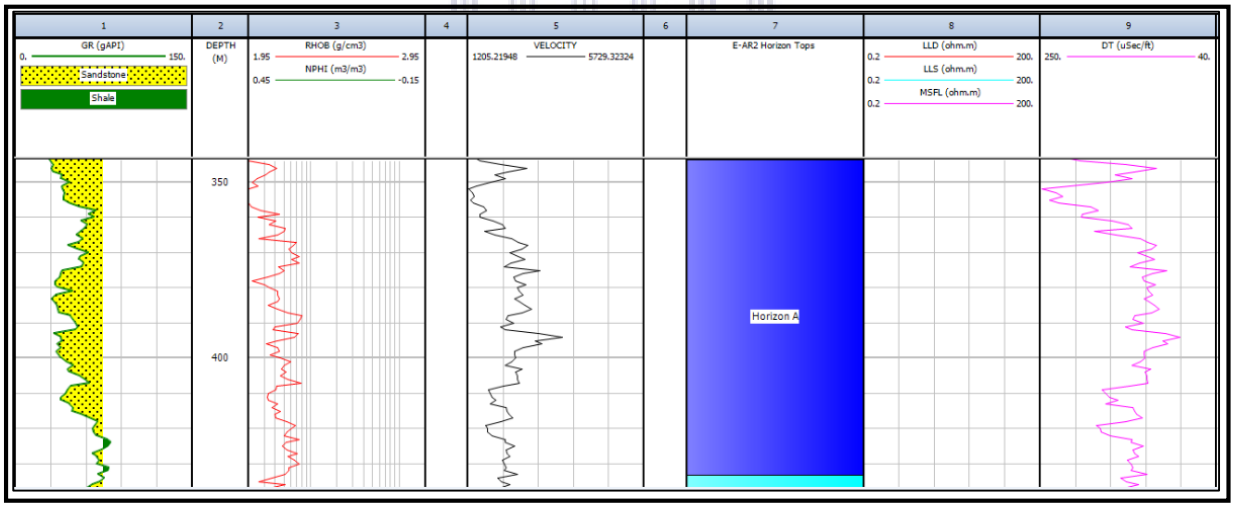

Figure 38: (Left to Right) Gamma ray, density, velocity and sonic logs representative of zone (A).

Increased velocities (~5356 m/s) are found at a depth of 319m that is coupled with a higher sonic reading. These results together with the gamma ray indicate the presence of a sandstone package. A general sharp increase in velocity can be noted with densities averaging 2.092g/cm. At approximately 390 m, velocities are noticeably higher within the sandstone package as compared to the base of zone (A). This may be an indication that the sandstones at this depth

are composed of quartz minerals other than clay minerals such as feldspars. Quartz minerals are harder, hence a higher velocity can be expected.

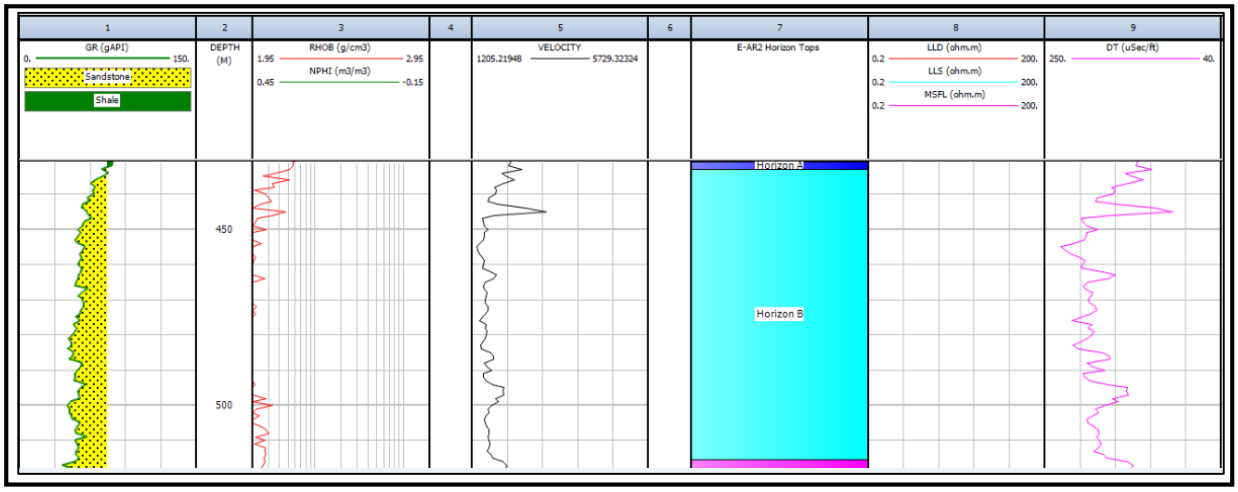

Figure 39: (Left to Right) Gamma ray, density, velocity and sonic logs representative of zone (B).

Zone B is representative of a lower velocity trend, however shows a positive change in velocities with depth. A change in velocity is noted at the interchange between zone A and B where the sandstone unit is divided by a thinner shale package. A sharp increase in velocity is recorded at 445m, although within the sand package, this may be indicative of a mineralogical change causing a sharp variation in velocities. A relatively uniform unit of sandstone below 445m does not show any erratic change in velocities for this zone. These velocities increase from ~1623 to 2011 m/s.

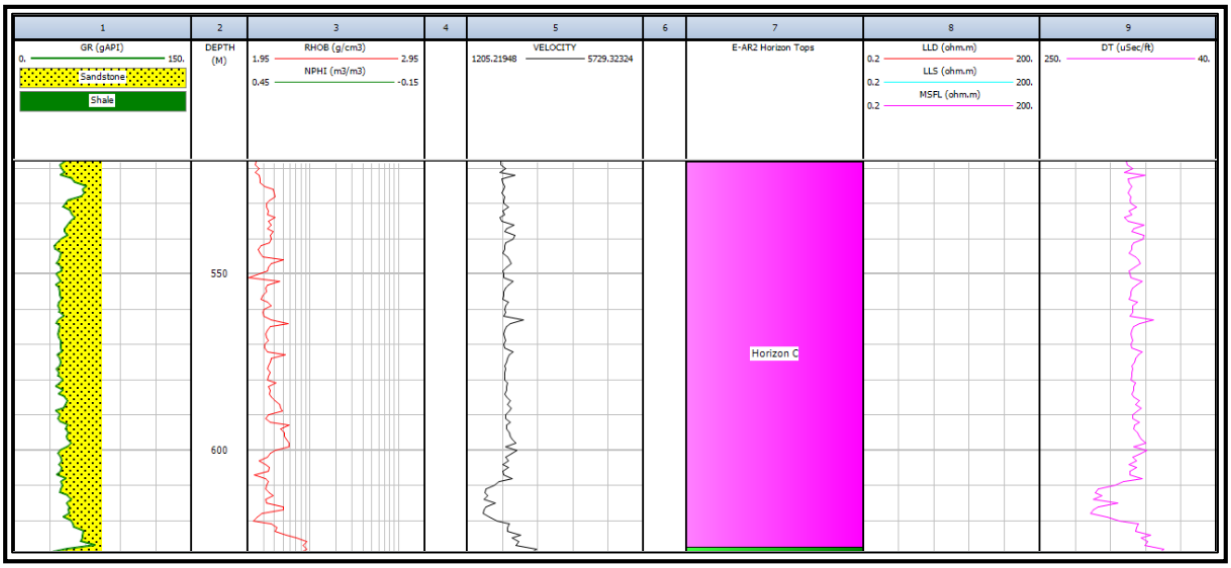

Figure 40: (Left to Right) Gamma ray, density, velocity and sonic logs representative of zone (C).

This zone is representative of a uniform sand package where distinctive variation in velocities are only eminent where lithologies become finer at the base of zone C. Zone C is a sand unit that is connected to zone B however shows a relatively higher constant velocity (~2400 m/s). These variations in velocities are possibly due to mineralogical changes. Feldspathic sandstones are characteristic of lower densities as compared to quartzitic sandstones. The variation in velocity within the same sand unit can be attributed to its mineral composition.

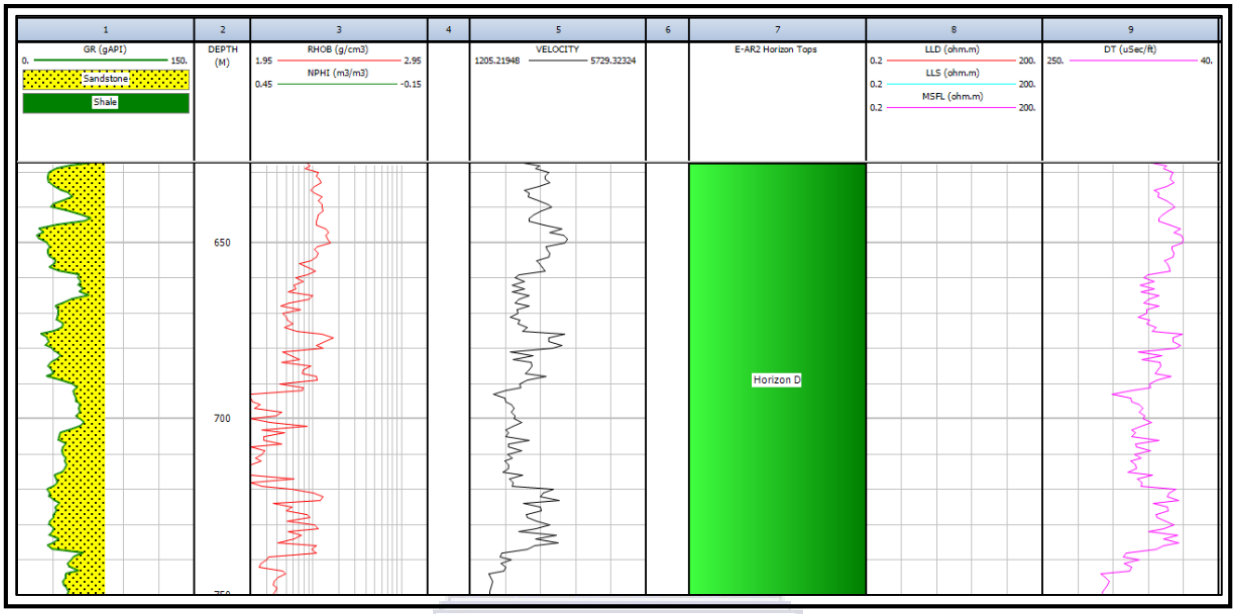

Figure 41: (Left to Right) Gamma ray, density, velocity and sonic logs representative of zone (D).

Zone D is marked by an increase in velocity that is strongly supported by changes in the gamma ray log. This change in velocity, as shown by the gamma ray log confirms a strong change in the composition of the sandstone unit. These sandstone units represent pulses of coarser sediments followed by deposition of finer sediments. Erratic changes in velocities within this zone is linked to the continuous change in configuration of the sandstone package, either becoming more fine or coarse grained. Sharp increase in velocities reach a maximum of 3640 m/s within the sand unit.

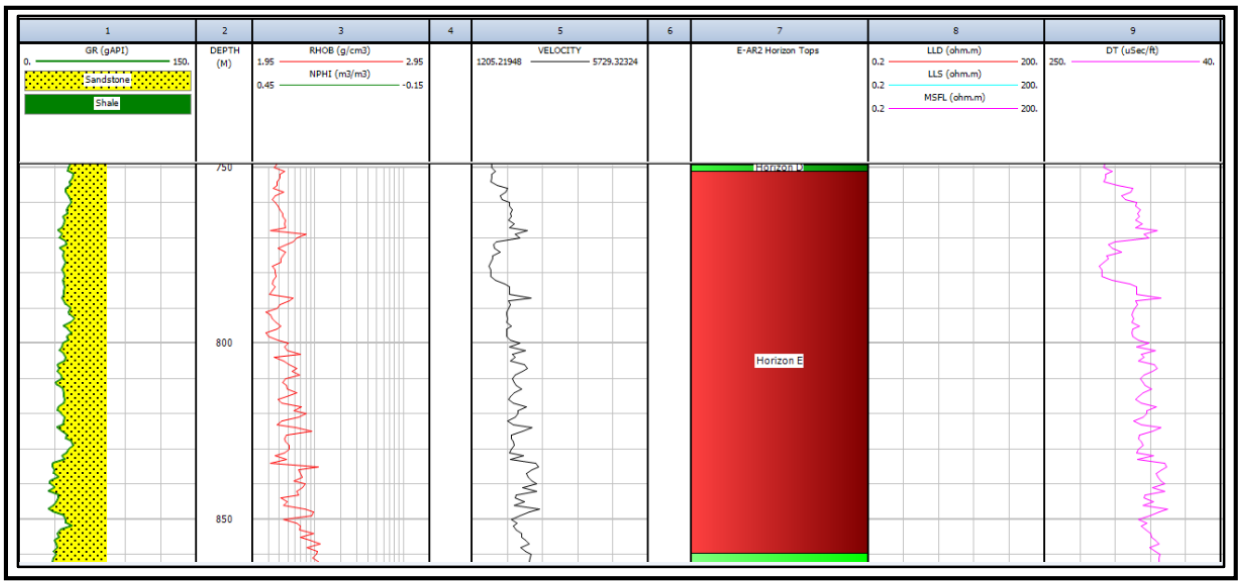

Figure 42: (Left to Right) Gamma ray, density, velocity and sonic logs representative of zone (E).

Zone E is representative of a continuous sand package with an average density of ~2.1 g/cm, suggesting a feldspathic sandstone composition. The changes in velocities are highly responsive to the change in density. Velocities respect a similar trend to the density log where increases in sediment density are observed with an increase in velocity. Velocities do not vary erratically within the sandstone unit.

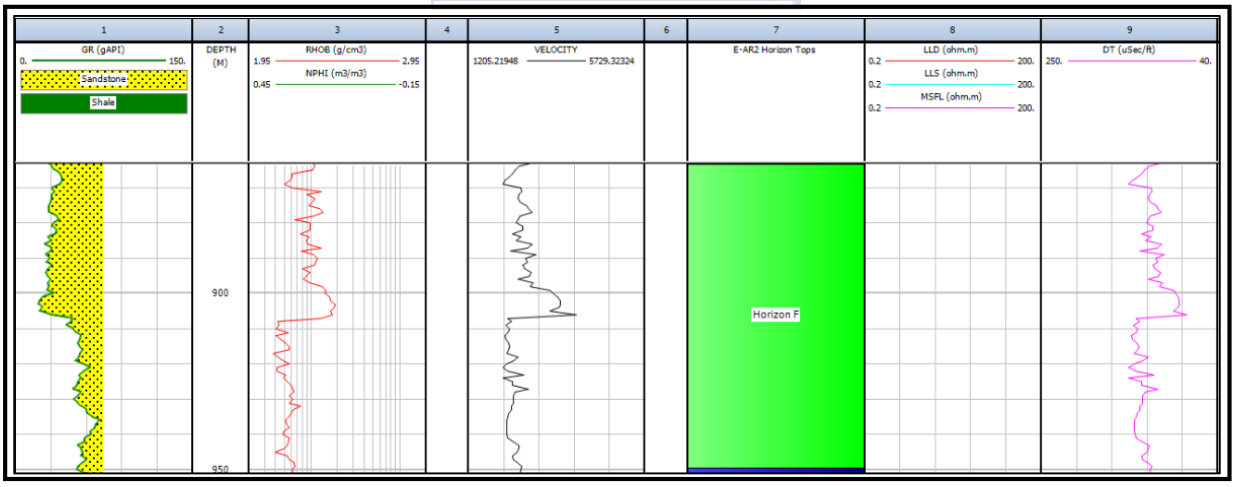

Figure 43: (Left to Right) Gamma ray, density, velocity and sonic logs representative of zone (F).

Zone F is characteristic of a sharp increase in velocity (3968 m/s) as a result of an increase in the gamma ray reading. The gamma ray indicates a change from a very coarse sandstone unit to a finer sand interval. The change in velocities as shown in this zone are primarily due to the transition of different sediments within the zone and illustrate that velocities are highly variable depending on the type or composition of the present lithology.

Mineralogical changes in the sandstone package are also factors that contribute to this variation. Quartz are more resistive minerals as compared to feldspars. Using this known mineral characteristic, it may be used to suggest why velocities vary to a certain extent within the same sand unit.

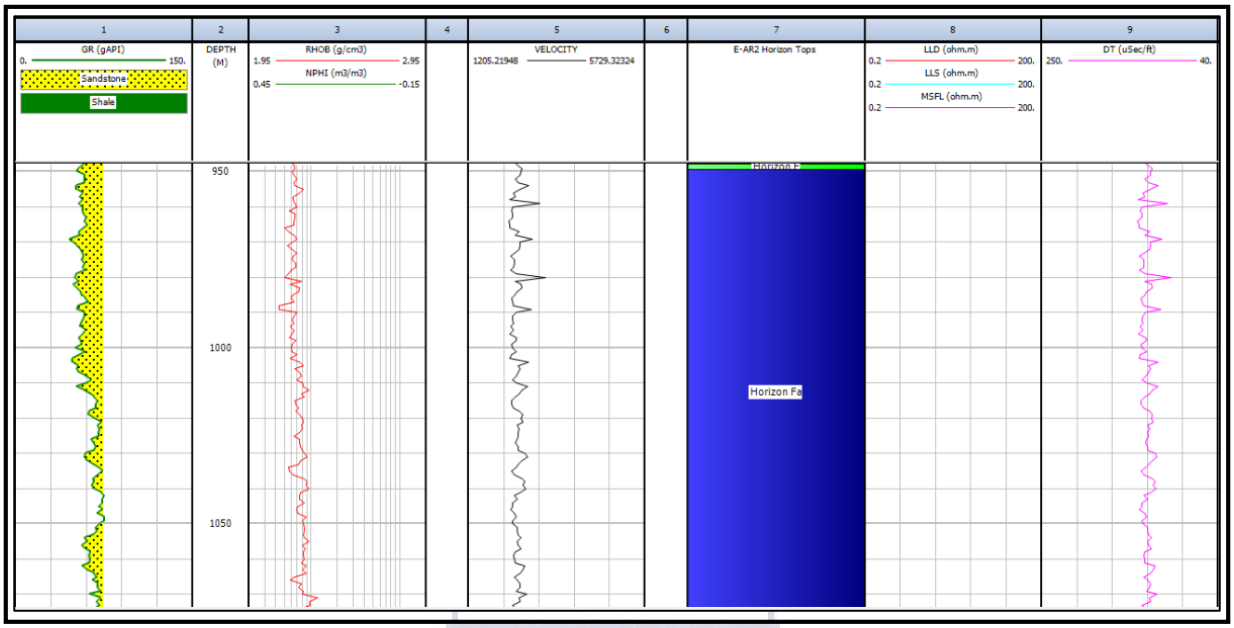

Figure 44: (Left to Right) Gamma ray, density, velocity and sonic logs representative of zone (Fa).

Zone Fa follows a relatively uniform velocity of ~2300 – 2600 m/s with smaller intervals of sandstones reaching ~3400 m/s. The interchange between coarser and finer sand packages may suggest a change in deposition (feeder channels to lobe deposits). Zone C to F is noticeably coarser as compared to Zone Fa. These large scale changes may support the change in deposition, since feeder channels are characteristic of coarser sandstones as compared to lobe deposits. This type of deposition is likely to occur in a submarine fan setting.

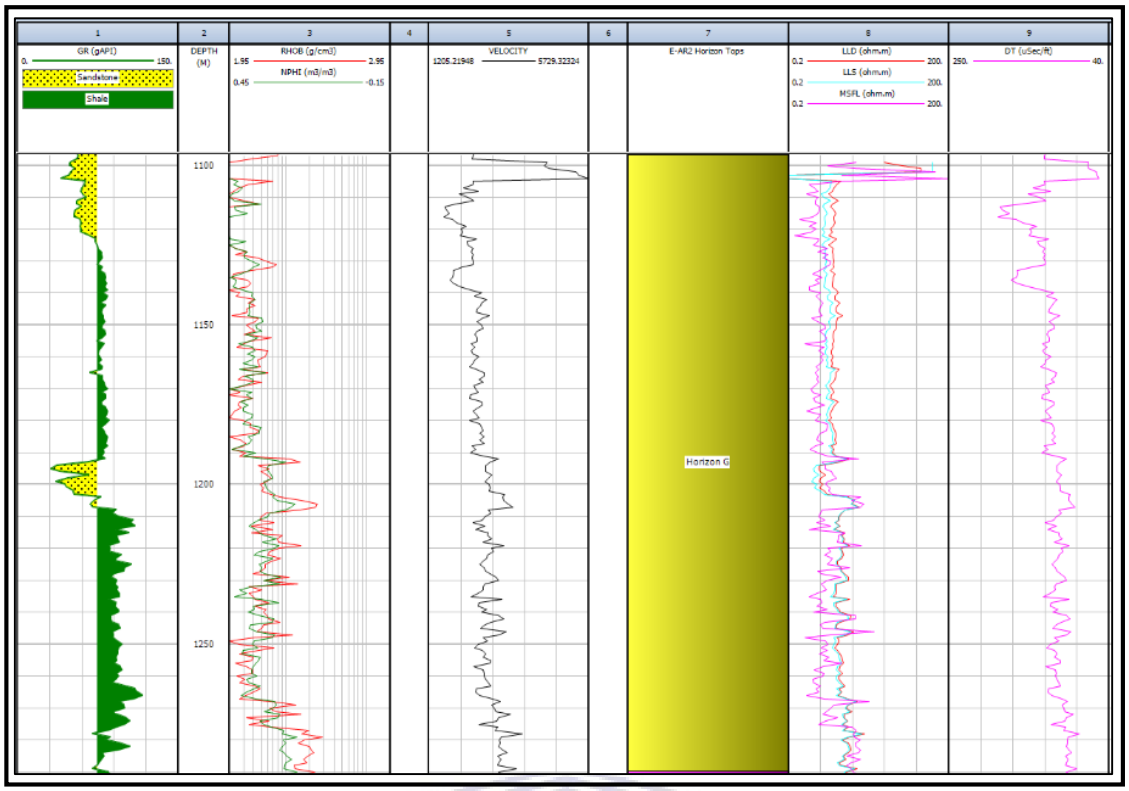

Figure 45: (Left to Right) Gamma ray, density/neutron, velocity, resistivity and sonic logs representative of zone (G).

Zone G is marked by a sharp change in velocity (~2400 m/s – 5000 m/s) related to a sharp change in the gamma ray log. This change is depicted by a transition towards a finer type sediment. Zone G is characterized by two thick layers of shale units that show distinctive variations in velocities, however an overall increase in velocity with depth. At ~1200 m a smaller sand package is noted, where a minor cross-over between the neutron and density log is present. However, resistivity measurements are fairly low for this specific interval. This nature suggests the presence of a water-bearing zone. A distinct change in the velocity can also be noted at this interval. Velocities in this package are higher as compared to the upper sandstone packages.

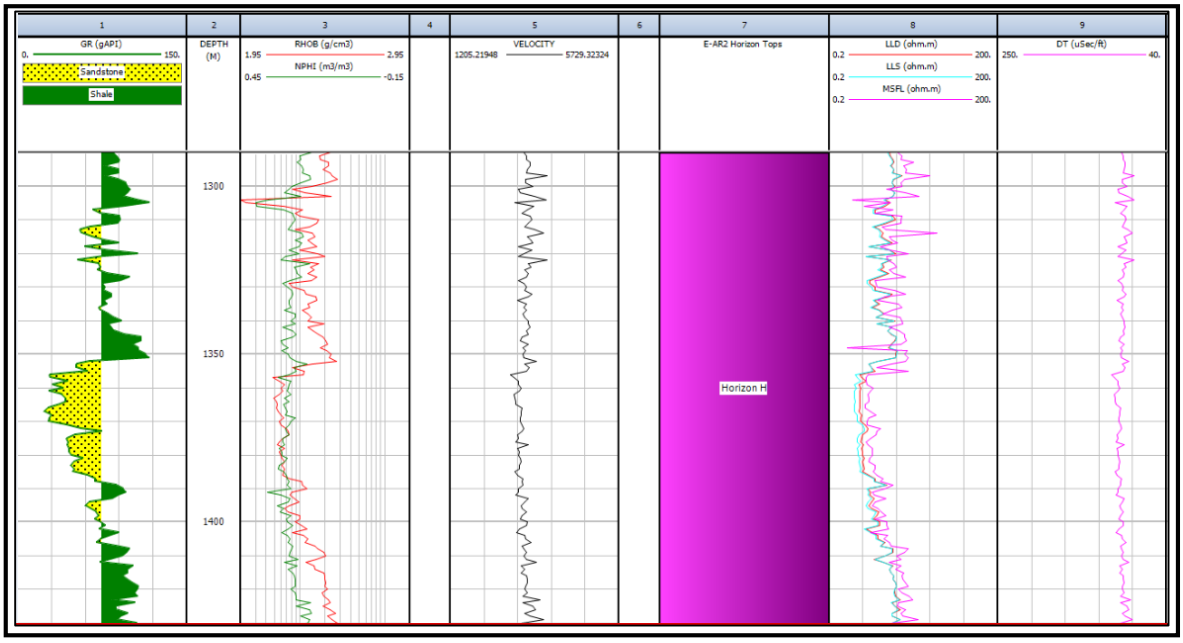

Figure 46: (Left to Right) Gamma ray, density/neutron, velocity, resistivity and sonic logs representative of zone (H).

Zone H is characteristic of well-defined intercalating shale and sandstone packages. A distinct pattern in the velocity profile can be observed from these two types of lithologies. Velocities are relatively uniform within the sandstone unit as compared to the shale packages. Erratic variations in the velocities can also be observed at the interchange between the sand and shale units. Velocities are expected to be greater within shale type sediments as compared to the sandstones as a result of higher densities. A second water-bearing zone is represented by the sandstone package, indicative by the cross-over between the density and neutron log as well as a lower resistivity reading. These characteristic features contribute to the heterogeneity of the subsurface and can be supported by the variation in velocities.

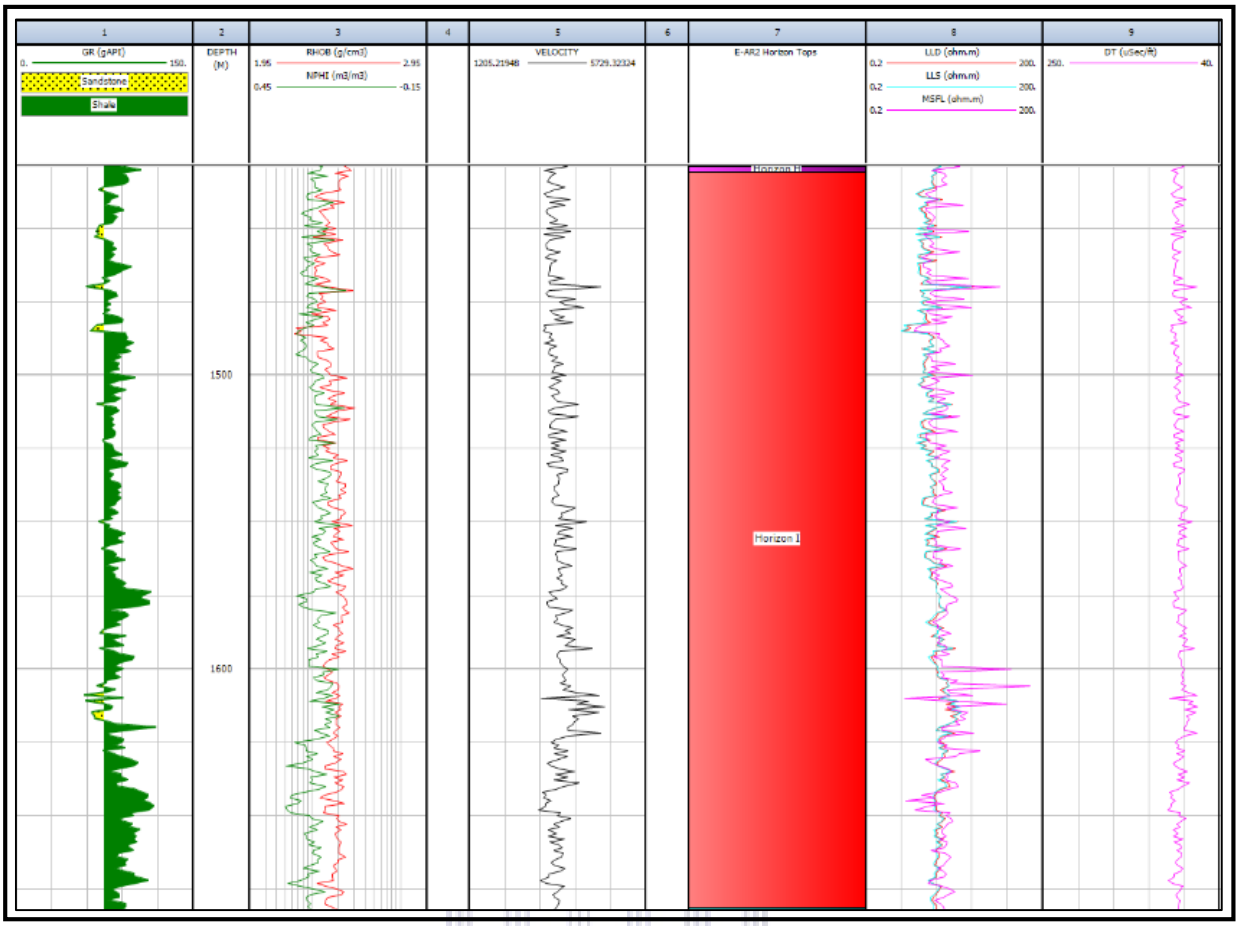

Figure 47: (Left to Right) Gamma ray, density/neutron, velocity, resistivity and sonic logs representative of zone (I).

Zone I is representative of an extensive shale interval with densities averaging 2.4 g/cm, however zone I is characteristic of intermittent variations in velocities at the interchange between smaller sand and shale intervals. This zone, being predominantly shale in composition, is a clear indication of a change in environment. This is confirmed by observing the volume of shale characteristic of zone I as compared to those zones mentioned above.

Comparing the above mentioned zones, velocity profiles are quite distinctive. Variations are significant on a zonal scale and are supported by their respective lithological make-up. Considering the heterogeneity of the subsurface, these changes are significant enough to have a substantial impact on the velocities. Hence, these variations as per zone are relevant for the construction of a velocity model which respects the geology.

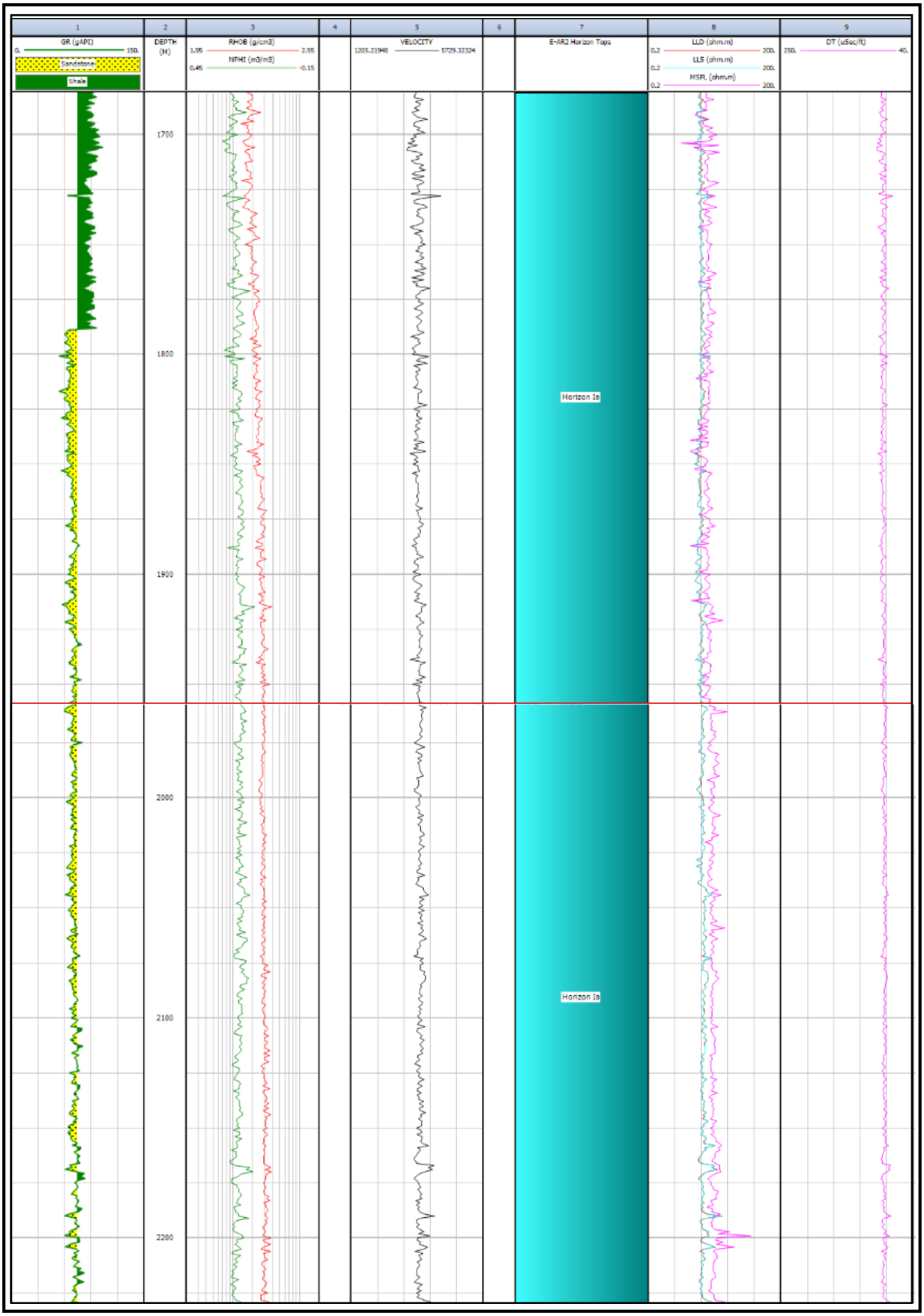

Figure 48: (Left to Right) Gamma ray, density/neutron, velocity, resistivity and sonic logs representative of zone (Ia).

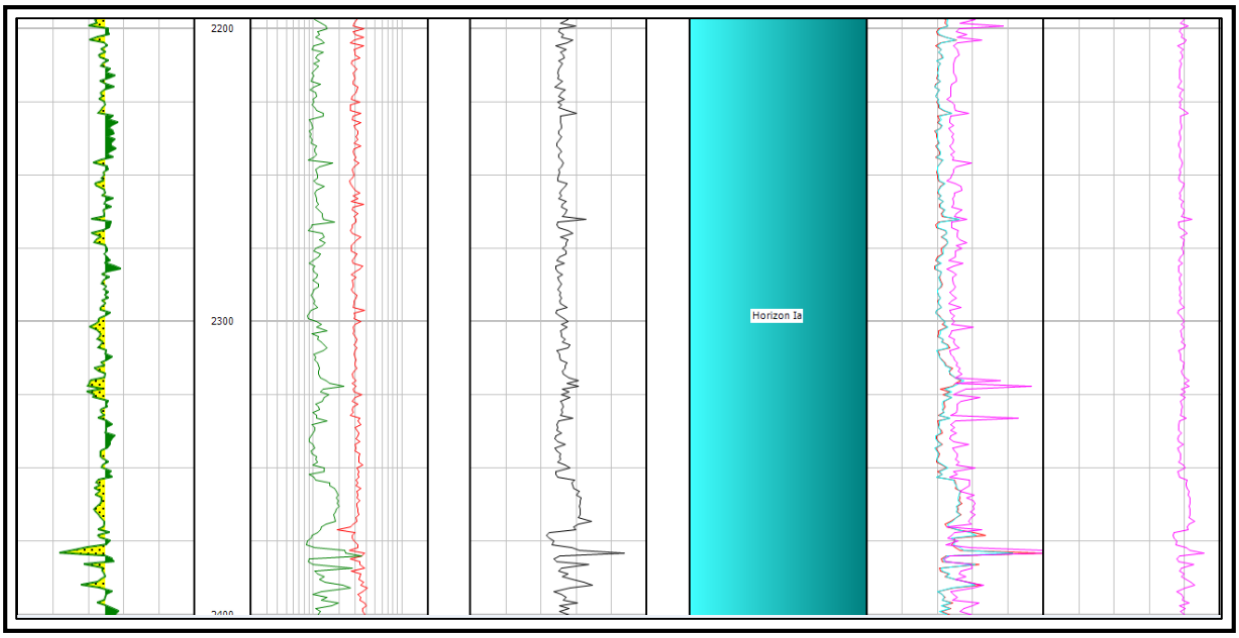

Figure 49: Continued zone Ia displaying (Left to Right) Gamma ray, density/neutron, velocity, resistivity and sonic logs.

Zone Ia is distinctive of a very uniform trend in velocity, except in areas where lithologies differ along the gamma ray baseline. Zone Ia is predominantly a sandstone package with an average gamma of 65 gAPI. Velocities for this continuous package (silty sandstone) range between ~3200 and 3900 m/s. A relatively uniform distribution of velocity can be directly related to the uniform distribution of this continuous silty-sandstone interval. Velocities are noticeably higher at this depth compared to those sandstone packages above zone G. This is may be an indication of a change in the mineralogical make-up of these sandstones packages. A change in the mineralogical make-up may suggest a change in an inter-depositional setting. A characteristic feature of this zone is that the sandstone interval here is much more continuous, however much finer as compared to sandstones observed above zone G. A significant difference in these sandstones is the apparent higher velocities.

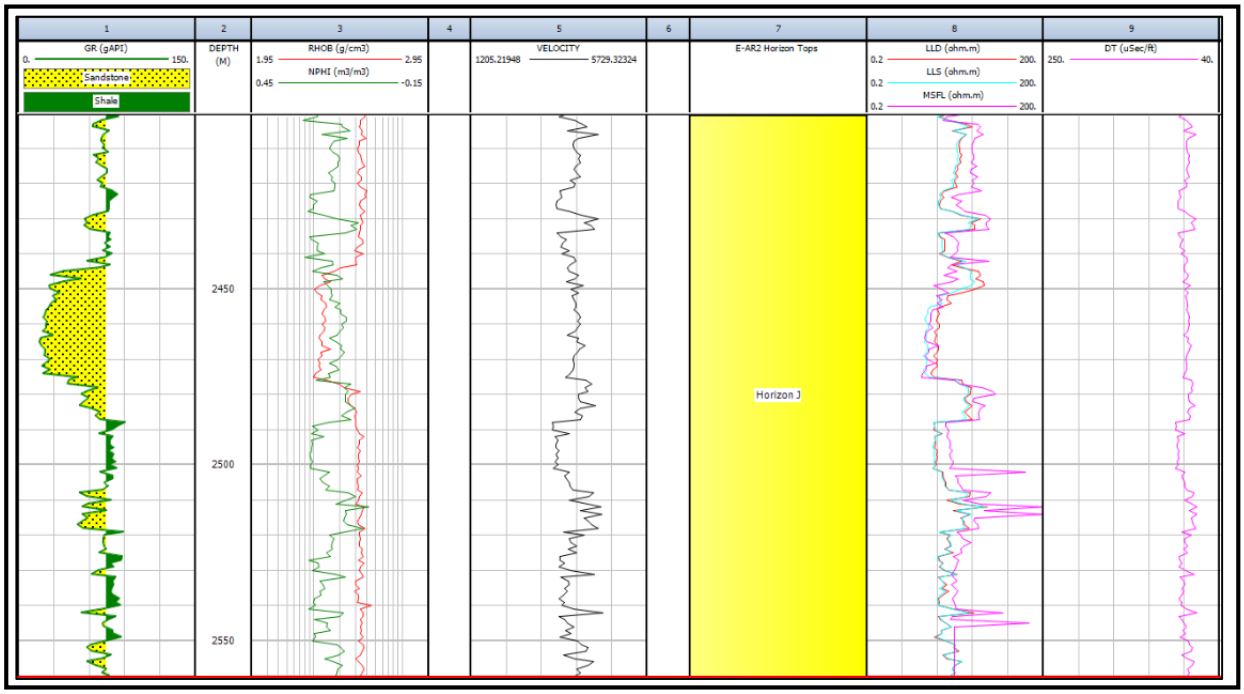

Figure 50: (Left to Right) Gamma ray, density/neutron, velocity, resistivity and sonic logs representative of zone (J).

Zone J is characterized by a much more erratic velocity profile as compared to zone Ia. This is due to the typical intercalation of sand and shale packages. Higher velocities, in some cases, are found in the sand packages. This occurrence may indicate an increase in quartz minerals within the sand unit. These velocities change by an average of 800 m/s where changes in lithologies are observed. A coarser sand unit as shown by the gamma ray is representative of a cross-over between the density and the neutron logs, however linked to a higher deep resistivity reading. This is suggestive of a hydrocarbon-bearing zone. Densities in this sand package are ~2.34 g/cm with velocities of ~3900 m/s. It is evident from this package that the changes in lithology are prominent factors influencing the variation in velocities, not only within the zone but at the boundaries of these zones.

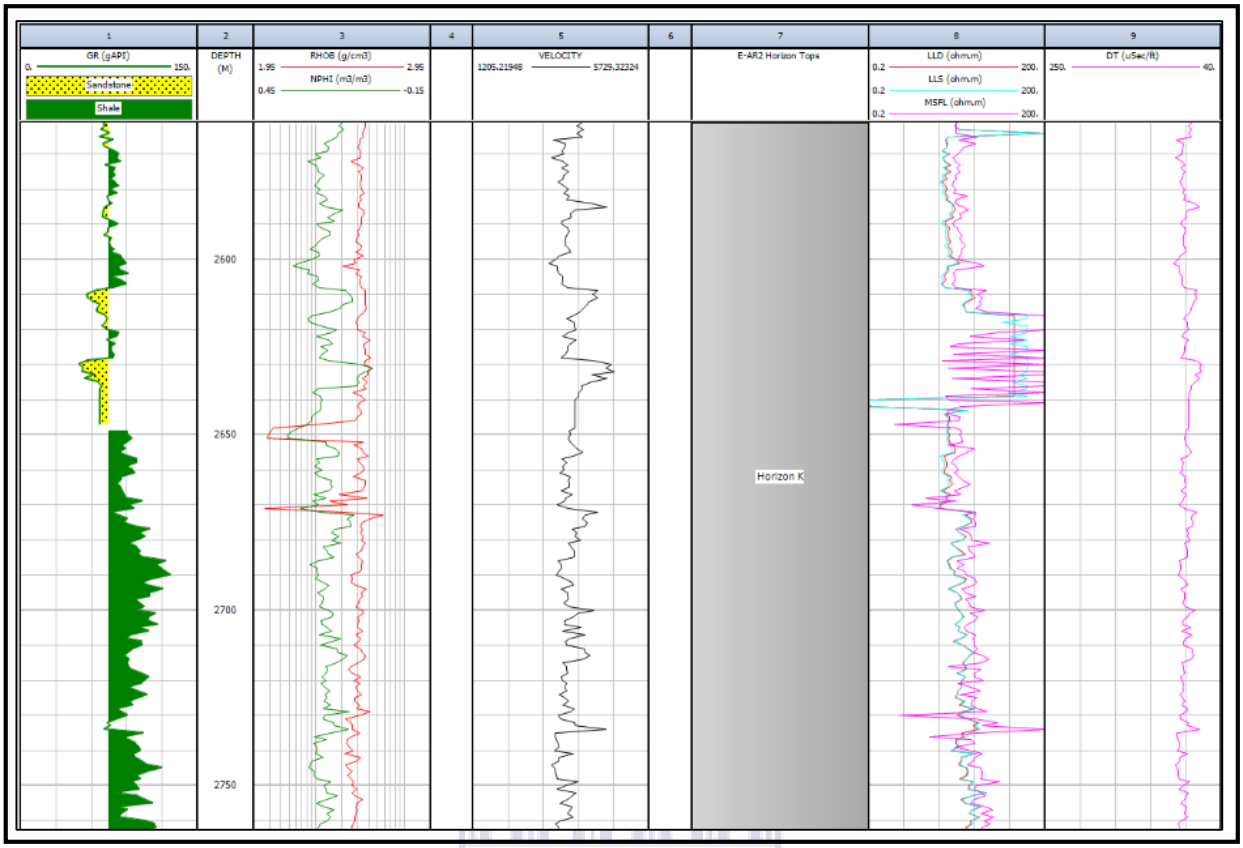

Figure 51: (Left to Right) Gamma ray, density/neutron, velocity, resistivity and sonic logs representative of zone (K).

Zone K is dominated by a shaly interval that is representative of sharp contrasts in velocities. These variations are strongly related to the intensity of the gamma ray log. A sand package is also present within this zone, exhibiting a general decrease in velocity. However, velocities sharply increases at the interface of the sand and shale units. Velocities do not remain uniform and are strongly the result of lithological changes.

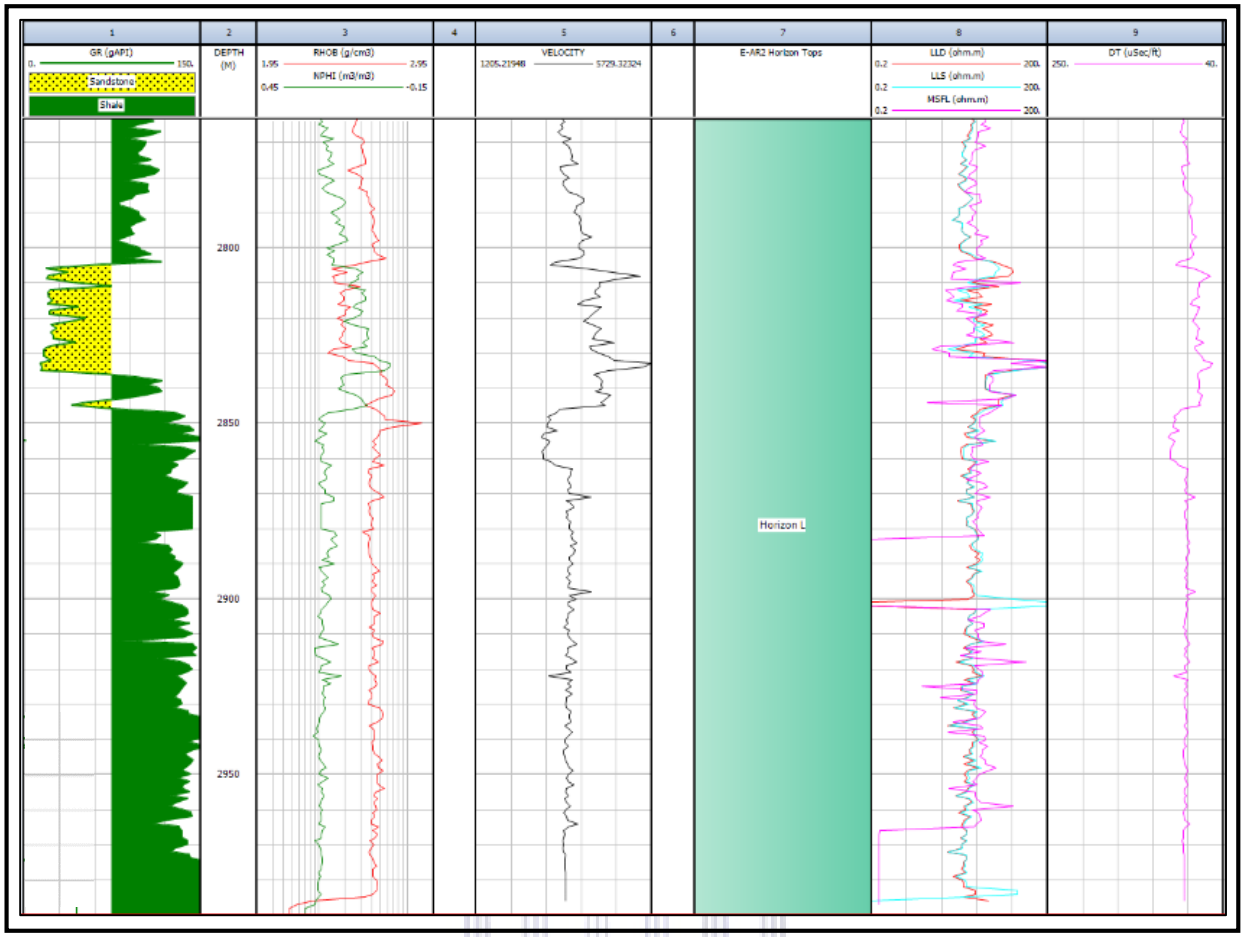

Figure 52: (Left to Right) Gamma ray, density/neutron, velocity, resistivity and sonic logs representative of zone (L).

Zone L is predominantly comprised of a shale unit where velocities display a relatively uniform trend. Velocities in the shale unit average at ~4000 m/s. A significant pulse of sandstone, represented by a sharp decrease in gamma ray is linked to a sudden increase in velocity, higher resistivity and a distinct cross-over between the neutron and density logs. This may be indicative of a hydro-carbon bearing zone, hence indicating that the composition forms an influential factor that controls the variation in velocities.

The variations in velocities are unique to the characterized zones and are represented by unique velocity profiles which are representative of the geology present per zone. The changes per zone in terms of geology and velocities are also significant. These changes are due to factors such as depositional environment or lithology, however significant variations in the velocity profile are also prominent within these zones at the interface of varying lithologies, either being entirely lithological or pertaining to its mineral composition.

4.4 Mineral Plots

Mineral plot analysis was completed in order to determine the mineral composition of the lithologies identified within well E-AX. Due to the limitation of available wireline logs for well E-AX, mineral plots could only be generated from zone G to L. These mineral plots describe the spread of the data between various fields (mineral indicators) between the x and y axis. It is from these plots that the variation in mineralogy relating to the lithology of any zone can be understood.

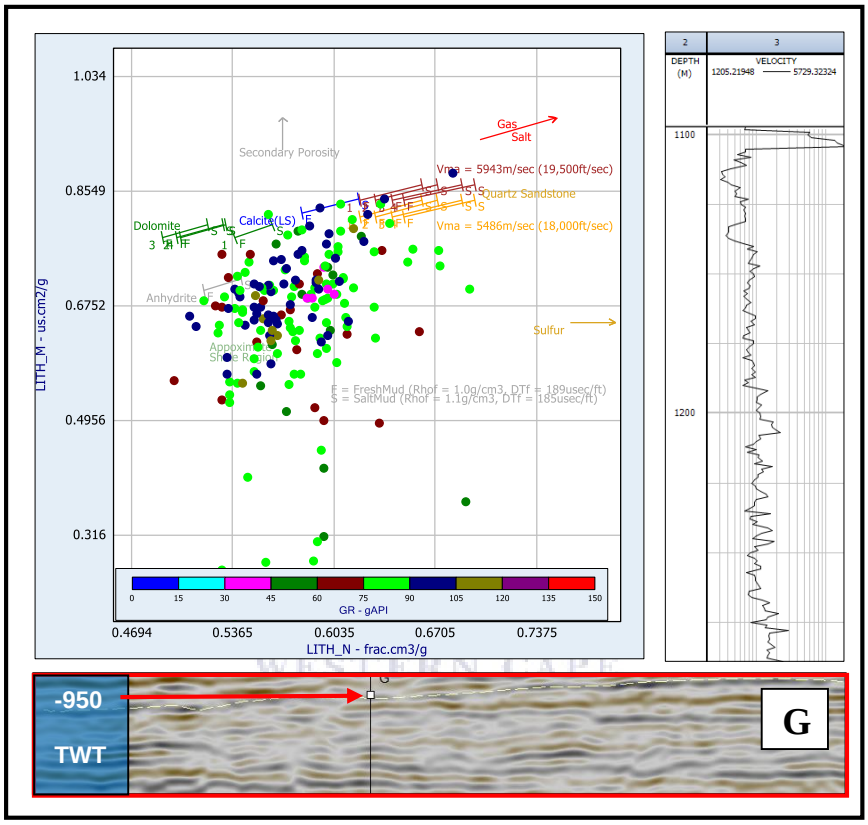

Figure 53: Mineral plot indicating the mineral composition for zone (G).

Zone G, characterized at the top by a significant variation in velocity; is shown to be more shaly in composition as evident by the mineral plot. Data points reveal a distinct mineral composition that is predominantly composed of fine sediments. These points plot mainly between the shale and calcite region with minimal points indicating the presence of quartzitic sandstone as well. Anhydrite minerals, as shown by the mineral plot, may also be present within zone G subsequently cementing this particular zone where sandstones are present. The velocity profile for zone G has an overall positive trend with an increase in velocity as the shale sediments become prominent.

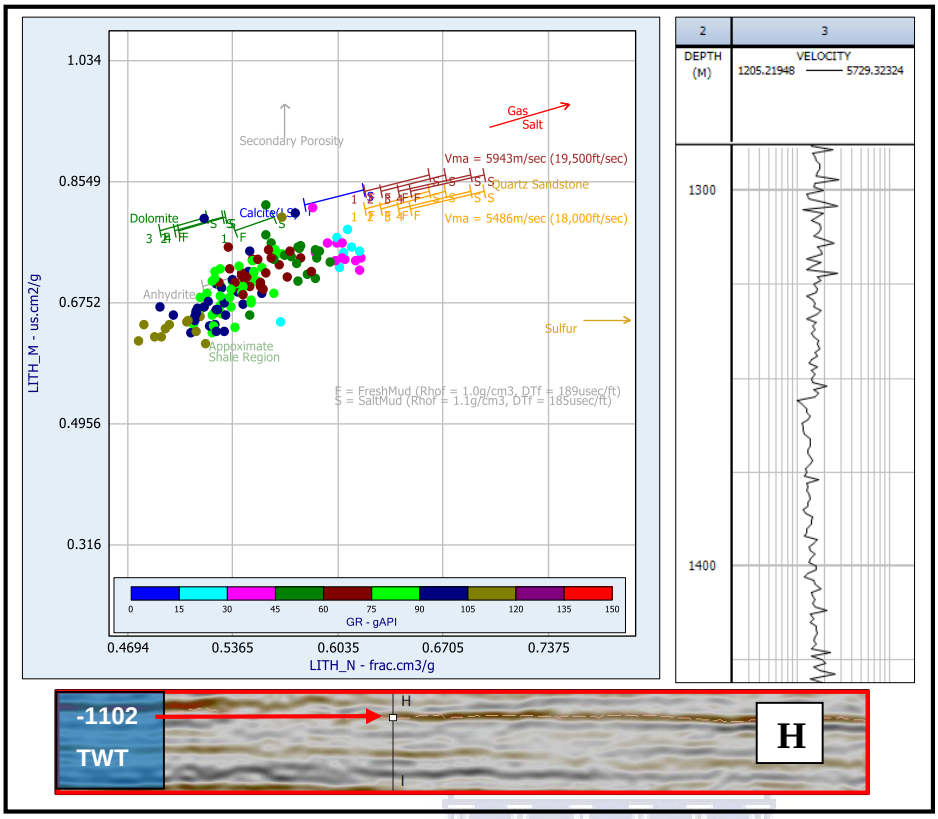

Figure 54: Mineral plot indicating the mineral composition for zone H.

Zone H is characteristic of a more uniform velocity profile as compared to zone G. The mineral plot reveals that the data points cluster between the dolomite and shale region. Velocities are higher in this zone and may be due to the presence of less sandstone. The mineral plot indicates a strong shale/clay composition. Dolomite stringers may also be present within this zone as shown by the mineral plot.

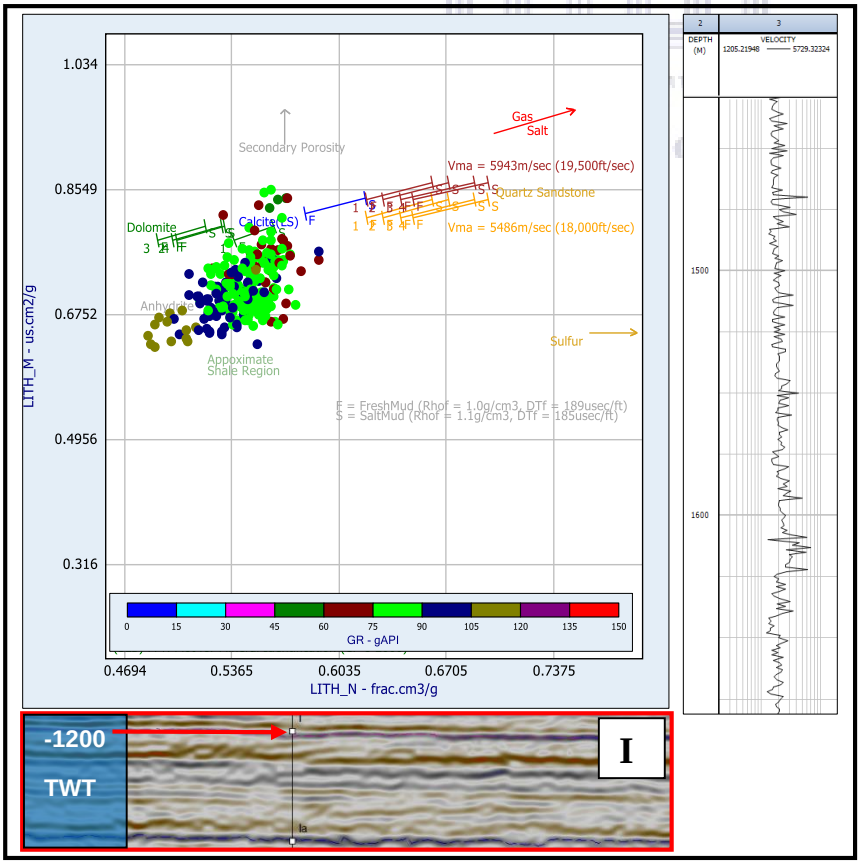

Figure 55: Mineral plot indicating the mineral composition for zone I.

Zone I displays a more erratic velocity profile as compared to zone H. Zone I is evidently more calcitic in composition as data points cluster between the calcite and shale region. Zone I is also characteristically more concentrated with dolomite minerals. The increase in these fine minerals within zone I is explains the reason for the erratic velocity profile as compared to zone H. These minerals impact the densities of these sediments which ultimately impacts the velocity. No quartz minerals are present within this zone.

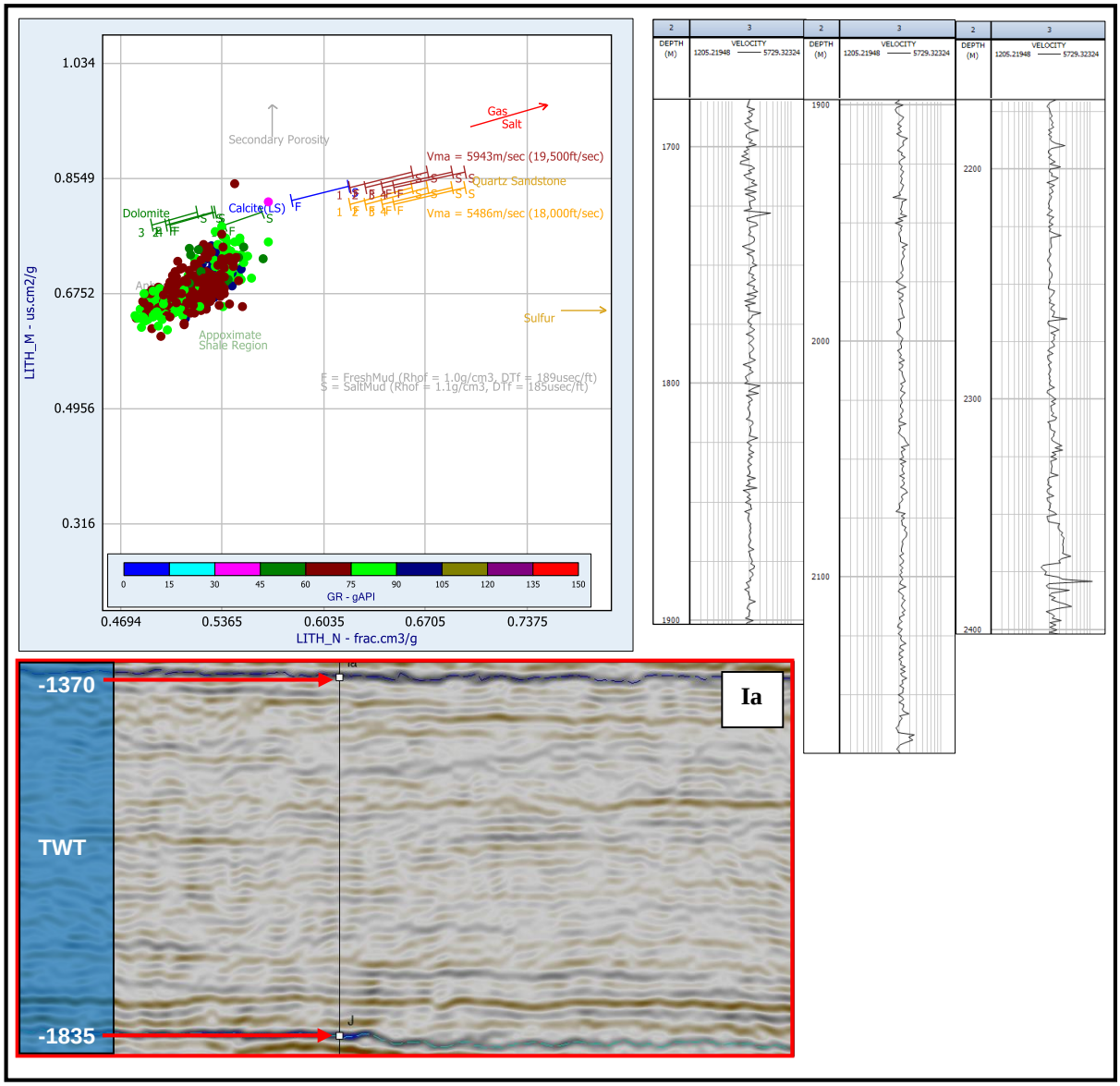

Figure 56: Mineral plot indicating the mineral composition for zone Ia.

Zone Ia is evidently more silty-sandstone rich as previously indicated by the gamma ray log, however higher velocities are indicative of this zone as compared to the velocities for the sandstones above ~ 1000 m. This is explained by examining the mineral plots. The mineral plot shows that the sandstone packages within zone Ia are characteristically higher in clay minerals which may have potentially resulted in the cementation of these sandstone sediments. This generally increases the density of the sediments which impacts the variation in velocities. The gamma ray ranges between 60 and 75 gapi, which supports the continuous silty-sandstone interval, however data points from mineral plot are predominantly found between the dolomite and shale region. This is an indication that the silty-sandstones may be considerably cemented.

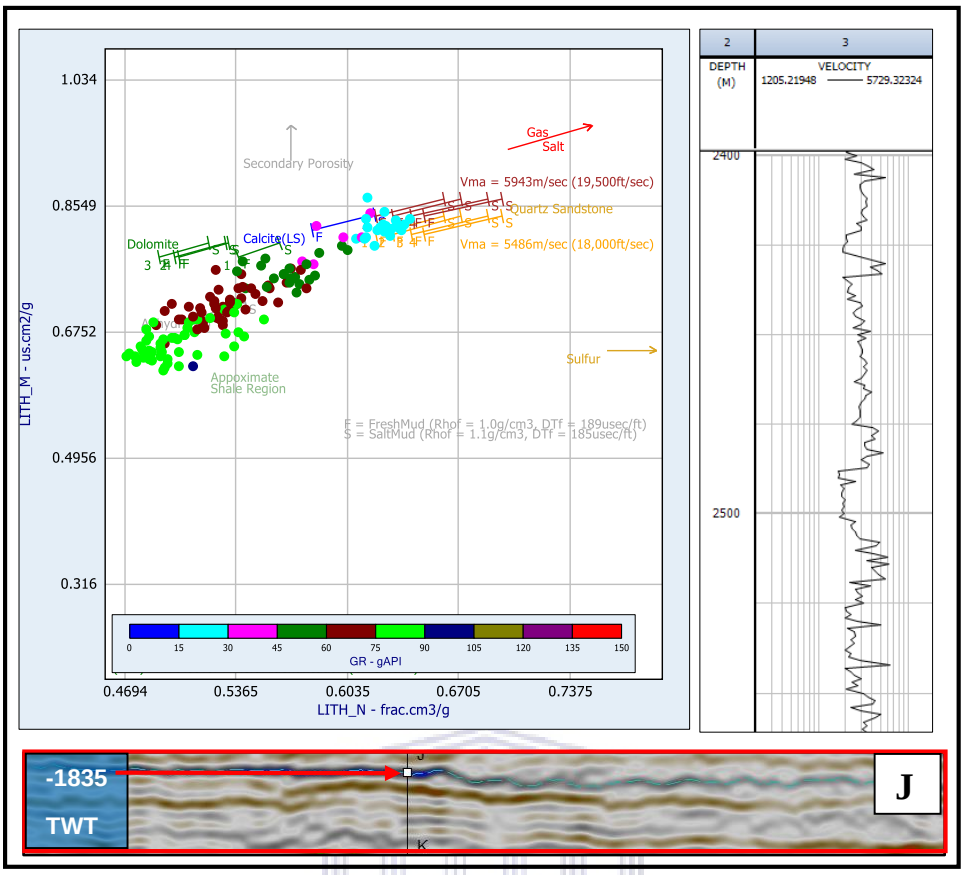

Figure 57: Mineral plot indicating the mineral composition for zone J.

Zone J, as shown by the gamma ray is distinctly made up of a greater composition of sandstone. Coarser sandstones are present within this zone as compared to zone Ia. Sandstones are evidently composed of clay minerals, however quartzitic sandstones are also present, as shown by the light blue cluster on the mineral plot. This may directly explain why velocities are higher within sandstone packages that are composed of quartzitic minerals. Velocities are observed to be more erratic within zone J which may be indicative of greater contrasts in lithologies as well as with variation in mineral composition. Higher velocities are recorded in the sandstones once more, and are consequence to the presence of clay minerals. Clay coating of sandstone grains contribute to a degree of cementation of these sediments which ultimately may result in higher velocities.

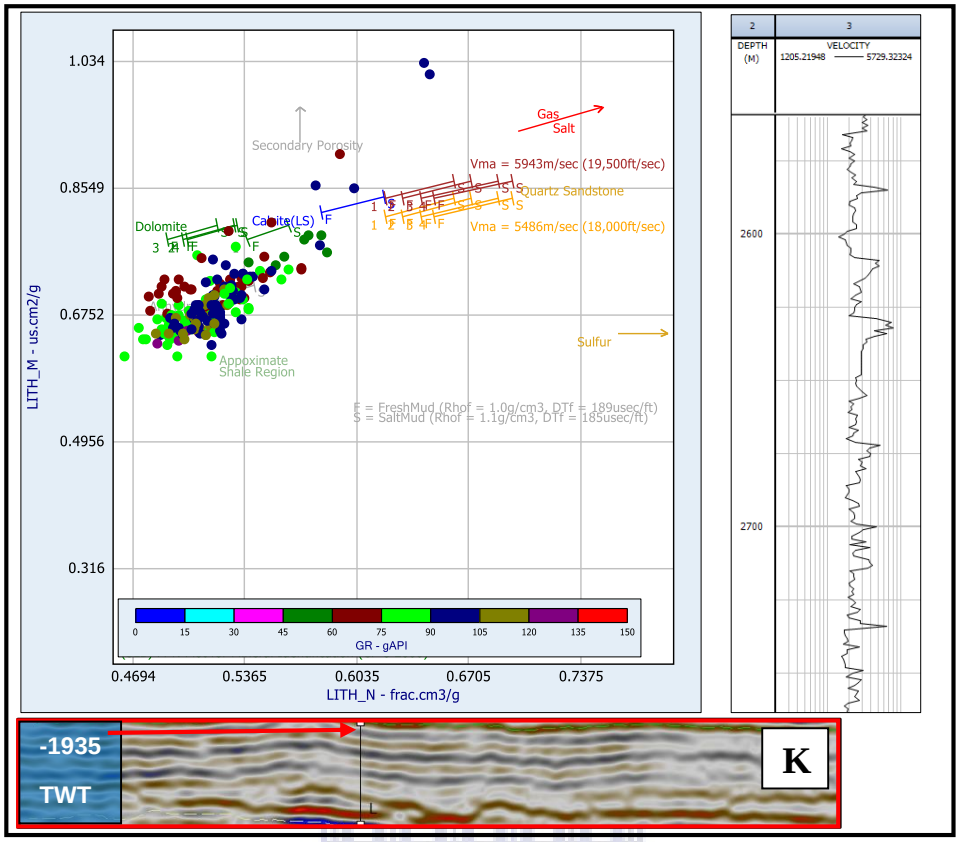

Figure 58: Mineral plot indicating the mineral composition for zone K.

Zone K is typical of less sandstones as compared to zone J, however higher velocities are still evident within the sandstones as compared to the shales. The gamma ray log which indicated the presence of sandstone sediments for this zone are illustrated by a strong clay composition (between the dolomite and shale region) on the mineral plot which could explain why velocities are typically higher for the sandstones.

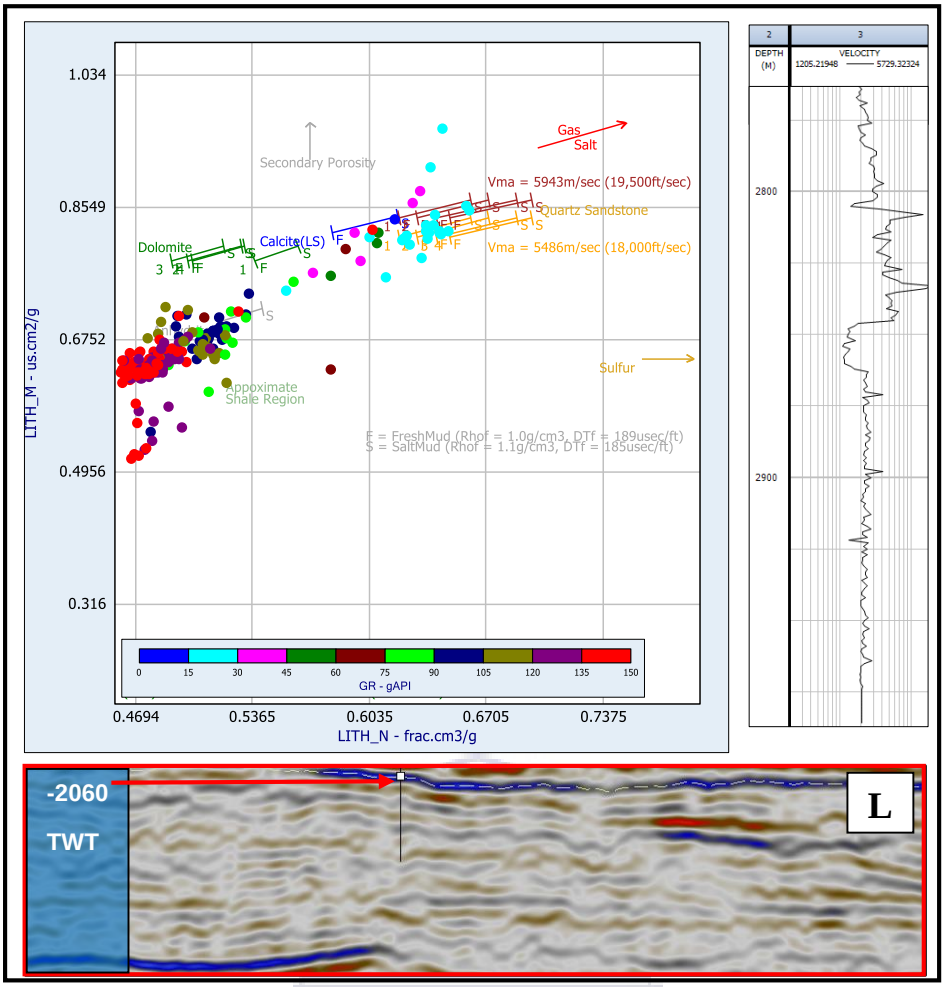

Figure 59: Mineral plot indicating the mineral composition for zone L.

Zone L is predominantly a shaly zone that is characteristic of very high gamma ray readings. The mineral plot shows a strong cluster of data points within the shale zone. A distinctive increase in velocity can be observed within the sand package of zone L. This is supported by the mineral plot which indicates that the sandstone sediments plot fairly in the quartzitic sandstone region. Quartz being a hard mineral should essentially result in a higher velocity response. This explains why velocities significantly increase within this sandstone package. Velocities are fairly uniform above and below this sandstone package. This uniform velocity can be related to the fairly uniform package of shales with a consistently higher gamma ray response. The combination of the mineral plot, gamma ray, velocity, neutron + density (cross-over) and resistivity logs within the sandstone package of zone L indicate the possibility of a hydrocarbon bearing zone.

Velocities are significantly higher within well E-AX below ~1000 m. Formations above this depth are predominantly sandstone, however mineral compositions for these zones cannot be justified due to limitation of wireline logs for zones above zone G. As a result of the limitation

of well logs above 1000 m, no mineral plots could be generated above this depth. However, studying the heterogeneity from zones G to L, it is clear that velocities are higher within the shale layers as well sandstones whose mineral compositions are made up of clay and/or quartz minerals.

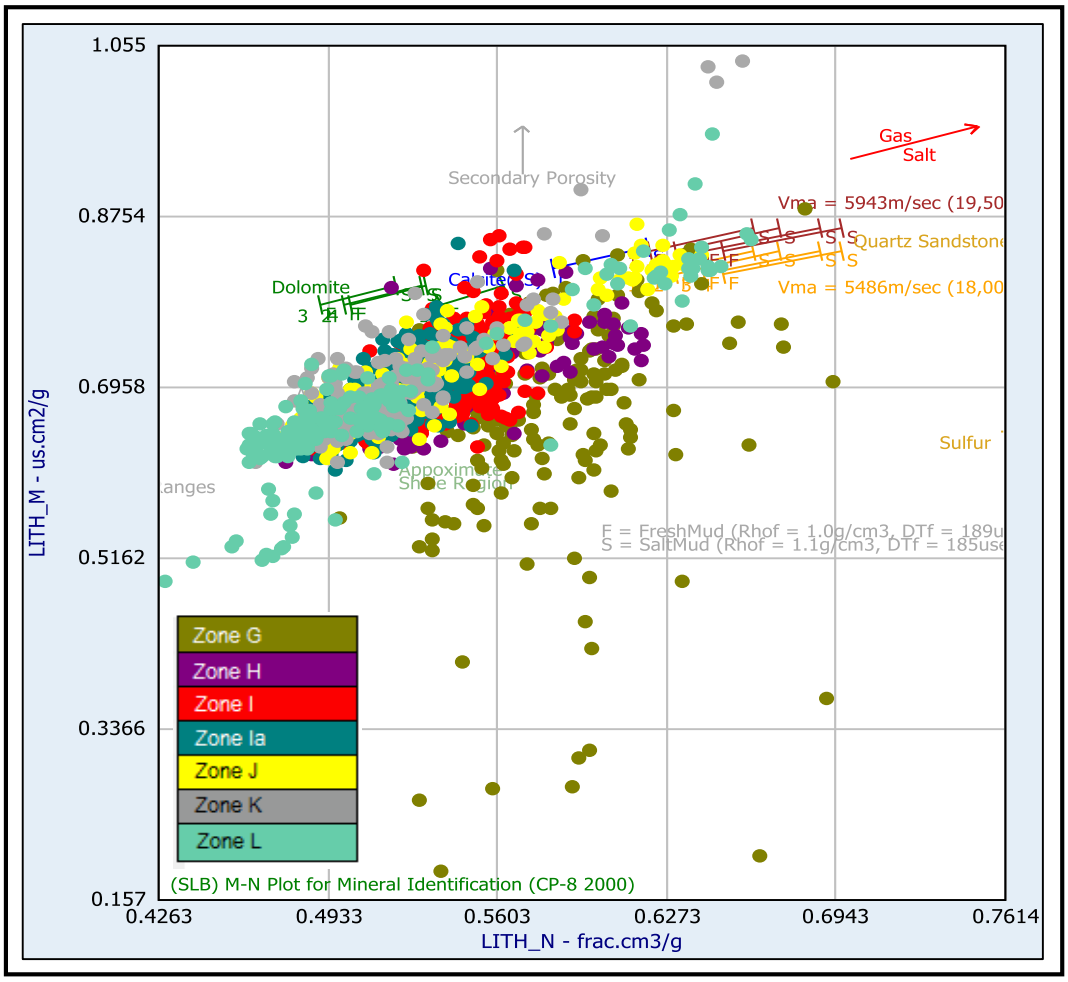

Figure 60: Mineral plot displaying the distribution of the mineral composition for zones (G) to (L)

The above figure illustrates the mineral distribution per zone. It is evident that the variation in mineral compositions are distinctive to the zones, however the variation of minerals per zone are apparent as well. The mineral plot above also illustrates that the predominant mineral composition ranges between the shale, dolomite and calcite region. Velocities from zones (G) to (L) are also evidently higher as compared to zones (A) to (Fa). This may be due to the clay volume from zones (G) to (L) being much greater in volume as compared to the zones above zone (G). Hence the mineral plots indicate that the mineral composition of these subsurface lithologies play a significant role in the variation of the velocity.

CHAPTER 5 – Discussion

This chapter deals with discussing results of analyses derived from velocity data, seismic facies, wireline log and lithology analysis as well as deciphering the mineral composition presented by the lithologies in the researched area. This discussion aims on elaborating key points established in the results section to address the problem statement.

5.1 Velocity model construction and investigation

Velocities as a response to subsurface heterogeneities were investigated in this study. The variation in the velocities as a result of existing subsurface heterogeneities were used to construct a velocity model for the purpose of constructing such a model that respects the geology. The velocity model was built based upon the velocities studied. The velocity model as constructed from these velocities were representative of subsurface variations for the entire extent of the well and seismic data. This was done in order to emphasise the complexity of the variation in velocities as opposed to only considering velocities recorded at formation well tops when building a velocity model. The purpose of this study was then fulfilled by understanding the impact of these subsurface heterogeneities on the variation in velocities.

The velocity data was acquired using a calculation from the sonic log. The sonic log was also used to tie the well to the seismic data in order to improve the control on the accuracy of the interpretation. Velocities used in this study were purposefully selected based upon distinct variations in the velocity profile for the well as a response to subsurface heterogeneities. These velocities were characterized into zones representing unique velocity profiles bounded by a top and base velocity distinctive of each zone. These zones were the basis for subdividing significant variations in the geology based upon the velocities. Sheriff, cited in Silva, 2008 stated the prevalent use of sonic logs to help construct a velocity model since the model is a measure of time over depth.

A total of fourteen horizons were mapped which are representative of the variation in the velocities. The sum of all mapped horizons are a direct indication that velocities are not constant within the subsurface, thus indicating the presence of subsurface heterogeneities. In order for a model to be constructed with respect to the geology, these velocities were incorporated.

Fourteen zones were distinguished, namely: Zones A to L alphabetically. It is evident from these zones that their unique velocity profiles are the result of geological implications. Velocities vary differently per zone. Zones A to Fa have velocity ranges significantly lower

than those velocities recorded below zone G. Velocities from zone A to Fa range from ~1400 to 3500 m/s as compared to velocities of ~3000 to 4800 m/s for zones G to L respectively.

In comparison of velocity variations for two groups of zones, namely: A - Fa and G - L, it is apparent that shales become prominent below zone G. The range in velocities for three representative zones above zone G, namely zone B, D and F range from ~1700 to 2000 m/s; ~1800 to 3500 m/s; and ~2400 to 2600 m/s respectively. Taking three representative zones below zone G, namely: zone H, Ia and K, velocities range from ~3000 to 3500 m/s; ~3400 to 3600 m/s and 3300 to 4800 m/s respectively. From this comparison, it can be observed that velocities are substantially higher below zone G. The rate of change in velocity is also significant per zone. This is attributed to factors such as changes in inter-depositional systems, lithologies as well as variations in the mineral compositions.

Significant variations in velocities can be found in zone G with a velocity range of 2200 m/s as compared to zones such as zone Ia, where the range of velocities are substantially lower (~690 m/s). The significant range in velocity observed in zone G can be attributed to the fact that this particular zone marks the first recorded shale packages, as shown by the gamma ray. Low variations in the velocity profile observed in zone Ia are attributed to the uniform deposition of the continuous silty-sand package, characteristic of low amplitude reflections.

A TDR (time-depth relation) by sonic calibration and a synthetic seismogram was generated to ensure that the desired velocities matched well with the amplitude reflections on the seismic data. Pandey et al., also argued the significance of a time – depth conversion to remove structural ambiguity inherent in time and verify structure. This provides a model which conforms to the depth domain. The position of the intervals representative of the selected velocities were justified by the position of the zone tops on the seismic data.

5.2 Seismic Facies Analysis

The study of the subsurface heterogeneity included the investigation of seismic facies, lithology analysis from the wireline logs as well as the mineral composition of the lithologies from the generation of mineral plots.

The seismic facies analysis involved studying the reflector patterns and amplitudes per zone with relation to the velocities. Brighter amplitudes associated with higher acoustic impedances are generally associated with higher velocities, as observed from the study. Each zone studied, exhibited unique seismic facies. Features such as contorted and chaotic seismic reflectors were

present in most zones, however more prevalent in zones such as zone Ia and L. According to Lin (2006), these features represent a disordered arrangement of reflection surfaces exhibiting little or no continuity. These configurations may be attributed to soft sediment deformation or deformation of strata in high energy environments. These seismic facies were linked to unique velocity profiles. The result of studying these seismic facies showed that velocities are substantially responsive to the variations in reflector patterns and amplitudes of the respective facies. The configuration of the seismic facies being geologically related.

The first recorded formation well top was captured at 1268m (1140ms (TWT)). It is observed from this study that velocities vary to a substantial degree above this depth, hence these velocities would be either ignored or averaged when only considering those velocities at the formation well tops.

Zone A is characterized by dimmed parallel seismic reflector patterns representing a uniform depositional rate on a uniformly subsiding surface (Lin, 2006). Velocities are observed to increase with brighter amplitude reflections. Lower velocities are found in zone B and C as compared to zone A, although having similar seismic reflector patterns. These lower velocities are attributed to dimmer amplitude reflections exhibited by zone B and C. The velocity profile observed in zone B was found to be less uniform as compared to zone C. This is the result of varying amplitude reflections.

A clear distinction in seismic facies can be seen in zone D. This zone is characterized by higher amplitude reflections, prominent parallel reflectors and significantly higher velocities as compared to zone E. These differences are attributed to changes in the type of sandstones present, as shown by the gamma ray in figure 26. Brighter amplitudes in zone D can be related to high acoustic impedance contrasts, hence greater variation in velocities.

Seismic facies found between zone I and Ia vary distinctly as well. The velocity profile for zone Ia (as shown by figure 34) is much more uniform as compared to zone I. Zone I is characteristic of more sub-parallel reflector patterns with greater contrasts in seismic amplitudes as compared to zone Ia. Zone Ia is characterized by contorted and chaotic reflector patterns, however a very uniform velocity profile attributed to its continuous fine-grained sand-silt package. This may be due to a change in inter-depositional systems between these zones. Seismic facies indicate that these two zones are divided by varying rates of deposition and distinct variation in reflector patterns. This was verified by examining the differences in lithologies and seismic facies in figures 31 to 34.

Varying rates of deposition can also be observed between zones J, K and L (as shown by figure 35). Zone K is characterized by well-defined sub-parallel reflectors with brighter amplitude reflections indicating faster rates of deposition on a uniformly subsiding surface. Zone L is represented by highly discontinuous seismic reflectors with predominant chaotic features as compared to zones J and K. These chaotic features are due to soft sediment deformation or deformation of strata in high energy environments (Lin, 2006). Velocities are relatively uniform above and below the sand package of zone L as a result of a prominent shale package exhibiting minimal variation on the gamma ray (figure 36).

Seismic facies display a wide variation in reflector patterns, these patterns are an indication of a variation in depositional rates and on a larger scale, changes in inter-depositional systems. Velocities conclusively respond to these changes as shown by the seismic data. The variation in seismic amplitudes can be integrated with the lithologies, since acoustic impedance contrasts are the response of lithological boundaries of varying density and velocities. These changes are quite significant when studying the seismic data as a whole, and vary depending on the existing heterogeneity. This statement is further supported by Posamentier and Kolla (2003) who described the use of seismic data in a deep basin-floor setting offshore Nigeria, Indonesia and the Gulf of Mexico to identify five depositional elements, from turbidity-flow leveed channels to debris-flow channels, lobes and sheets. Each depositional element representative of unique morphologies and seismic expressions. (Posamentier and Kolla, 2003). Anomneze et al., (2015) incorporated the use of reflection geometries and amplitudes to define seismic facies in the eastern Niger Delta Basin, Nigeria. This method in turn was used to make qualitative lithological predictions away from existing well control.

It is observed from the study that low amplitude reflections are generally represented by a uniform velocity profile. A uniform velocity profile with low amplitude reflections are the result of low acoustic impedance contrasts by the presence of a continuous lithological package displaying minor variations in properties such as grain size. This is observed within zone Ia characterized by its continuous fine silty-sandstone package, as revealed by the gamma ray log. The trend in the velocity is therefore distinct per zone as each zone is characteristic of a particular combination of seismic reflector patterns and amplitudes.

5.3 Log and Lithology Analysis

A suite of wireline logs were used to identify and characterize lithologies within the study area and how these lithologies impact the variation in velocities. Velocities are observed to be highly responsive to lithological disparities. Lithologies that are higher in terms of density generally have higher velocities, as shown by integrating the study between lithologies and velocity.

Velocities in some lithological units are observed to decrease resulting in an overall negative gradient for the respective zone. These may be due to factors such as formation pressure increases or overpressures. Uniform lithological units, especially those interpreted as sandstones are represented by a uniform velocity profile. Sharp variations in velocities are observed at the interface of varying lithologies and can be attributed to the acoustic impedance contrast between these lithologies. Within the characterized zones, sandstones of similar nature exhibit distinctly different responses on the velocity profile. This is the result of differences in mineral composition within these lithologies. Mineral plots indicate that zone J is more quartzitic in composition as compared to the other zones studied, and velocities here are noticeably higher. Quartz minerals are harder and dense by nature and should explain why the resultant velocities are higher for the sandstone units of this zone.

Higher velocities are found deeper within the study area. A conclusive observation is that densities increase with depth as a result of natural processes such as increases in overburden pressures. These variations in velocities can be observed by integrating the density log and understanding the lithologies present. The response of velocities are highly dependent on the lithology present and vary substantially at lithological units of varying geologic properties. This is observed when comparing zones A – Fa with zones G – L. Velocities are higher from zones G to L as a result of prominent shale sediments. The densities for these sediments are higher, overburden pressures are greater and the ratio between shale and sandstones proliferate. These factors contribute to higher recorded velocities for zones G to L.

Zone L, (Figure 52) velocities are distinctly higher within the sandstone unit, as a result of its quartzitic composition. This observation supports the afore mentioned statement where the mineral composition impacts this variation in velocities, as it is expected that the shales with greater densities, deposited above and below this sandstone unit, should have higher velocities.

5.4 Mineral Plots

Mineral plots could not be generated for zones A to H, however well reports for the study area demonstrate that sandstones above 350 m as observed from the gamma ray log, are not entirely clean sandstones. The low gamma ray is a result of calcareous materials present. The sandstones are interbedded with calcarenite and are highly fossiliferous (Soekor, 1990).

Glauconitic sandstones with calcareous fossil content are mistaken to be very coarse sandstones on the gamma ray log, as a result of its low radiation. Sandstones are composed of calcareous and phosphate nodules as well as foraminifera. Shelly material within the upper sandstone units result in very calcitic sandstones. From ~500 to 630 m, formations are predominantly made up of limestone with Inoceramus and shelly material. Sandstones are cleaner below ~1300 m (Soekor, 1990). The presence of these calcareous and fossiliferous materials explain why velocities are lower above ~1000 m.

The impact on the variation of velocities by change in the mineral composition was understood by cross-plotting the lithology M against lithology N. The characterized zones were analysed and are observed to have varying mineral compositions. Zones G to L predominantly plot between the dolomitic and shale region indicating that these lithologies are concentrated with clay minerals. This explains why velocities are higher within these zones. Zones J and L are composed of quartz minerals indicating that the sandstones are quartzitic in composition. Sandstones within these zones show higher velocities as compared to the shales deposited above and below, as a result of its mineral composition.

Zones with higher clay composition may have caused pore cementation, most likely by the presence of pore filling minerals such as illite or chlorite, thus resulting in an increase in density. This change in density such as that observed in zone K results in a positive change in velocity. From these observations, it is evident that the composition of minerals influences the variation in velocities, substantially.

The integrated study encompassing the impact on the variation of velocities by existing subsurface heterogeneities have shown that velocities vary substantially depending on the present geology. Studying the seismic facies, results demonstrate that low amplitude reflections are associated with lower velocities, high acoustic impedance contrasts are associated with higher velocities and higher velocities related to faster rates of deposition. Zones were represented by unique seismic facies in terms of seismic reflectors and amplitudes and were

characteristic of distinctive velocity profiles. Variations in the velocities were highly affected by variations in the lithologies, as shown by results from the wireline log analysis.

Velocities and densities were observed to have a general direct relationship. Velocities increased substantially where shales became prominent and vary erratically at interfaces between shales and sandstones as a result of contrasts in densities. Uniform velocities as observed in zone Ia are attributed to a uniform distribution of silty sandstones as a result of subtle variations in density. Further investigation has also shown that mineral compositions for similar lithologies, such as the sandstones in the study area, exhibited varying velocities in comparison. This is attributed to minerals such as quartz distributed in zones such as J and L, and clay minerals distributed indiscriminately. Mineral plots reveal that the lithologies were predominantly composed of clay minerals, serving part of the influential factors impacting the variation in velocities. The analyses undertaken have shown that subsurface velocities are influenced by multiple factors on varying scales ranging from the seismic facies to the mineral compositions, hence is a significant representation of the relation between subsurface heterogeneities and velocities.

CHAPTER 6 - Conclusion

An integrated study of the geology and velocities were completed in accordance to the aims and objectives set at the beginning of this thesis. The study shows that subsurface velocities are highly responsive to existing heterogeneities and illustrates that the sole use of velocities at formation well tops will not entirely respect the heterogeneity of the subsurface. The integration of investigating subsurface heterogeneities by examining seismic facies, lithologies and the mineral compositions have shown, as a result, that velocities vary to a significant degree depending on the existing subsurface heterogeneities. These differences are quite significant from a scale of seismic facies to mineral composition.

Fourteen zones were identified representing unique velocity profiles. An average maximum velocity of 3500 m/s was found above zone Fa as compared to an average maximum velocity of 4800m/s below zone G. These significant variations in velocities were attributed to differences in lithologies, more specifically, as shale sediments were found to be more prominent below zone G. Brighter amplitudes with high acoustic impedance contrasts were found to be associated with higher velocities. These brighter amplitudes are observed within zones such as zone D reaching velocities of 3717 m/s as compared to dimmer amplitude reflections reaching a maximum velocity of 2933 m/s within zone E. Dimmed seismic reflectors as a result of subtle variations in lithologies displayed minimal variations in velocities. These minimal variations in velocities can be observed in zone Ia, where the range of the variation in velocities were observed to be only ~690 m/s over a thickness of 718.9m as compared to zone G, where the range of velocities were observed to be 2200m/s over a thickness of 213.3m. Zones such as I and Ia have shown distinct differences in terms of seismic facies where a more uniform velocity profile represented by zone Ia was attributed to its low acoustic impedance contrasts and minimal variation in the silty sandstone as shown by the gamma ray.

The rate of change in velocity due to lithologies was shown by studying the formation densities. Higher velocities are related to higher densities, particularly where shale sediments were present. Zones G to L being characteristically higher in dolomitic and shale sediments have shown to have higher velocities (~3000 – 4800 m/s), however where quartzitic minerals were present such as those found in zone L, velocities were higher (~4800 m/s) than the shales

sediments (~3600 m/s) deposited above and below the sandstone package. Hence indicating that velocities were strongly dependent on the densities and minerals present in the formation.

The variation of these velocities are therefore significant enough that it should be considered when constructing a velocity model which respects the geology of the study area.

The ability to examine the subtle or significant variations in the subsurface in terms of the geology from factors such as the seismic facies and able to link them to the velocity profile, may indeed improve the results of the velocity model. This will result in a model that is more complete and representative of the subsurface geology.

6.1 Recommendations:

For future construction of a velocity model with geological implication, the following could be considered:

- As velocities vary instantaneously with existing heterogeneities, it is therefore significant to consider these velocities as opposed to averaging velocities.
- Incorporate significant/key interval velocities which show distinct variation from the velocity profile as a result of geological differences.
- Velocities at formation well tops should be included when building the velocity model for the purpose of increasing accuracy when depth converting, in addition to the key interval velocities.
- Due to varying mineral compositions from similar lithologies, such as the sandstones studied, a petrographic study will aid to better understand the influence of overburden pressures as well as cementation of these minerals and its impact on the velocities.

References

Alaminiokuma, G. & Ugbor, C., 2010. Analytical Velocity Model for Depth Conversion in the Subsurface Facies of Agbada Formation in the Niger Delta, Nigeria.. *The Pacific Journal of Science and Technology,* 11(1), pp. 563-575.

Anomneze, D. et al., 2015. Application of seismic stratigraphy and structural analysis in the determination of petroleum plays within the Eastern Niger Delta Basin, Nigeria.. *Journal of Petroleum Exploration, Production and Technology,* Volume 5, pp. 113-122.

Brown, L. F. et al., 1995. Sequence Stratigraphy in Offshore South African Divergent Basins. In: *Geology #41 An Atlas on Exploration for Cretaceous Lowstand Traps by Soekor (Pty) Ltd.*. U.S.A: American Association of Petroleum Geologists (AAPG), pp. 19-37.

Dalfsen, W., Doornenbal, J. & Gunnink, J., 2006. A comprehensive seismic velocity model for the Netherlands based on lithostratigraphic layers. *Netherlands Journal of Geoscience - Geologie en Mijnbouw,* 85(4), pp. 277-292.

Davies, C., 1997. Unusual biomarker maturation ratio chnanges through the oil window, a consequence of varied thermal history.. *Organic Geochemistry,* 27(7/8), pp. 537-560.

Envoi, 2014. Offshore South Africa (Outeniqua Basin) Pletmos Inshore Block. p. United Kingdom s.n.

Feddersen, J. & Malan, J., 2001. *Geological well completion report: Proposal for the appraisal borehole E-AX,* s.l.: Soekor E & P.

Futalan, K., Mitchell, A., Amos, K. & Backe, G., 2012. *Seismic Facies Analysis and Structural Interpretation of the Sandakan Sub-basin, Sulu Sea, Philippines.* Singapore, AAPG International Conference and Exhibition.

Grobber, N., 2005. The Barrimian to Aptian Gas Fairway, Bredasdorp Basin, South Africa.. *World Petroleum Congress, Africa Session,* Volume 21.

IHS Energy, 2010. *Outeniqua Basin, South Africa.* s.l., Basin Monitor.

Kadi, E., Khalil, H. & Khalil, G., 2015. *Comparison Between Manual and Computerized Petrophysical Interpretation of Rudeis Formation, Belayim Marine Field, Gulf of Suez, Egypt.,* Egypt: Al Azhar University and Belayim Petroleum Company.

Lin, A., 2006. *Seismic Stratigraphy*, Taiwan: Unpublished: National Central University of Taiwan, Department of Earth Science.

Malan, J., 1993. Geology, potential of Algoa, Gamtoos Basins of South Africa.. *Oil Gas Journal*, 91(46), pp. 74-77.

McCarthy, T. & Rubidge, B., 2005. *The Story of Earth and Life: A southern African perspective on a 4.6-billion-year journey.* Johannesburg: Struik Nature.

McMillan, I., Brink, G., Broad, D. & and Maier, J., 1997. Late Mesozoic Sedimentary Basins off the South Coast of South Africa,. In: *Africa Basins. Sedimentary Basins of the World 3. Edited by R.C. Shelley, Series Editor K.J Hsu.* Amsterdam: Elsevier Science B.V., pp. 319-376.

Onajite, E., 2014. Understanding Seismic Interpretation Methodology. In: *Seismic Data Analysis Techniques in Hydrocarbon Exploration.* Nigeria: Elsevier, pp. 177-211.

Pandey, A. et al., 2013. *Seismic Velocity Model Building: An aid for better understanding of subsurface - a case study from Cambay Basin, India.*. Kochi, 10th Biennial International Conference and Exposition.

Petroleum Agency SA, 2004/5. *South African Exploration Opportunities.* pp 27 ed. Cape Town: South African Agency for Promotion of Petroleum Exploration and Exploitation.

Posamentier, H. W. & Kolla, V., 2003. Seismic Geomorphology and Stratigraphy of Depositional Elements in Deep-water Settings.. *Journal of Sedimentary Research*, Volume 73, pp. 367-388.

Rider, M., 2002. *The Geological Interpretation of Well Logs.* 2nd ed. Scotland: Whittles Publishing.

Roux, J., 1997. Soekor E&P: Potential Outlined in Southern Outeniqua Basin, off S. Africa. *Oil and Gas Journal*, Issue July 21, 1997.

Schalkwyk, H., 2005. *Assessment controls on reservoir performance and the affects of granulation seam mechanics in the Bredasdorp Basin, South Africa. MSc Thesis.*, Cape Town: Department of Earth Sciences, University of the Western Cape.

Schlumberger, 1997. M-N Plot for Mineral Identification. In: *Log Interpretation Charts.* Houston, Texas: Schlumberger Wireline and Testing, pp. 4-21.

Schlumberger, 2014. *Petrel E & P Software Platform 2014*, s.l.: Schlumberger.

Silva, M., 2008. *Comparison of Average Methods to Build a Velocity Model from Sonic Log.* Rome, Italy, 70th EAGE Conference and Exhibition.

Soekor, 1990. *Geological well-completion report of borehole E-AR2,* Cape Town: Soekor.

Tarek, F., A.M., S. a. M. & Ramadan, 2011. Well Logs Application in Determining the Impact of MIneral Types and Proportions on the Reservoir Performance of Bahariya Formation of Bassel-1x Well, Western Desert, Egypt.. *Journal of American Science,* 7(1), pp. 498-505.

Thomson, K., 1999. Role of continental break-up, mantle plume development and fault reactivation in the evolution of the Gamtoos Basin, South Africa.. *Marine and Petroleum Geology 16,* pp. 409-429.

Turner, J. R., Grobbler, N. & Sontundu, S., 2000. Geological modelling of the Aptian and Albian sequences within block 9, Bredasdorp Basin, Offshore South Africa. *Journal of African Earth Sciences, Geocongress 2000: A new millenium on ancient crust, 27th Earth Sciences Congress of the Geological Society of South Africa,* p. 80.

Yin, P. & Wo, S., 2010. *Creation of Mineral Log, Enhanced Oil Recovery Institute.* Wyoming, University of Wyoming.